

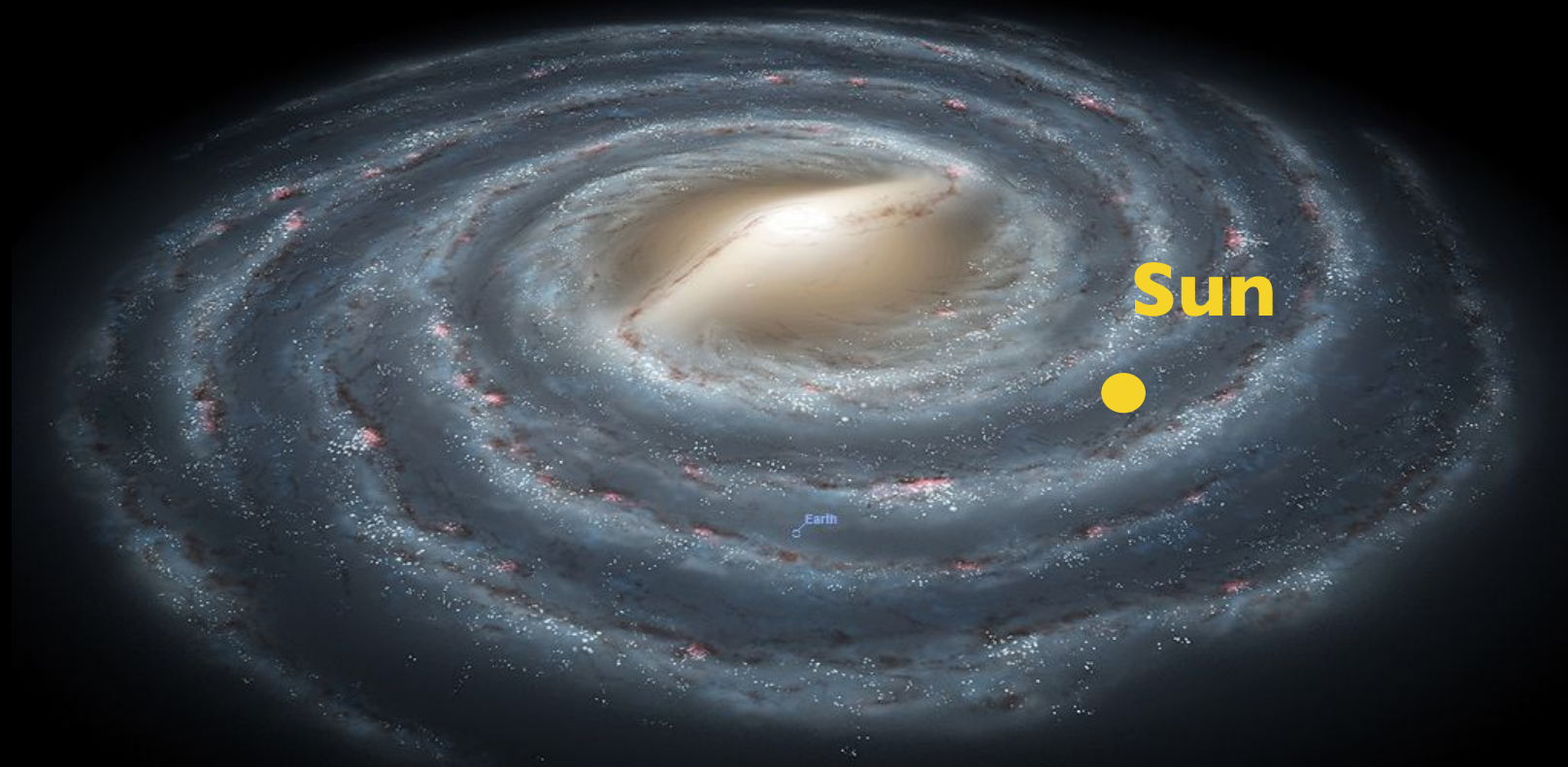
# Impact of simulation results for dark matter searches

Nassim Bozorgnia

Institute for Particle Physics Phenomenology  
Durham University

# Dark Matter distribution

*Signals in direct and indirect dark matter (DM) searches strongly depend on the DM distribution in our Galaxy.*

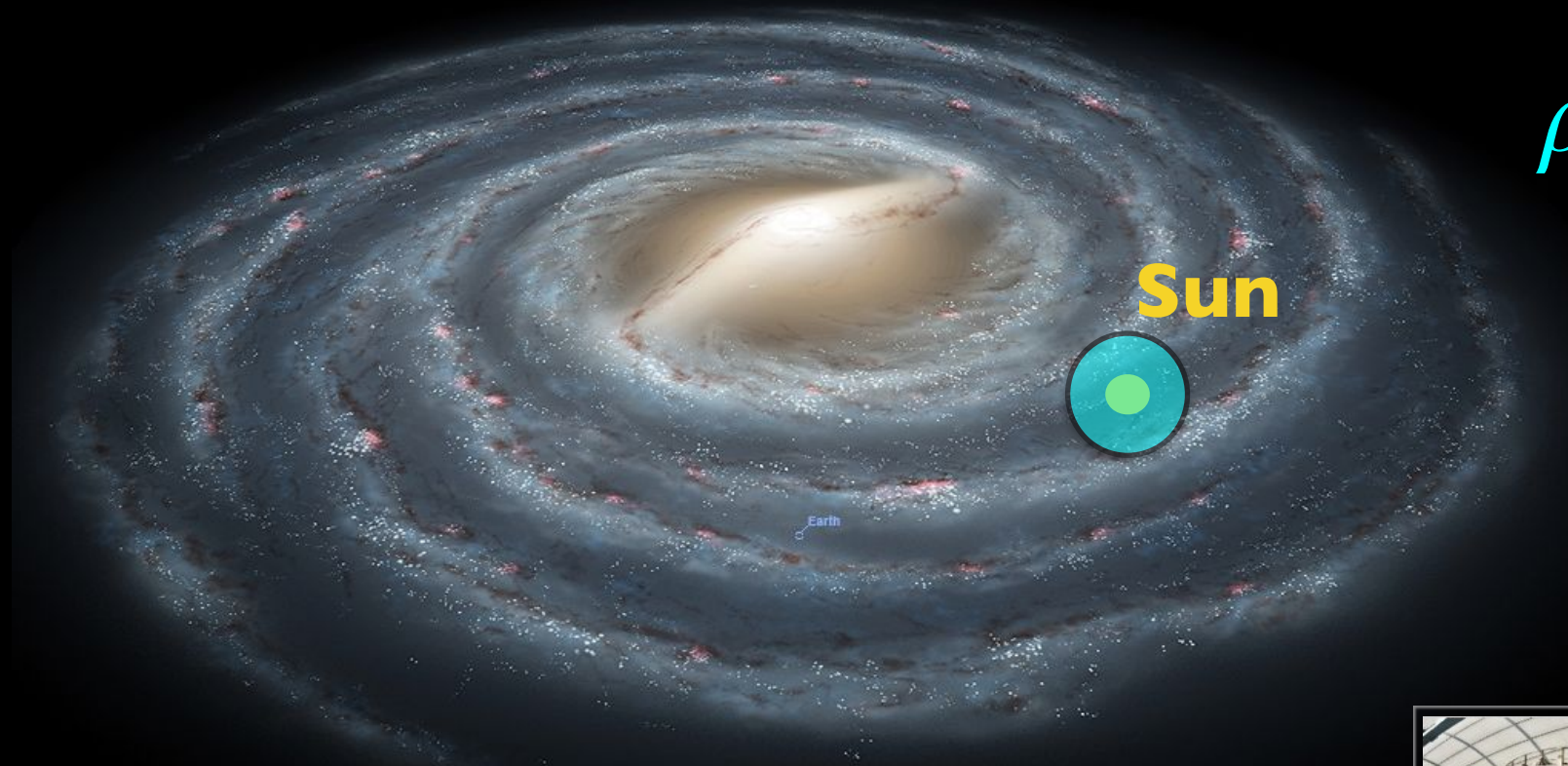


# Dark Matter distribution

*Signals in direct and indirect dark matter (DM) searches strongly depend on the DM distribution in our Galaxy.*

## Direct Detection

$$\rho_\chi, f(\mathbf{v})$$



# Dark Matter distribution

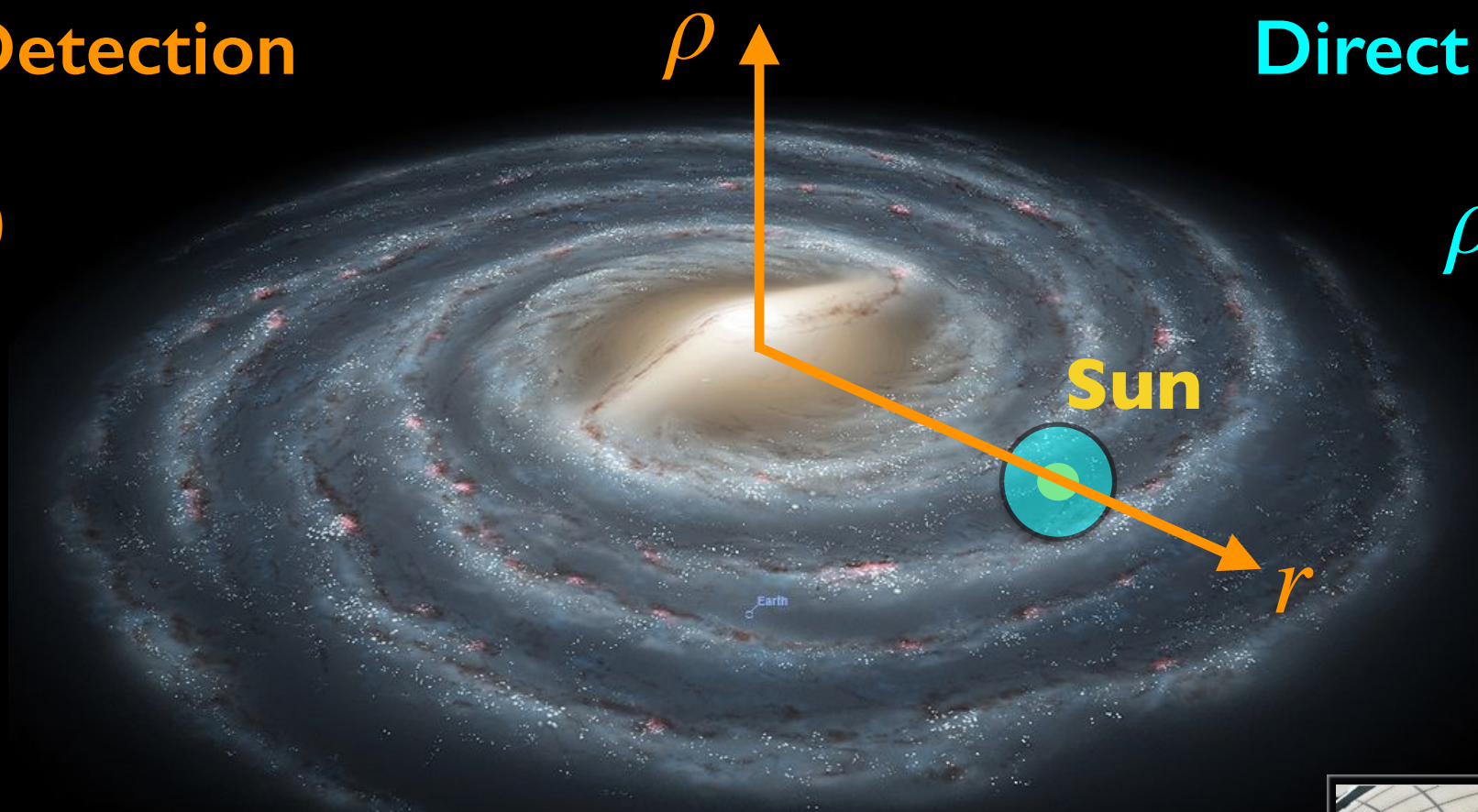
*Signals in direct and indirect dark matter (DM) searches strongly depend on the DM distribution in our Galaxy.*

## Indirect Detection

$$\rho(r)$$

## Direct Detection

$$\rho_\chi, f(\mathbf{v})$$



# Dark Matter distribution

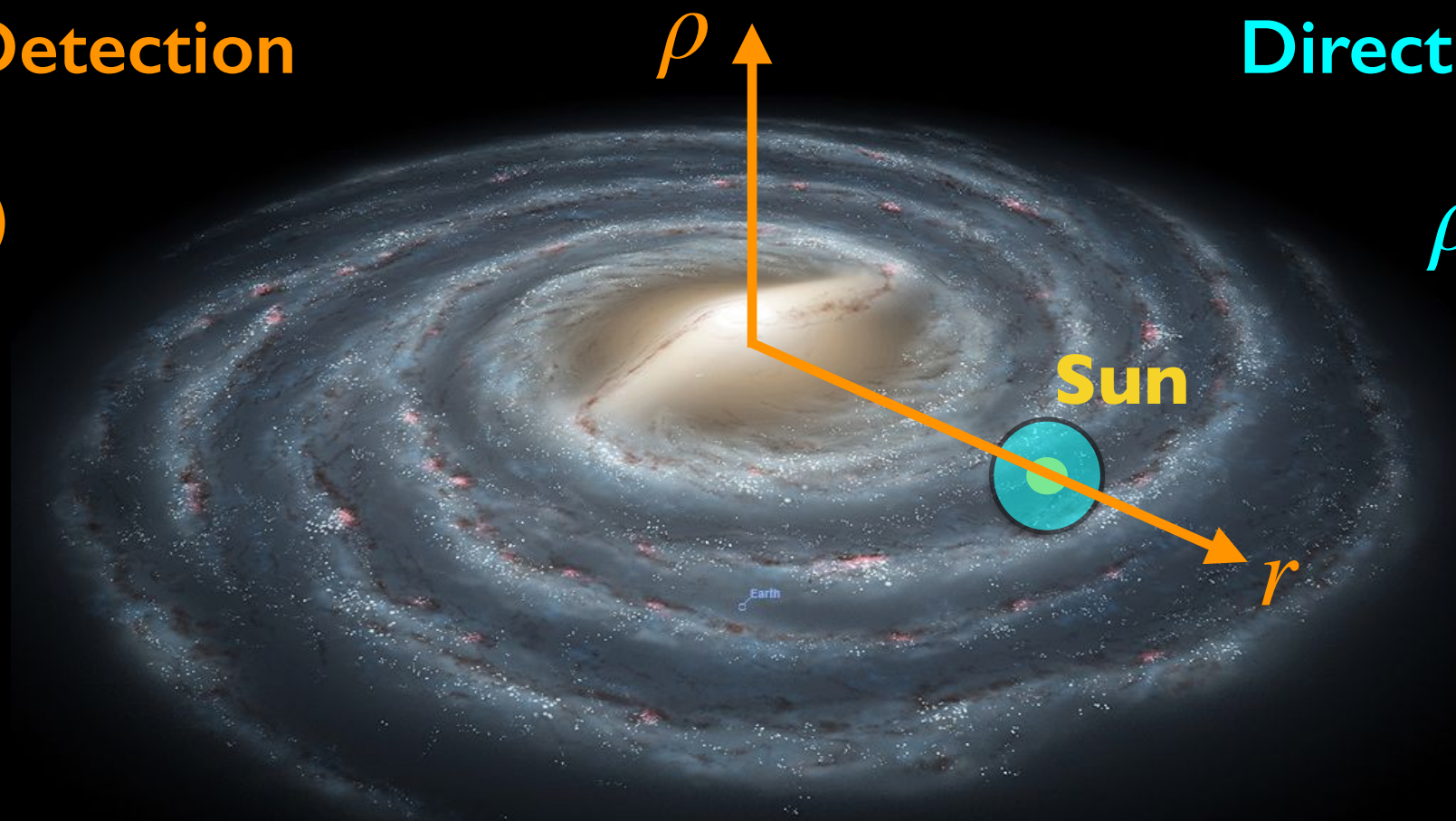
*Signals in direct and indirect dark matter (DM) searches strongly depend on the DM distribution in our Galaxy.*

**Indirect Detection**

$$\rho(r)$$

**Direct Detection**

$$\rho_\chi, f(\mathbf{v})$$



- Extract the DM distribution from high resolution cosmological simulations to make accurate predictions for DM searches.

# Prospects for direct DM searches

# Astrophysical inputs

$$\frac{dR}{dE_R} = \frac{\rho_\chi}{m_\chi m_N} \int_{v > v_{\min}} d^3v \frac{d\sigma_{\chi N}}{dE_R} v f_{\text{det}}(\mathbf{v}, t)$$

astrophysics

# Astrophysical inputs

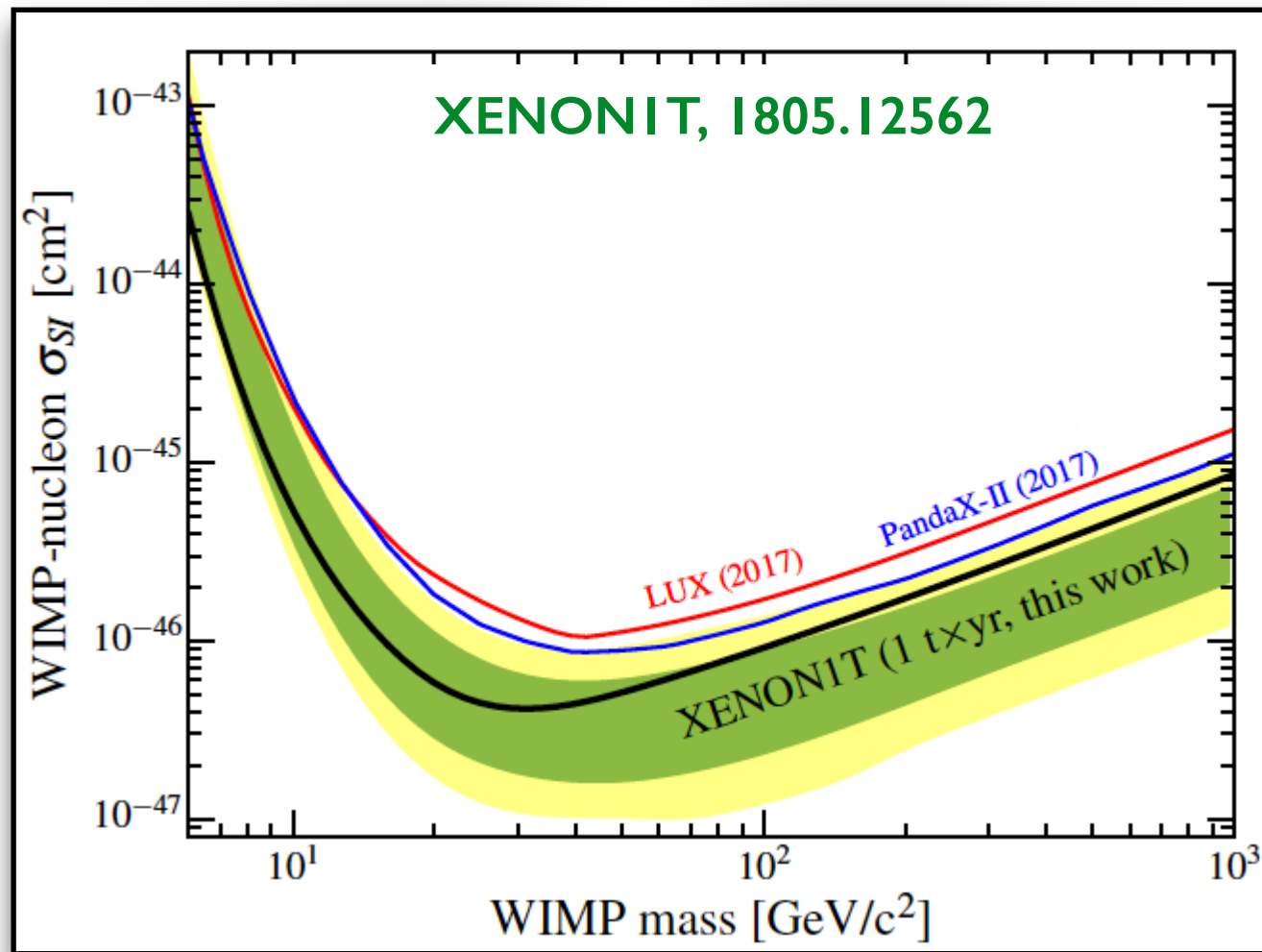
$$\frac{dR}{dE_R} = \frac{\rho_\chi}{m_\chi m_N} \int_{v > v_{\min}} d^3v \frac{d\sigma_{\chi N}}{dE_R} v f_{\text{det}}(\mathbf{v}, t)$$

astrophysics

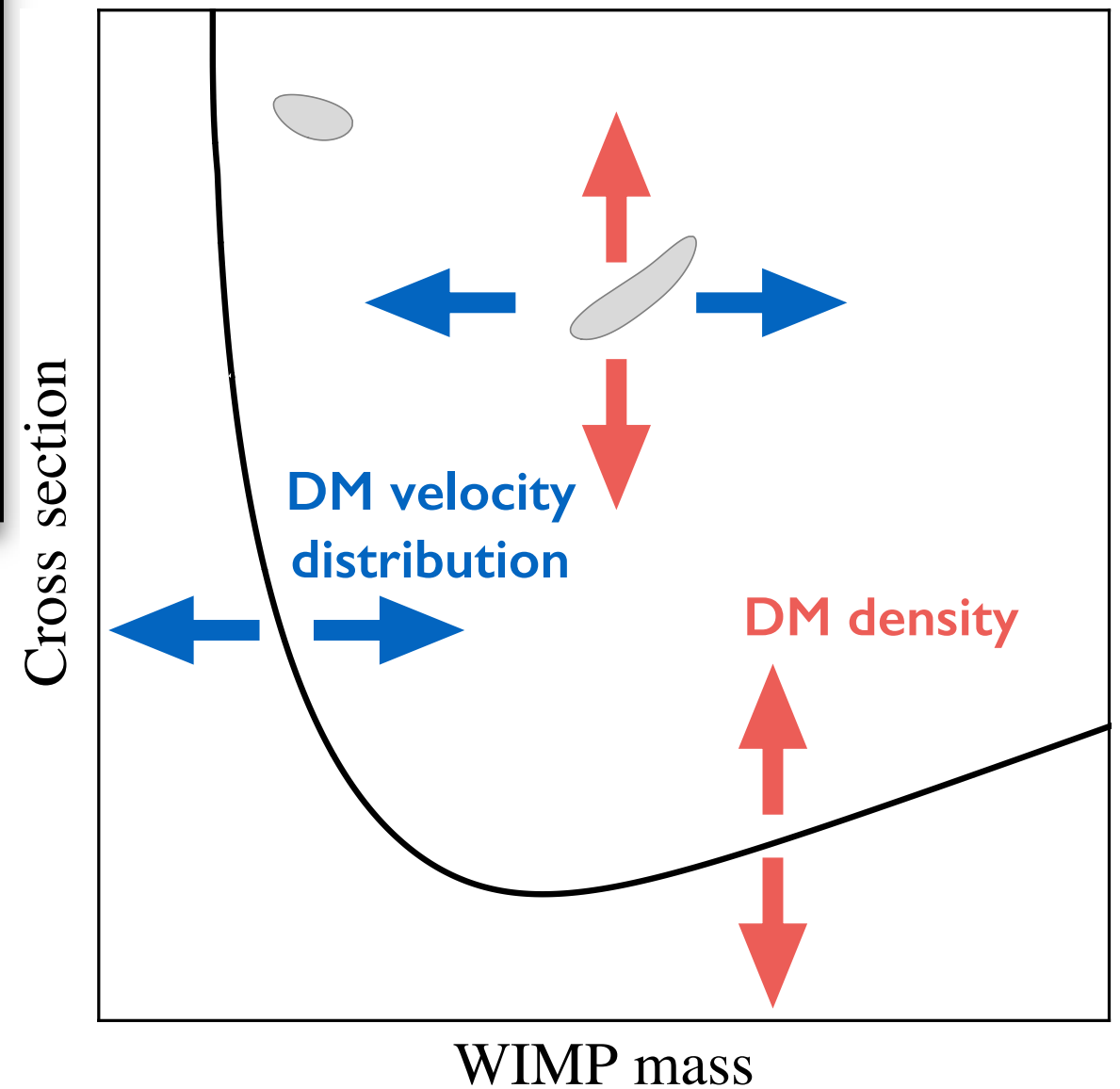
- **Standard Halo model (SHM)**: isothermal sphere with an isotropic Maxwell-Boltzmann velocity distribution with a **peak speed** equal to the **local circular speed** ( $\sim 220$  km/s).

$$f_{\text{gal}}(\mathbf{v}) = \begin{cases} N \exp(-\mathbf{v}^2 / v_c^2) & v < v_{\text{esc}} \\ 0 & v \geq v_{\text{esc}} \end{cases}$$

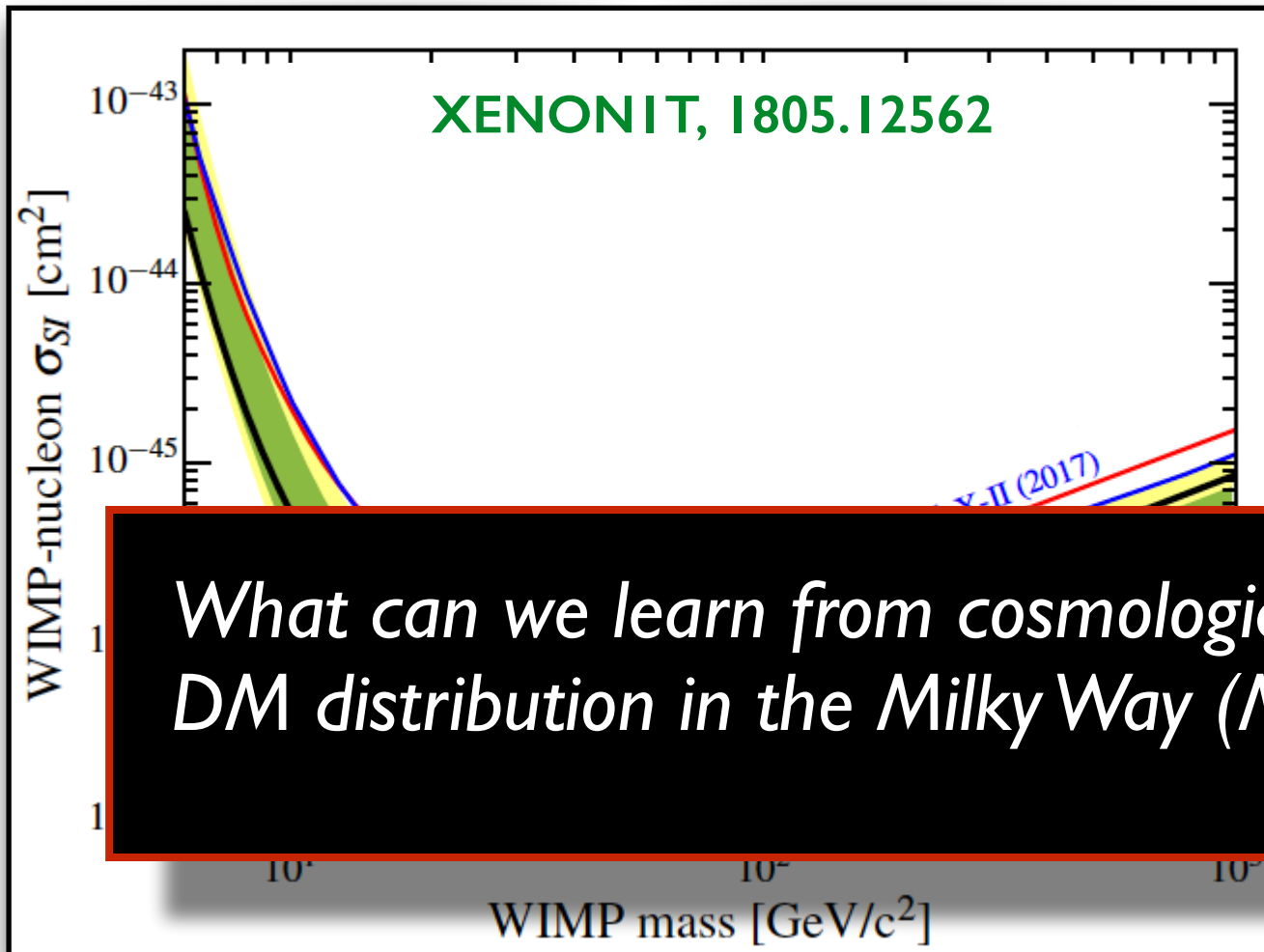
# Astrophysical inputs



Assumption: **SHM**

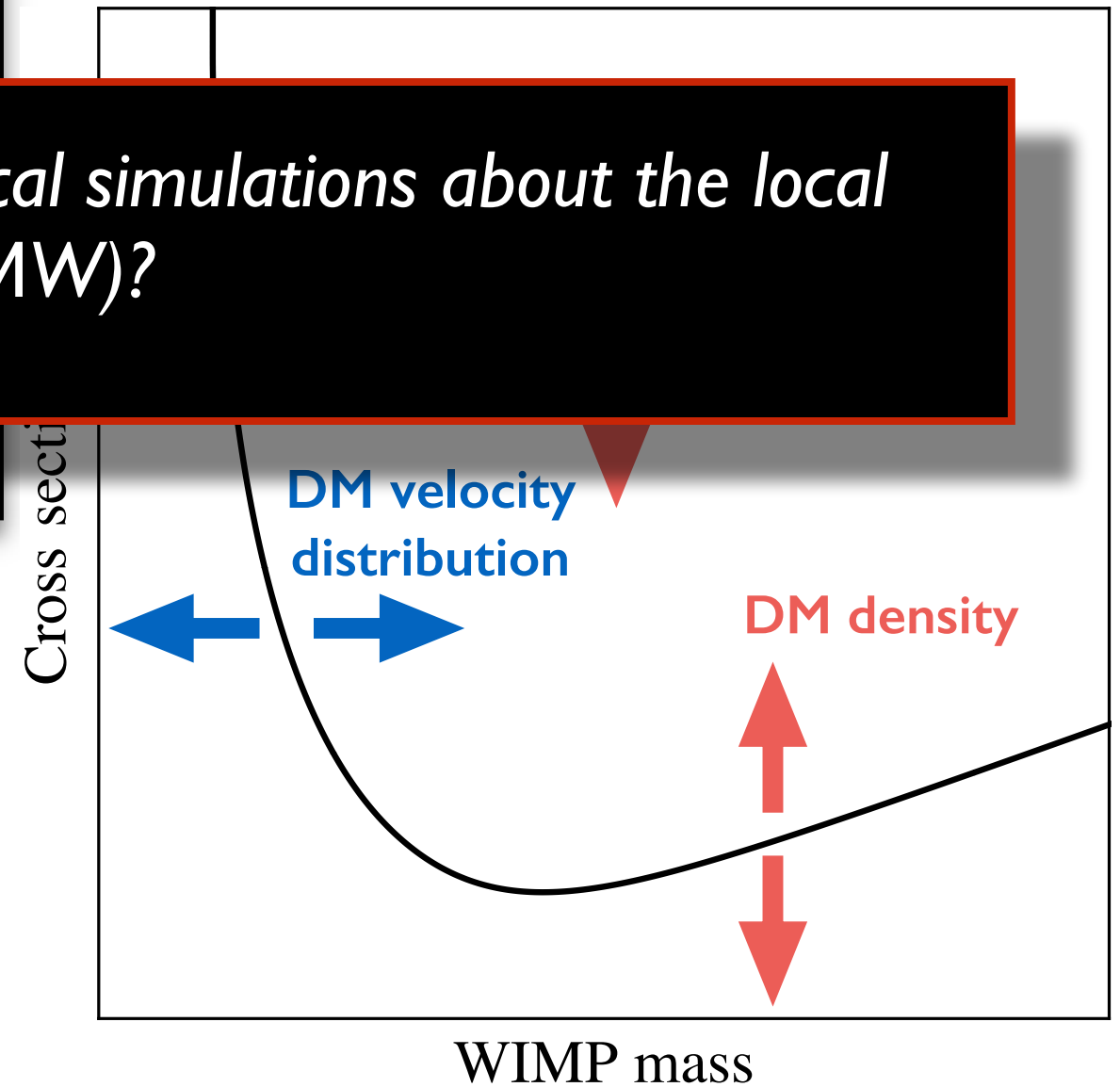


# Astrophysical inputs



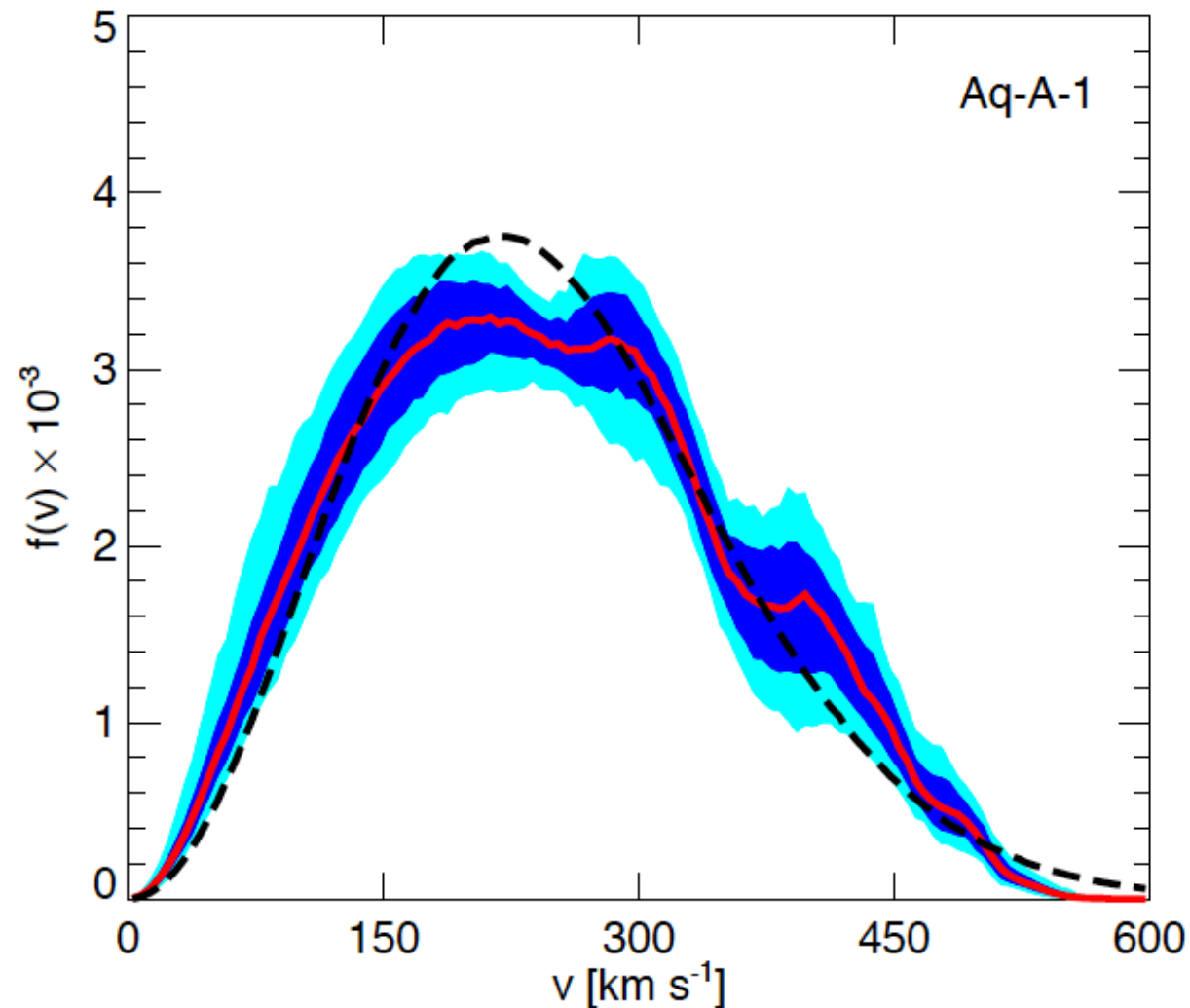
*What can we learn from cosmological simulations about the local DM distribution in the Milky Way (MW)?*

Assumption: **SHM**



# Dark Matter only simulations

- DM speed distributions from cosmological N-body simulations **without baryons**, deviate substantially from a Maxwellian.



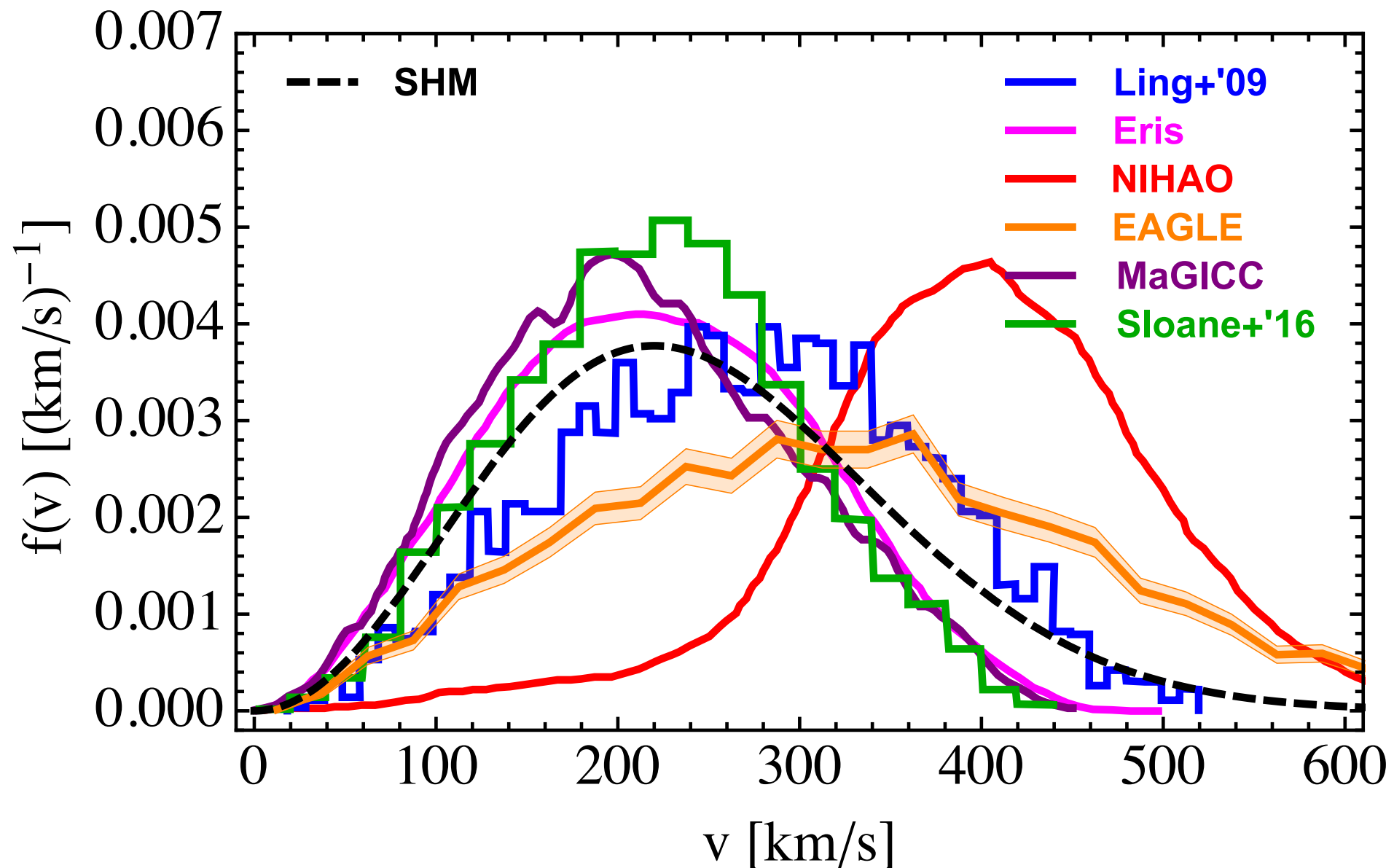
$$f(|\mathbf{v}|) = v^2 \int d\Omega_{\mathbf{v}} f(\mathbf{v})$$

Vogelsberger et al., 0812.0362

- Significant systematic uncertainty since the impact of baryons neglected.*

# Hydrodynamical simulations

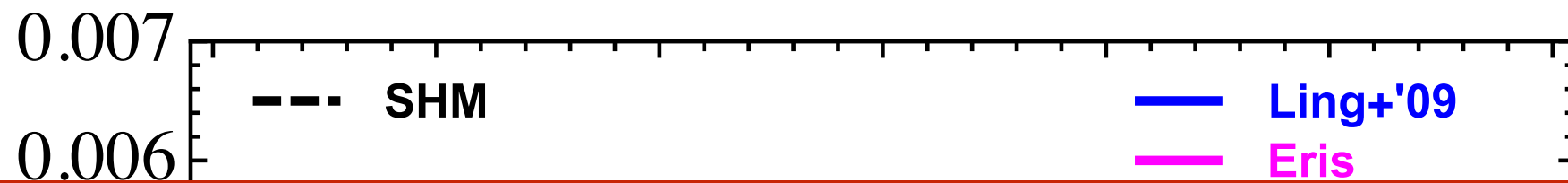
- Each hydrodynamical (**DM + baryons**) simulation adopts a different *galaxy formation model, spatial resolution, particle mass*.



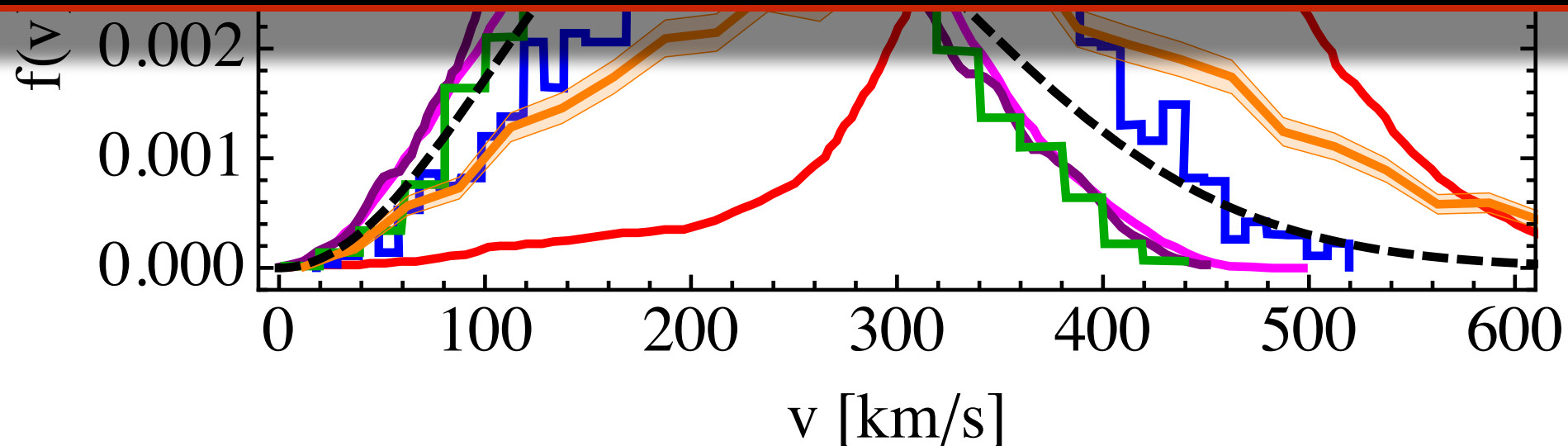
Bozorgnia & Bertone, 1705.05853

# Hydrodynamical simulations

- Each hydrodynamical (**DM + baryons**) simulation adopts a different *galaxy formation model, spatial resolution, particle mass*.



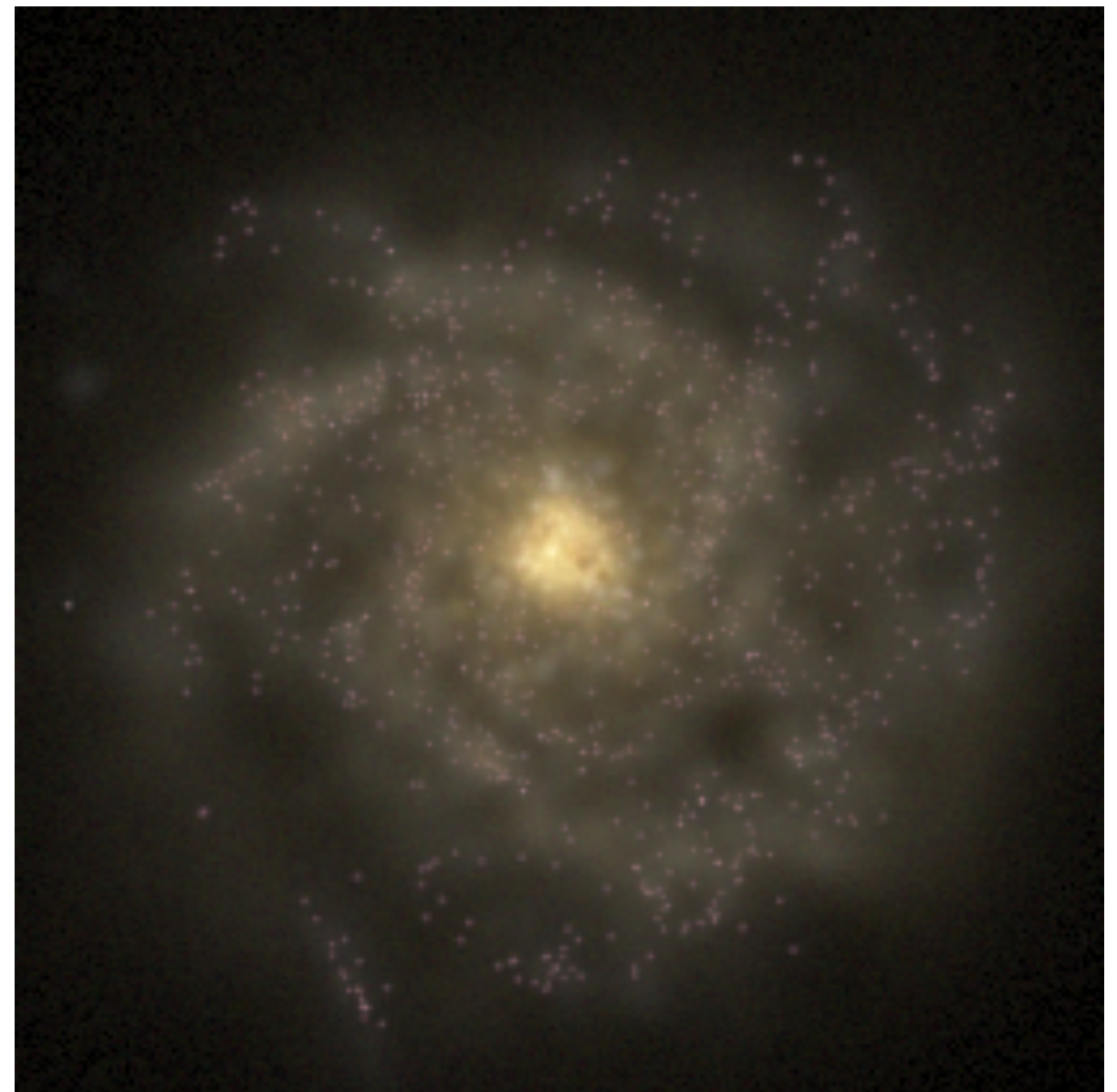
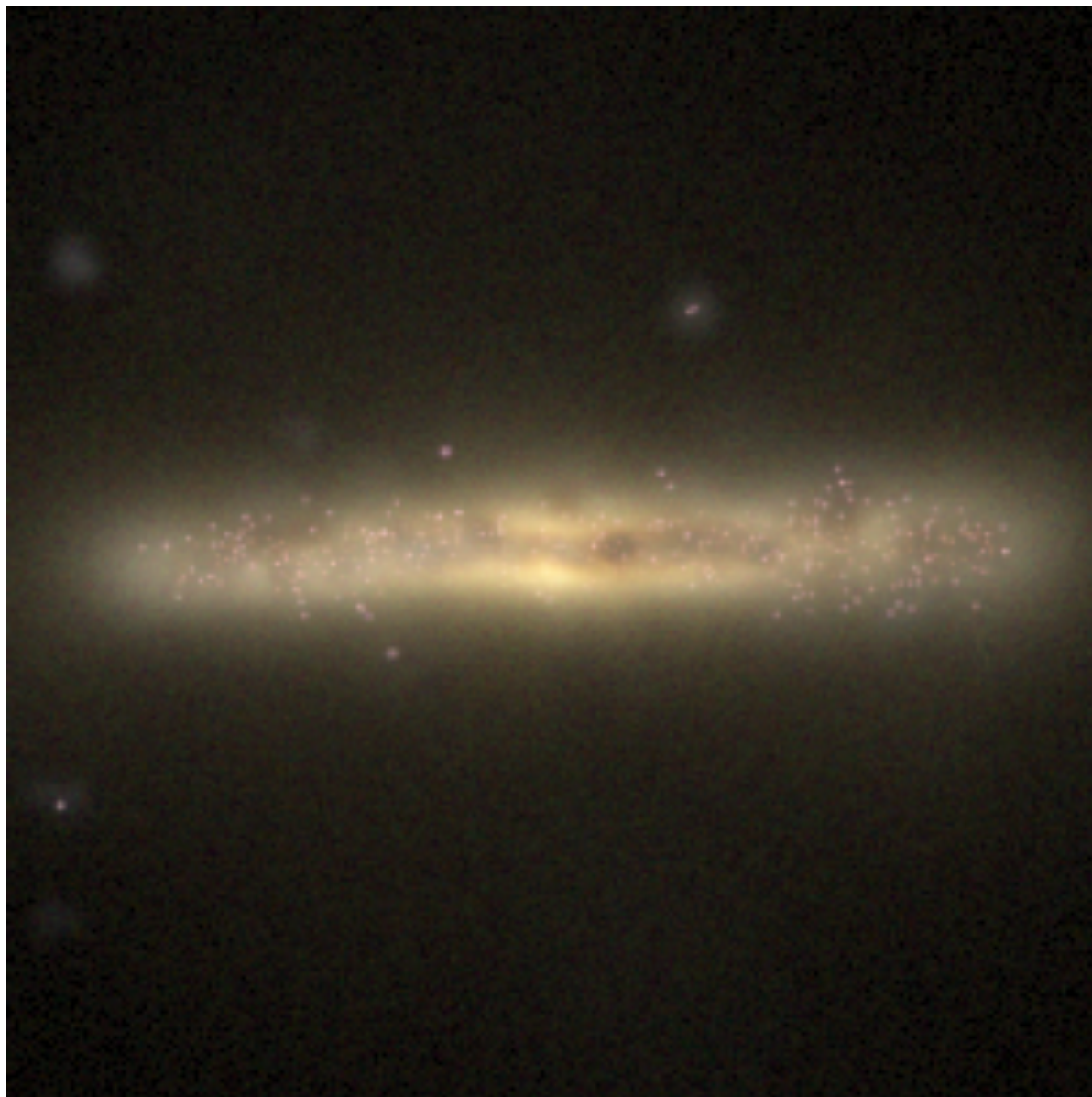
Different criteria used to identify MW-like galaxies among different groups. The most common criterion is the MW mass constraint, which has a large uncertainty.



Bozorgnia & Bertone, 1705.05853

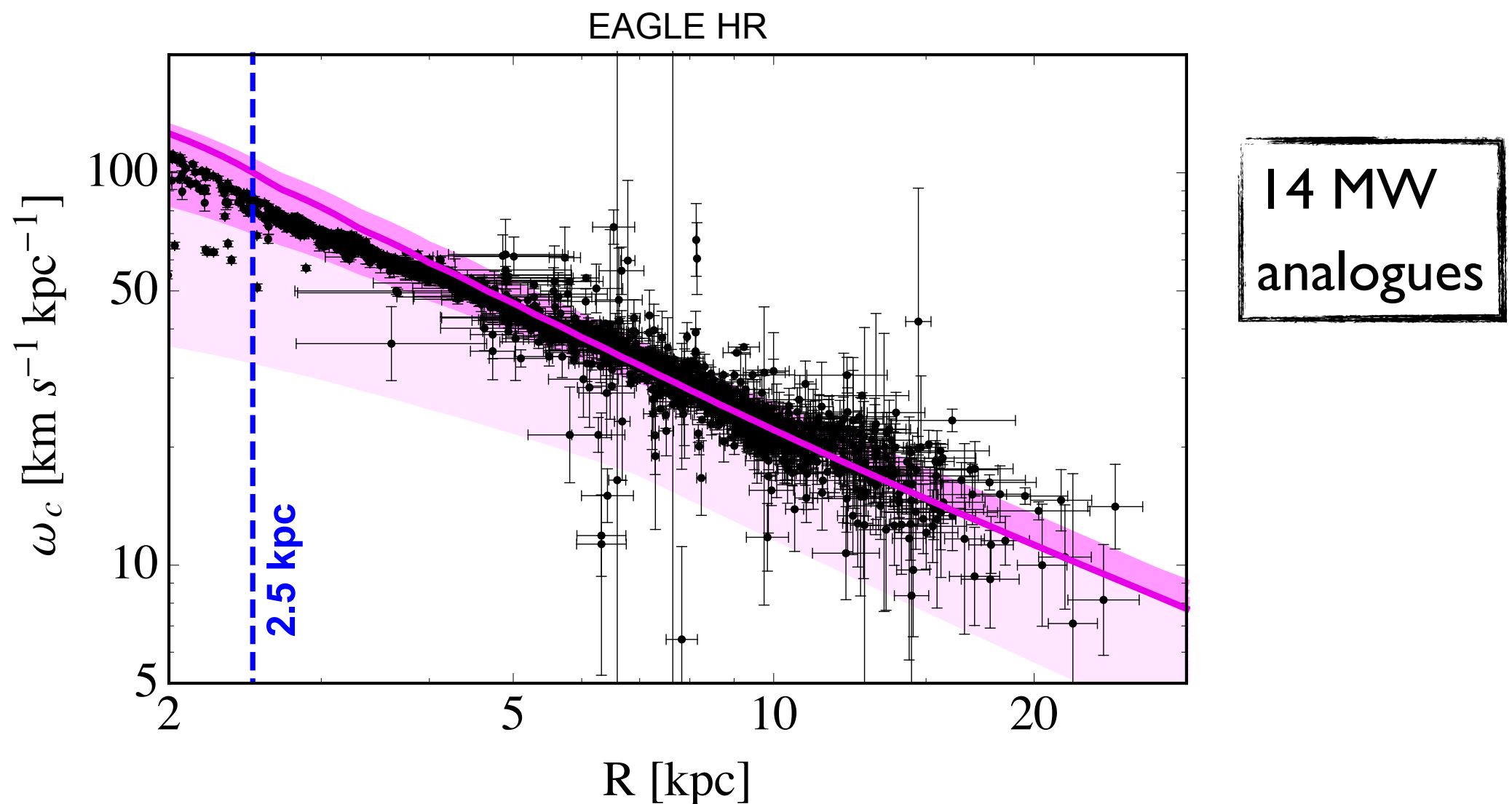
# EAGLE and APOSTLE

- We use the **EAGLE** and **APOSTLE** hydrodynamic simulations. *Calibrated to reproduce the observed distribution of stellar masses and sizes of low-redshift galaxies.*



# Identifying Milky Way analogues

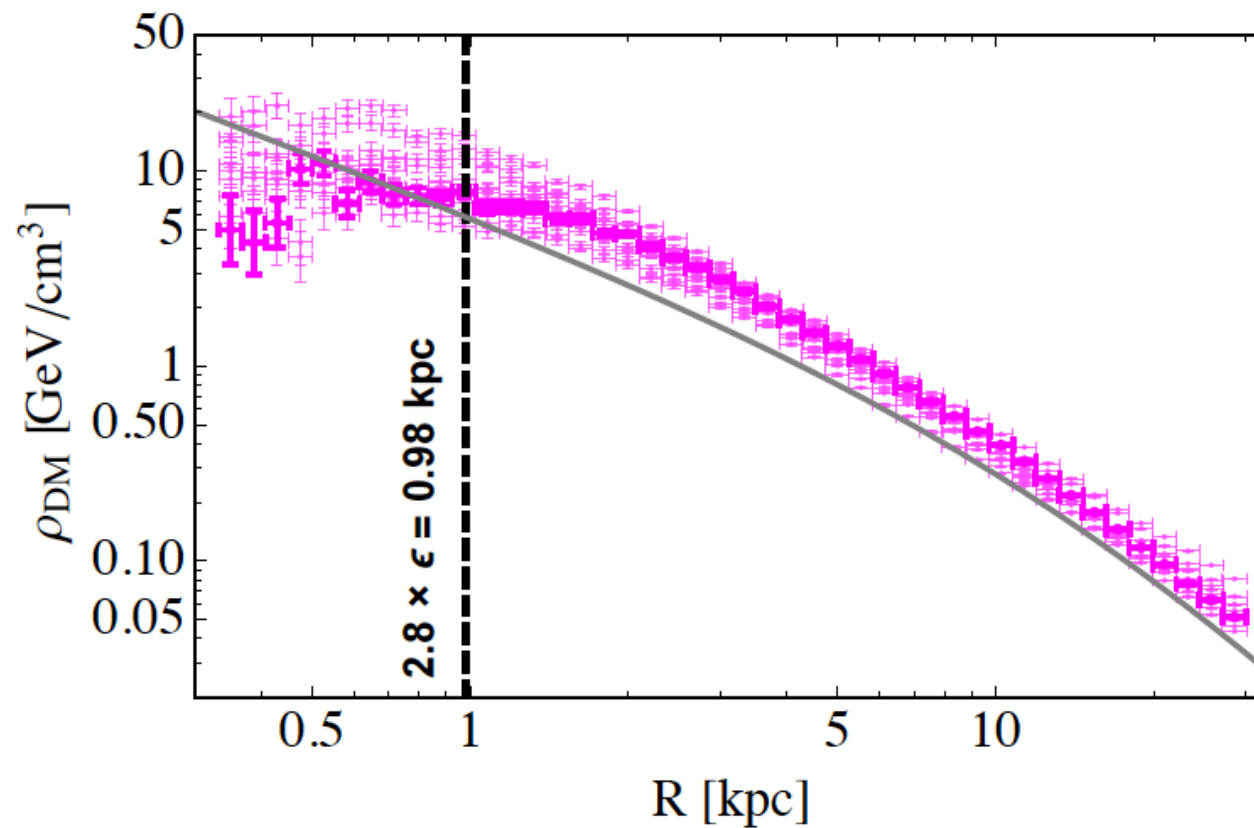
- Identify MW-like galaxies by taking into account observational constraints on the MW, in addition to the mass constraint:  
**rotation curves** [Iocco, Pato, Bertone, 1502.03821], **total stellar mass**.



Bozorgnia et al., 1601.04707  
Calore, Bozorgnia et al., 1509.02164

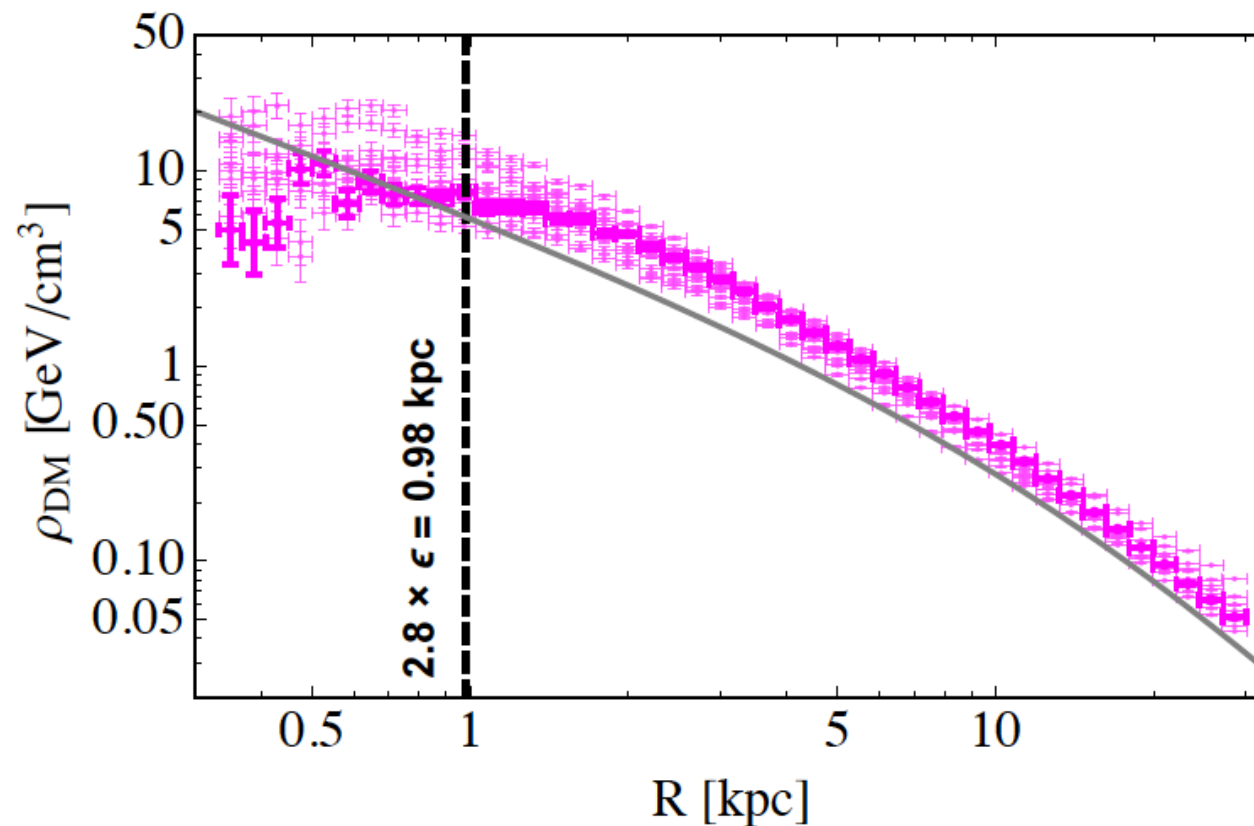
# Dark Matter density profiles

- Spherically averaged DM density profiles of the MW analogues:



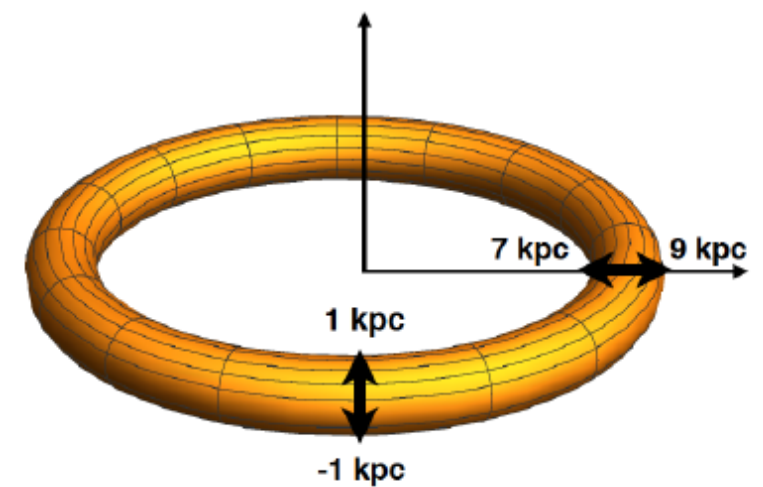
# Dark Matter density profiles

- Spherically averaged DM density profiles of the MW analogues:



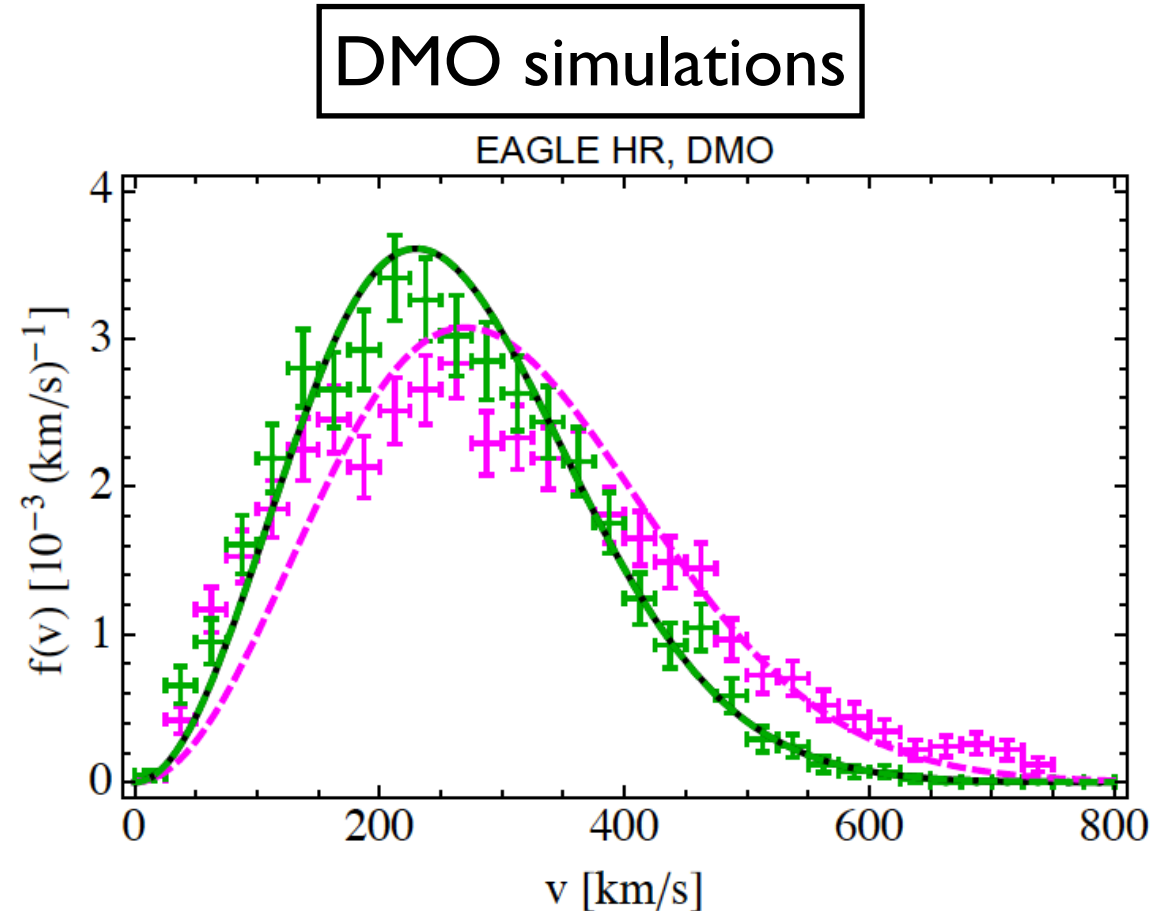
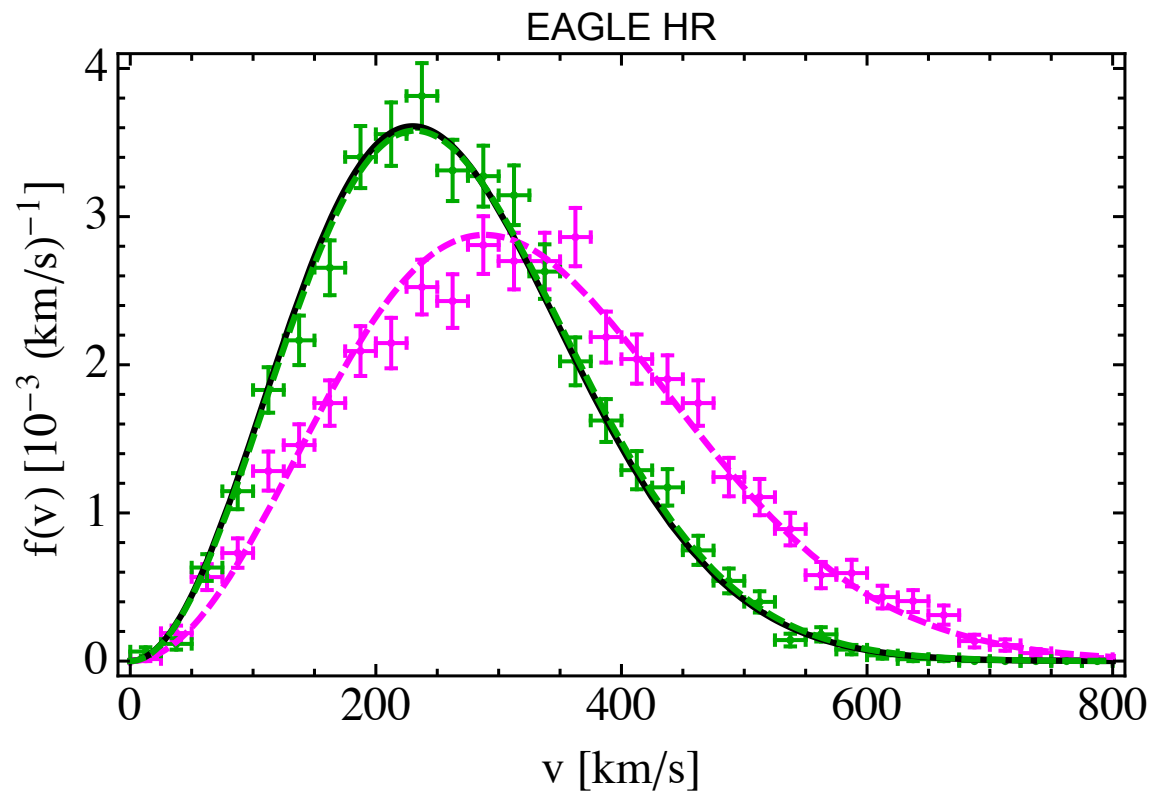
- To find the DM density at the position of the Sun, consider a torus aligned with the stellar disc.

$$\rho_{\chi} = 0.41 - 0.73 \text{ GeV}/\text{cm}^3$$



# Local speed distributions

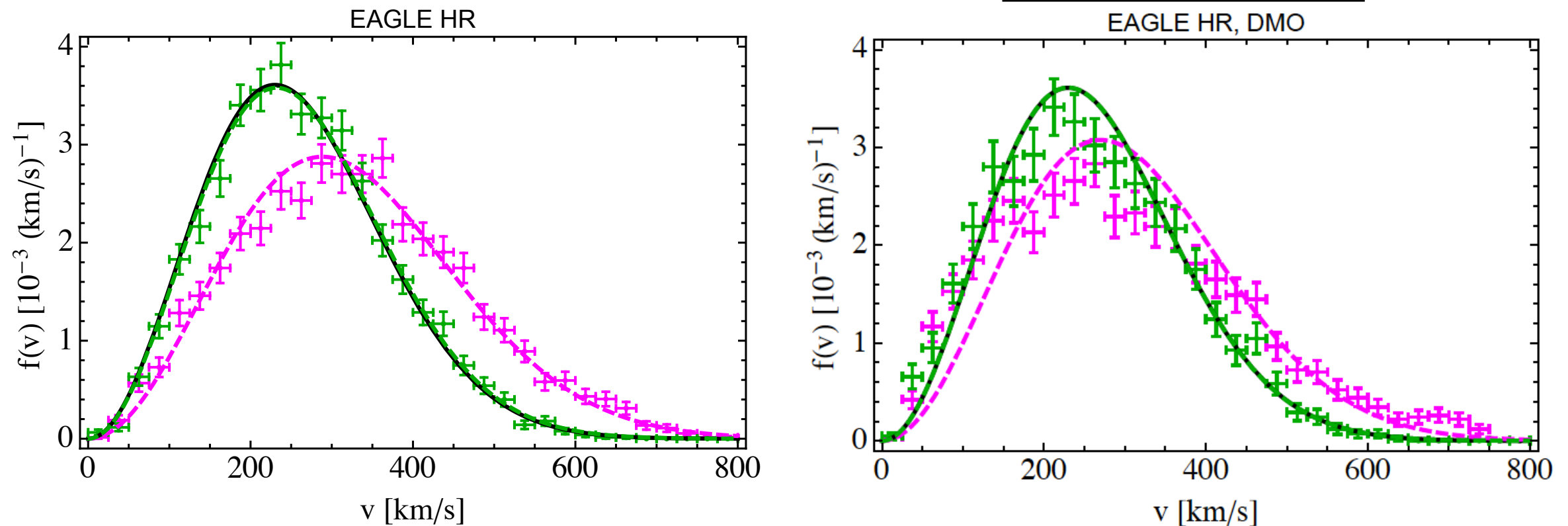
In the galactic rest frame:



Bozorgnia et al., 1601.04707

# Local speed distributions

In the galactic rest frame:



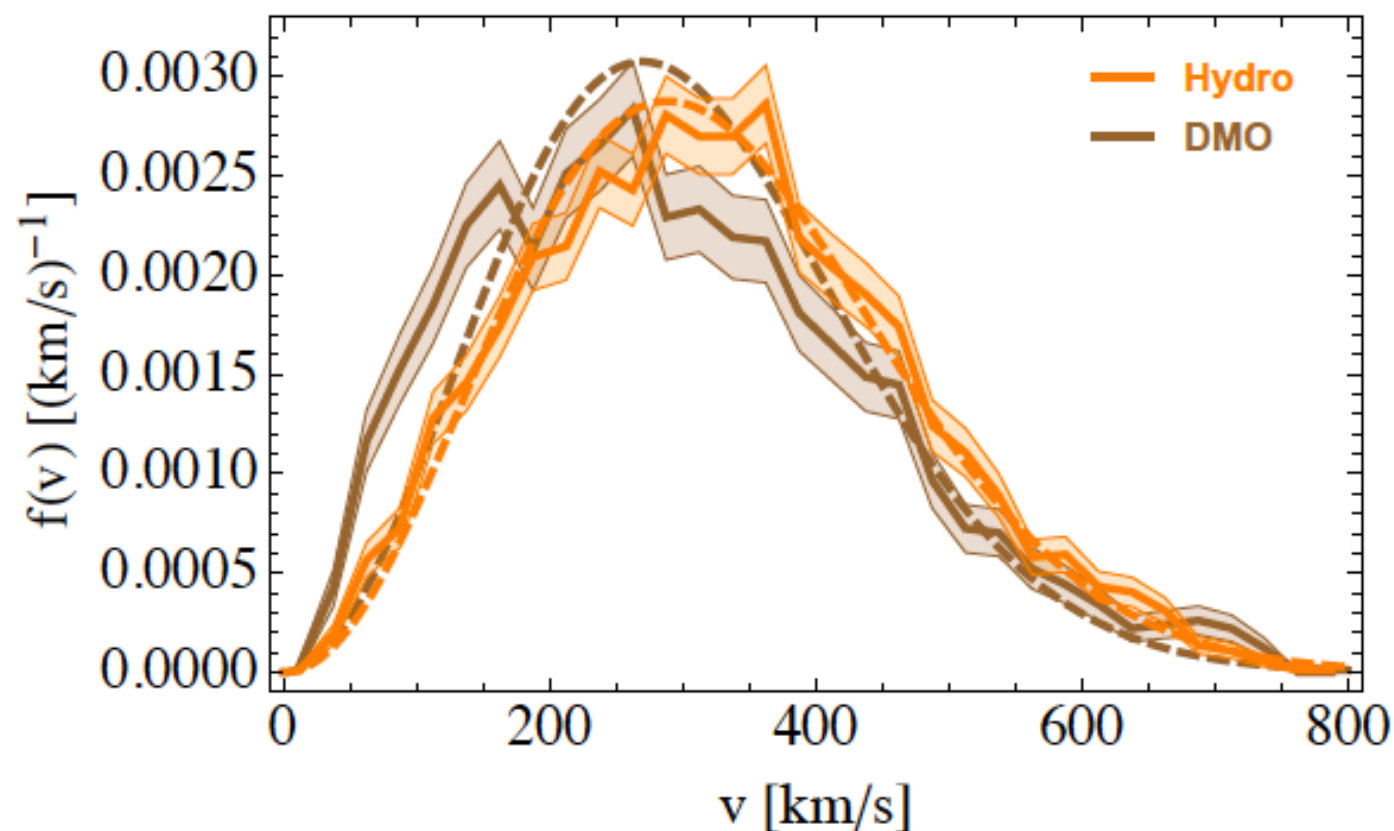
Bozorgnia et al., 1601.04707

- Maxwellian distribution with a free peak provides a better fit to haloes in the hydrodynamical simulations compared to their DMO counterparts.
- Best fit peak speed:  $v_{\text{peak}} = 223 - 289 \text{ km/s}$

# Local speed distributions

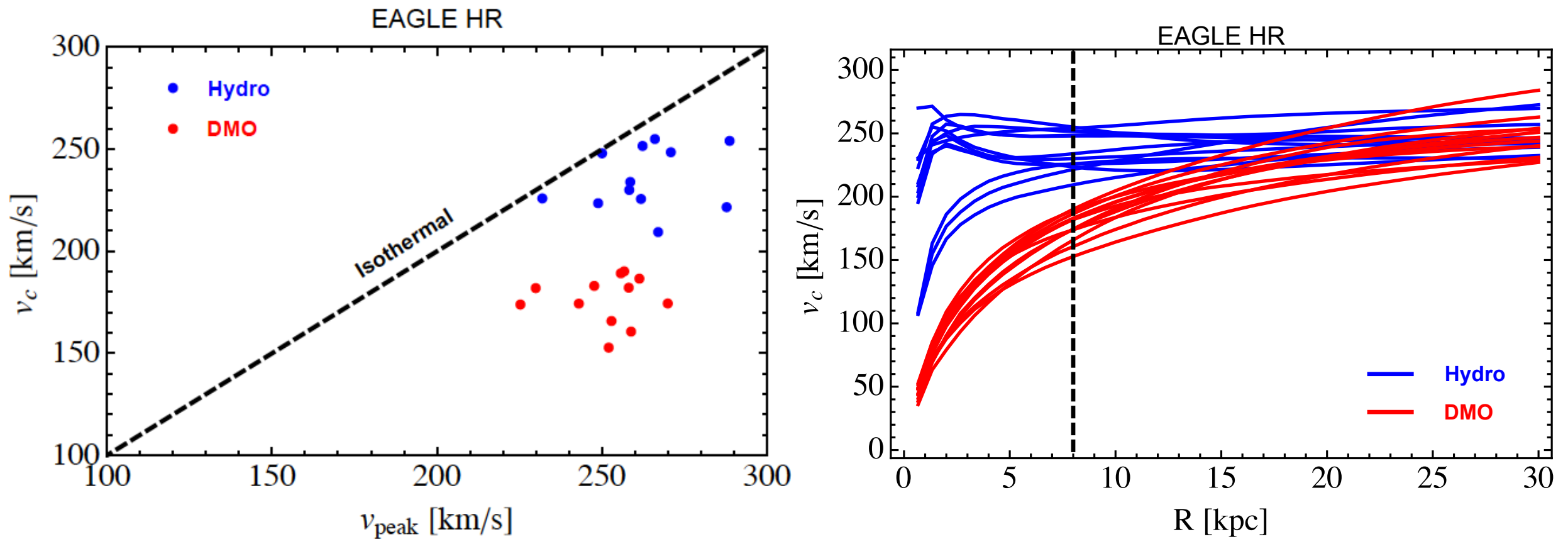
## Common trends in different hydrodynamical simulations:

- Baryons deepen the gravitational potential in the inner halo, shifting the peak of the DM speed distribution to *higher speeds*.
- In most cases, baryons appear to make the local DM speed distribution *more Maxwellian*.



Bozorgnia & Bertone, 1705.05853

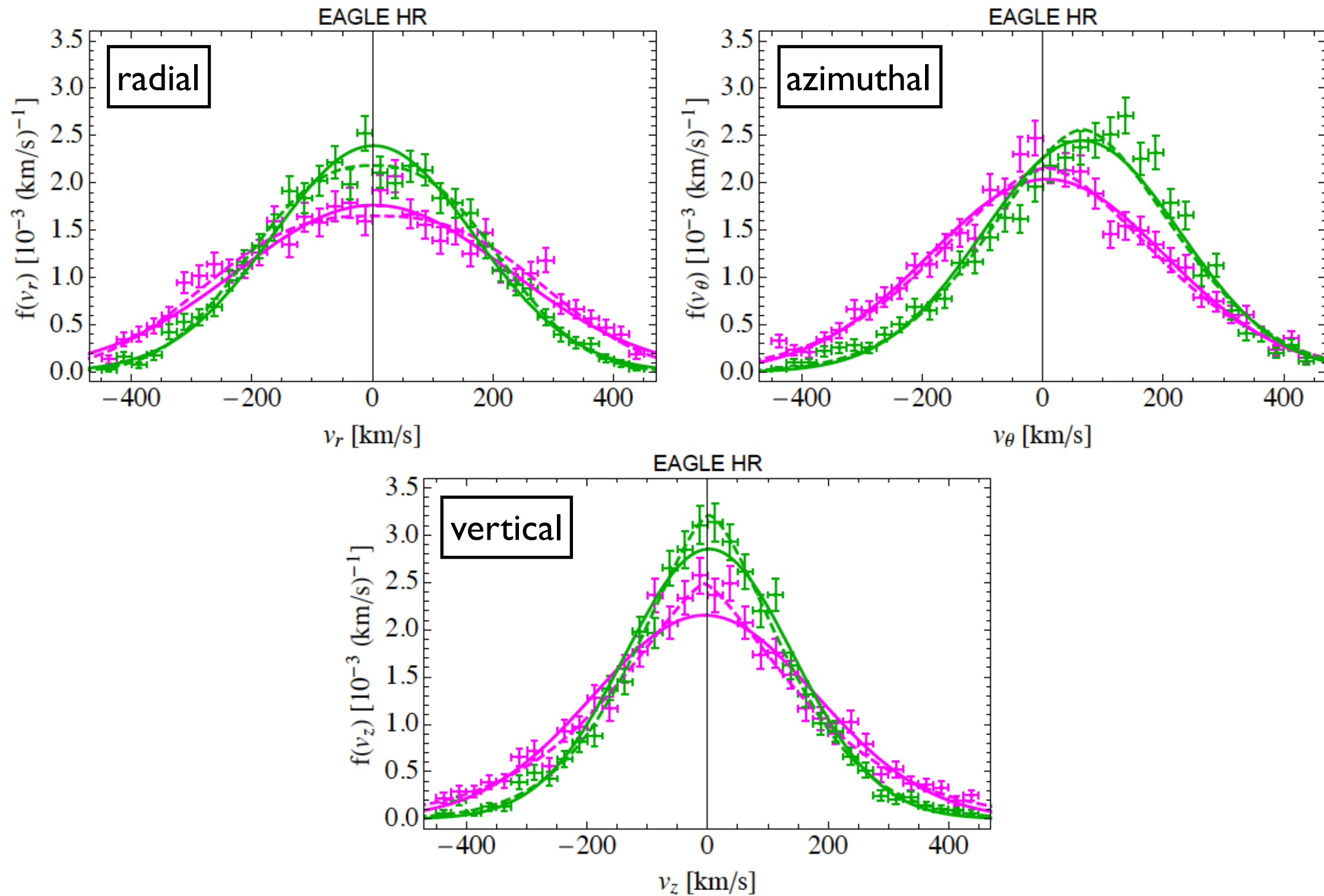
# Departure from isothermal



Bozorgnia & Bertone, 1705.05853

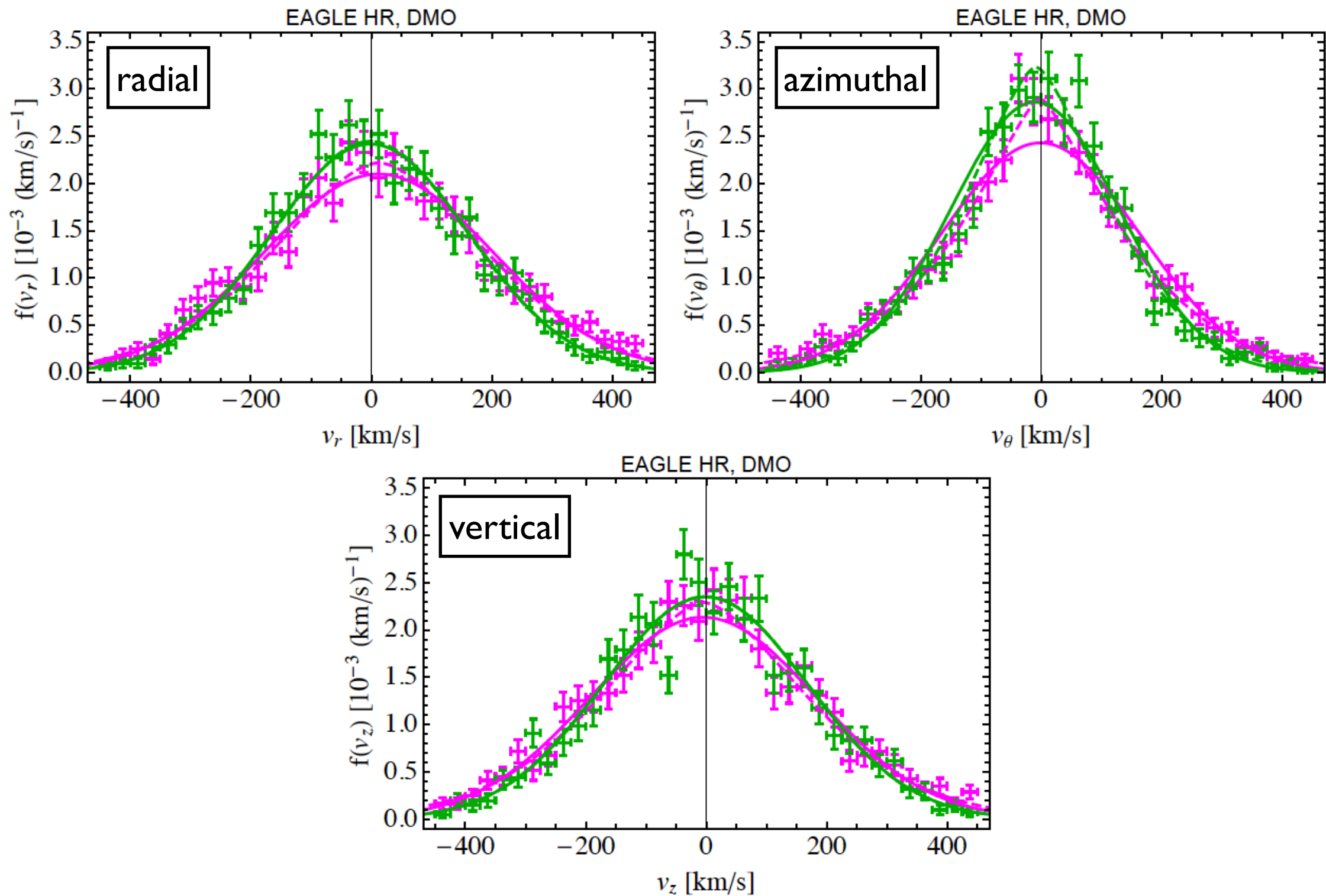
- At the Solar circle, haloes in the hydrodynamical simulation are closer to isothermal than their DMO counterparts.

# Components of the velocity distribution



Bozorgnia et al., I601.04707

# Comparison with DMO



Bozorgnia et al., [1601.04707](#)

# How common are dark disks?

- Clear velocity anisotropy at the Solar circle.
- Two haloes have a rotating DM component in the disc with mean velocity comparable (within 50 km/s) to that of the stars.

# How common are dark disks?

- Clear velocity anisotropy at the Solar circle.
- Two haloes have a rotating DM component in the disc with mean velocity comparable (within 50 km/s) to that of the stars.
- Hint for the existence of a co-rotating dark disk in 2 out of 14 MW-like haloes. → Dark disks are relatively rare in our halo sample.

Bozorgnia et al., 1601.04707

Schaller et al., 1605.02770

# How common are dark disks?

- Clear velocity anisotropy at the Solar circle.
- Two haloes have a rotating DM component in the disc with mean velocity comparable (within 50 km/s) to that of the stars.
- Hint for the existence of a co-rotating dark disk in 2 out of 14 MW-like haloes. → Dark disks are relatively rare in our halo sample.

Bozorgnia et al., 1601.04707

Schaller et al., 1605.02770

- *Sizable dark disks also rare in other hydro simulations:*
  - They only appear in simulations where a large satellite merged with the MW in the recent past, which is robustly excluded from MW kinematical data.

Bozorgnia & Bertone, 1705.05853

# The halo integral

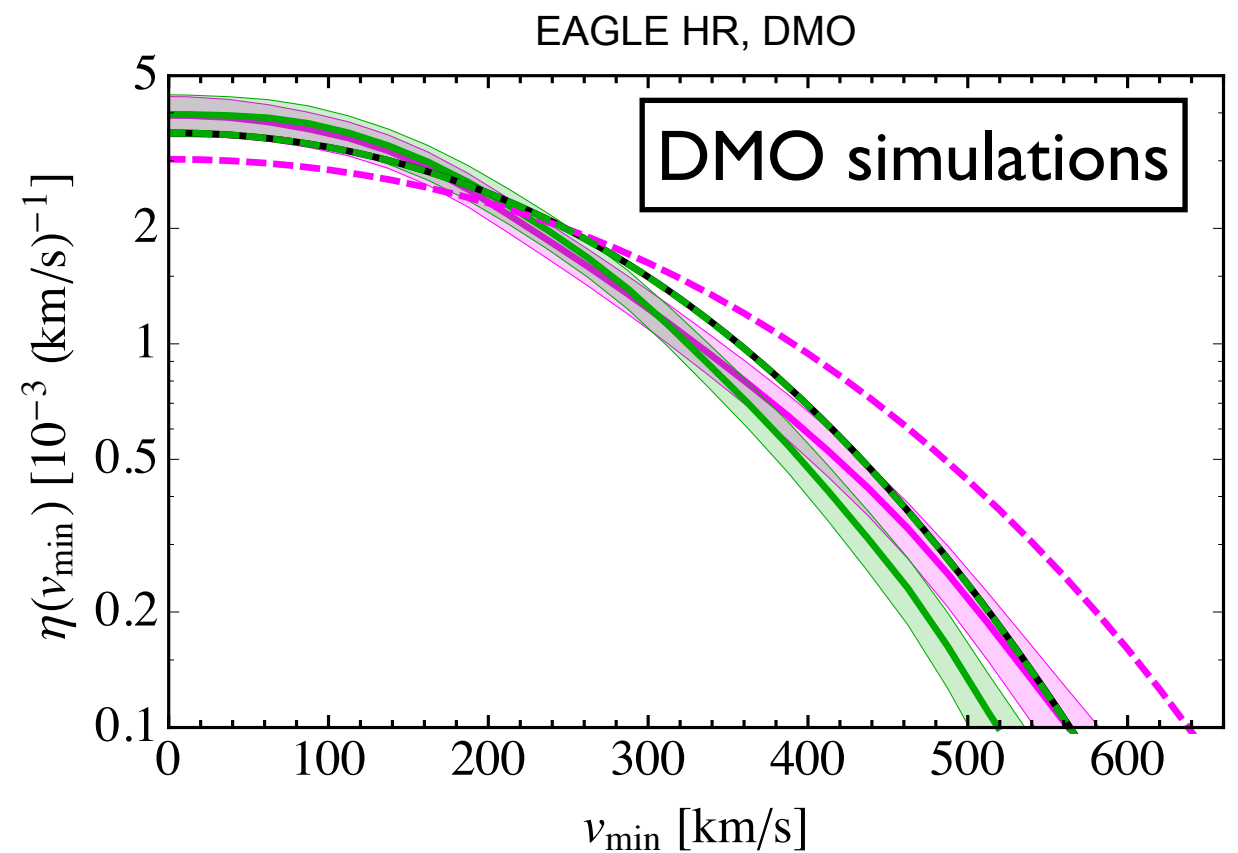
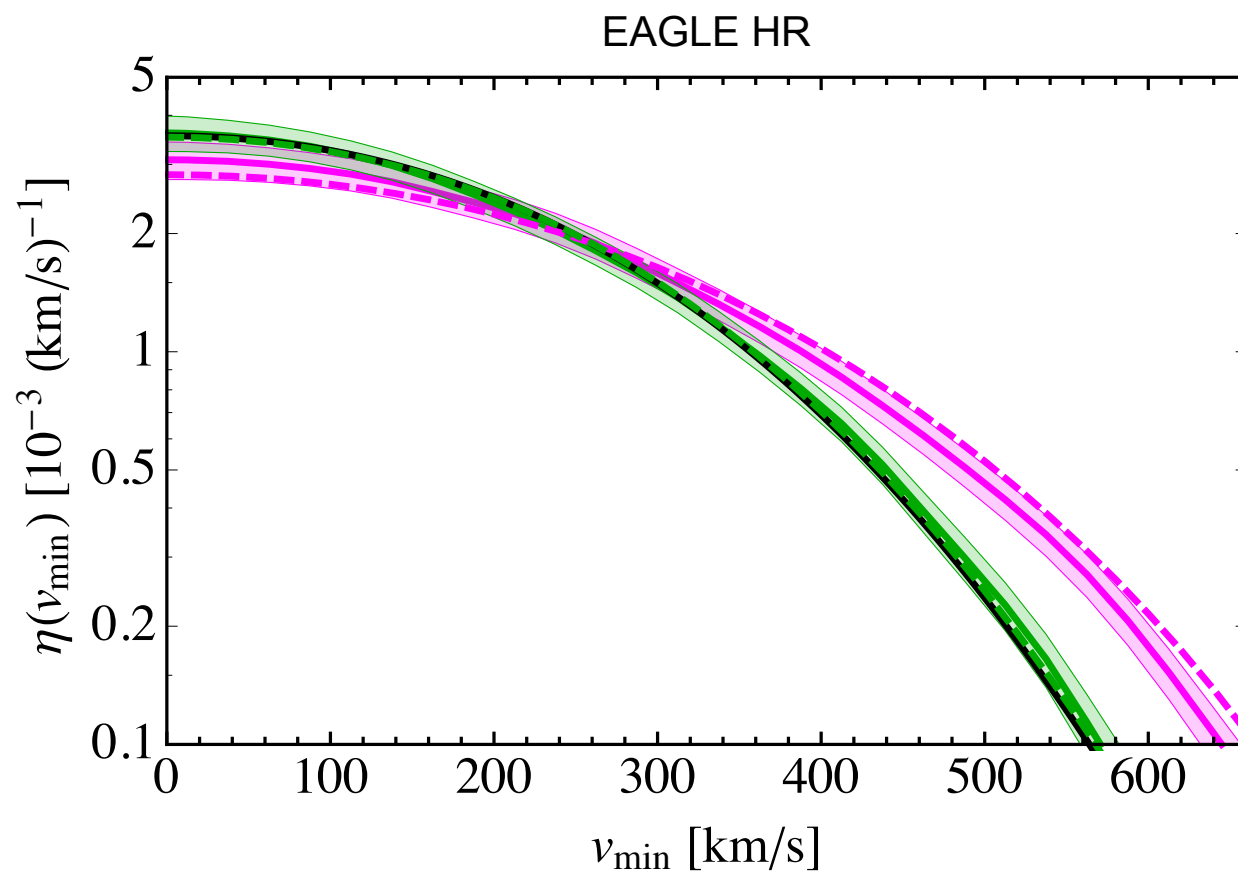
- For standard spin-independent and spin-dependent interactions:

$$\frac{dR}{dE_R} = \frac{\sigma_0 F^2(E_R)}{2m_\chi \mu_{\chi N}^2} \rho_\chi \eta(v_{\min}, t)$$

particle physics      astrophysics

$$\eta(v_{\min}, t) \equiv \int_{v > v_{\min}} d^3v \frac{f_{\text{det}}(\mathbf{v}, \mathbf{t})}{v}$$

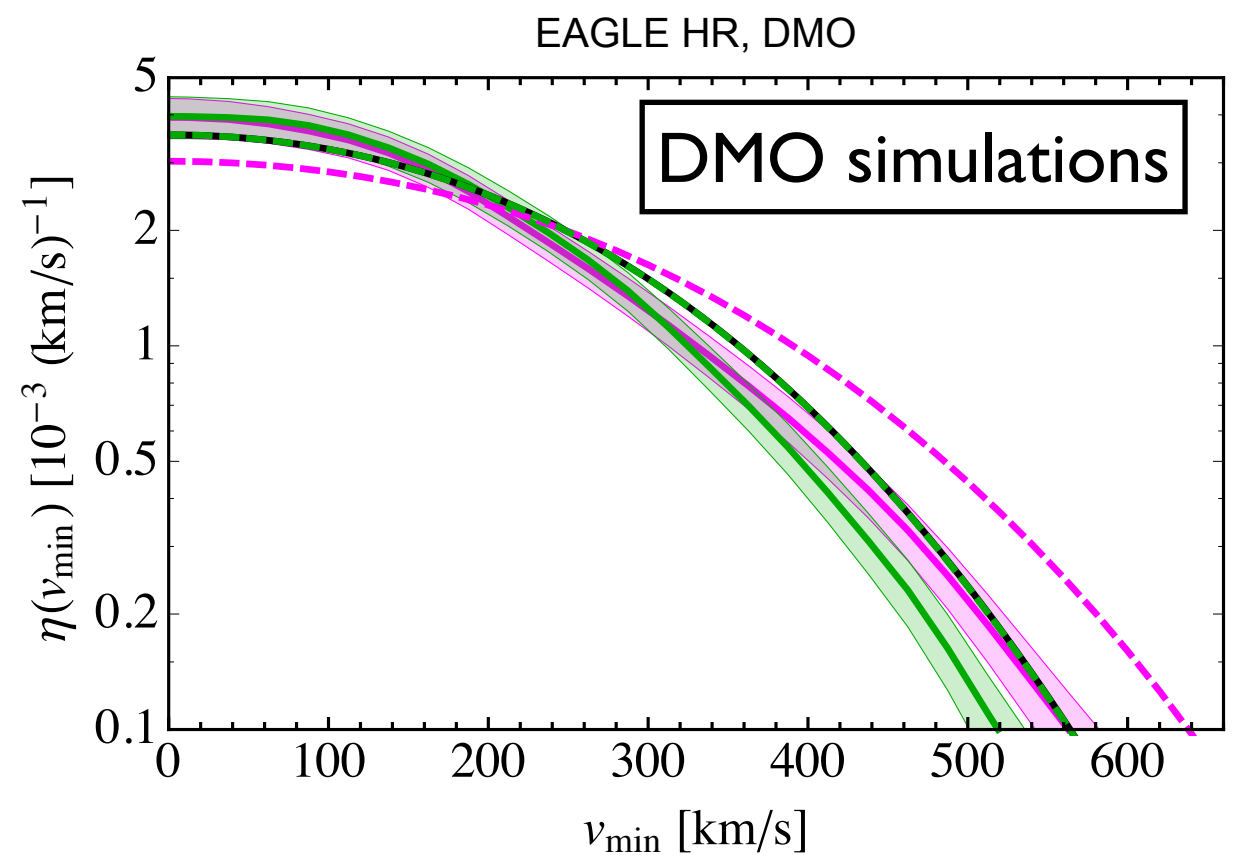
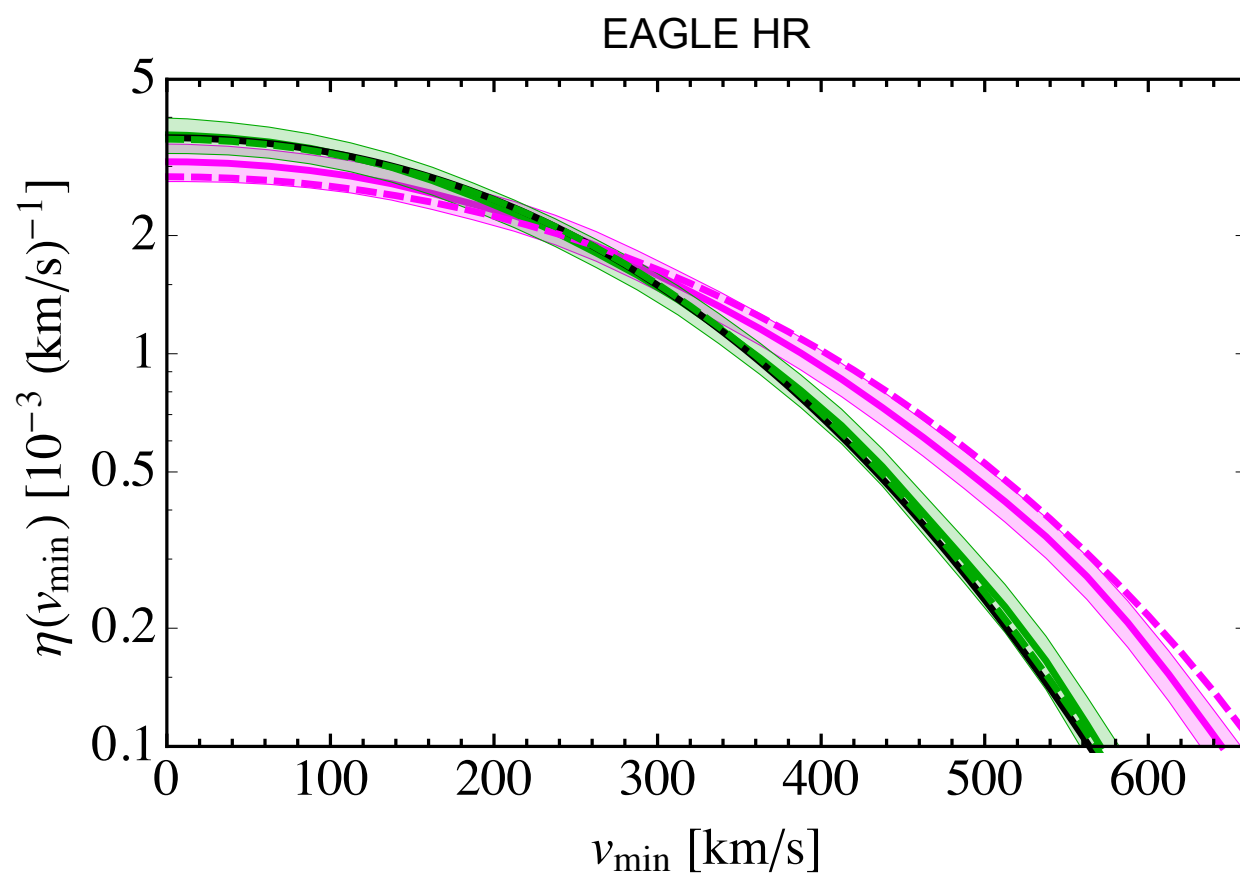
$$v_{\min} = \sqrt{m_N E_R / (2\mu_{\chi N}^2)}$$



Bozorgnia et al., 1601.04707

# The halo integral

- Halo integrals for the best fit Maxwellian velocity distribution (*peak speed 223 - 289 km/s*) fall within the  $1\sigma$  uncertainty band of the halo integrals of the simulated haloes.



Bozorgnia et al., 1601.04707

# The halo integral

## Common trend in different hydrodynamical simulations:

- Halo integrals and hence direct detection event rates obtained from a **Maxwellian velocity distribution with a free peak** are similar to those obtained directly from the simulated haloes.

Bozorgnia et al., 1601.04707 (EAGLE & APOSTLE)

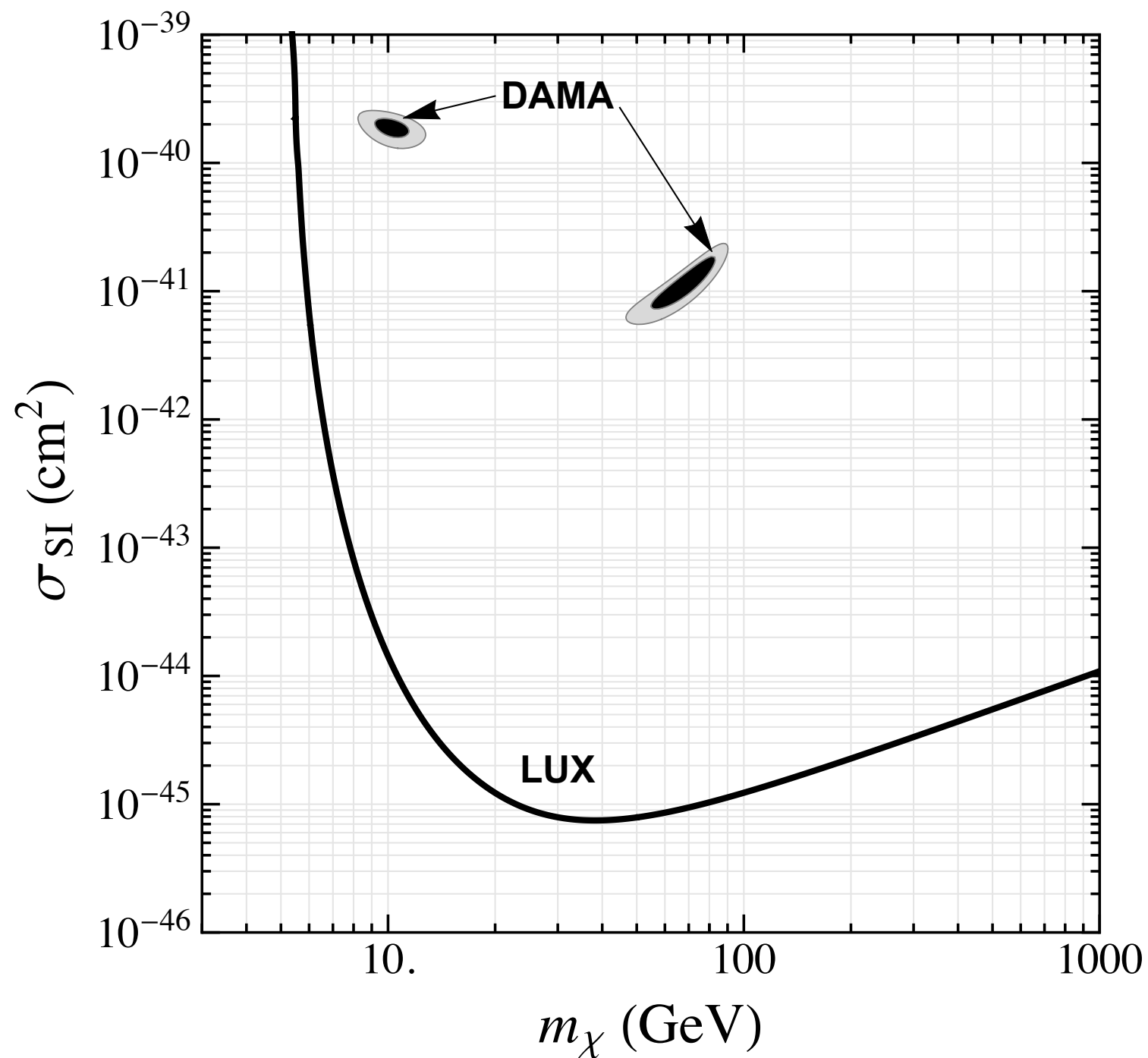
Kelso et al., 1601.04725 (MaGICC)

Sloane et al., 1601.05402

Bozorgnia & Bertone, 1705.05853

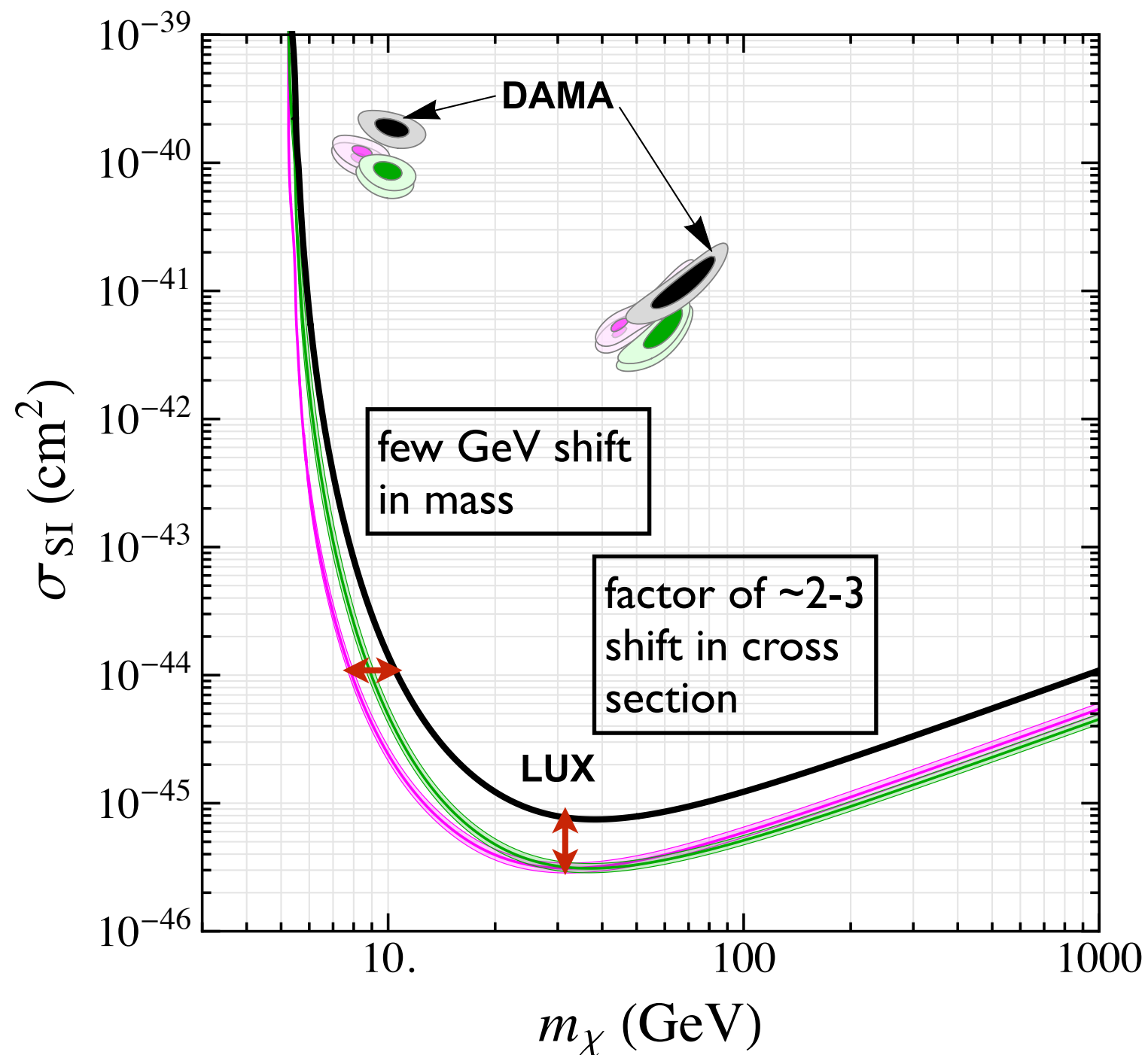
# Implications for direct detection

- Assuming the **Standard Halo Model**:

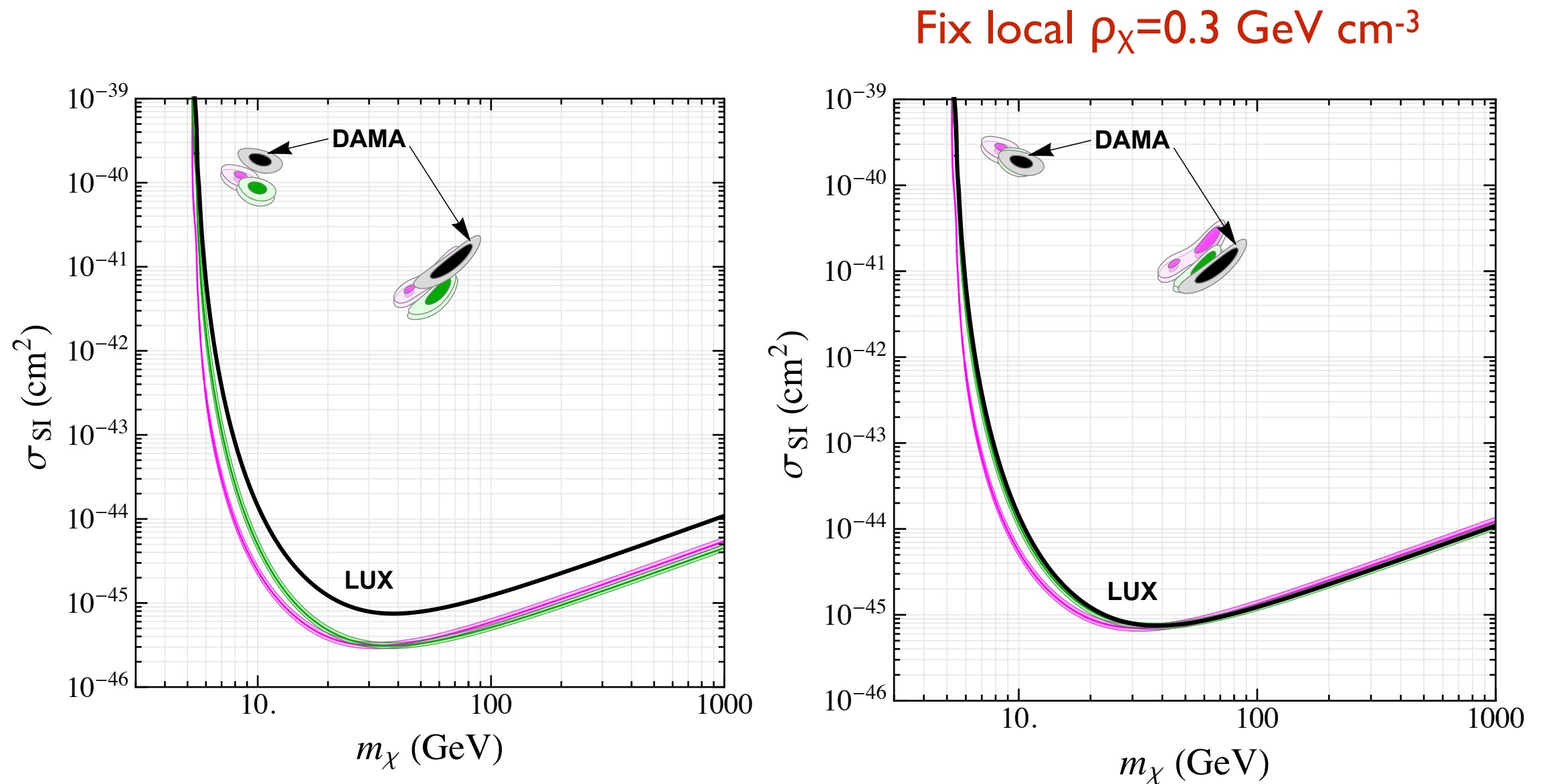


# Implications for direct detection

- Compare with simulated Milky Way-like haloes:



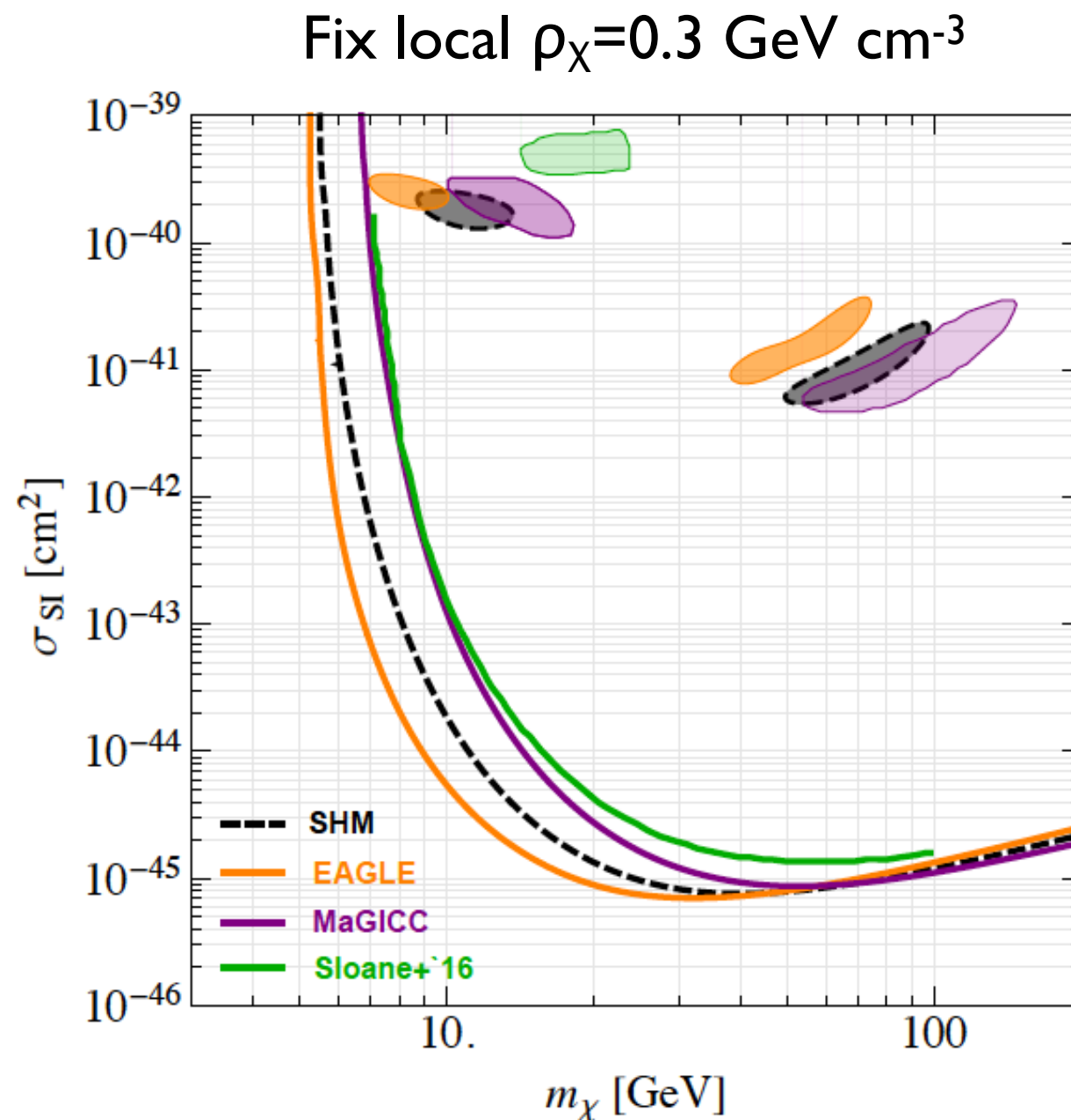
# Implications for direct detection



- Difference in the local DM density  $\rightarrow$  overall difference with the SHM.
- Variation in the peak of the DM speed distribution  $\rightarrow$  shift in the low mass region.

# Implications for direct detection

Comparison to other hydrodynamical simulations:



Bozorgnia & Bertone, 1705.05853

# Non-standard interactions

- For a very general set of non-relativistic effective operators:

Kahlhoefer & Wild, 1607.04418

$$\frac{d\sigma_{\chi N}}{dE_R} = \frac{d\sigma_1}{dE_R} \frac{1}{v^2} + \frac{d\sigma_2}{dE_R}$$

# Non-standard interactions

- For a very general set of non-relativistic effective operators:

Kahlhoefer & Wild, 1607.04418

$$\frac{d\sigma_{\chi N}}{dE_R} = \frac{d\sigma_1}{dE_R} \frac{1}{v^2} + \frac{d\sigma_2}{dE_R}$$

$\eta(v_{\min}, t)$        $h(v_{\min}, t) = \int_{v > v_{\min}} d^3v \, v \, f_{\text{det}}(\mathbf{v}, t)$

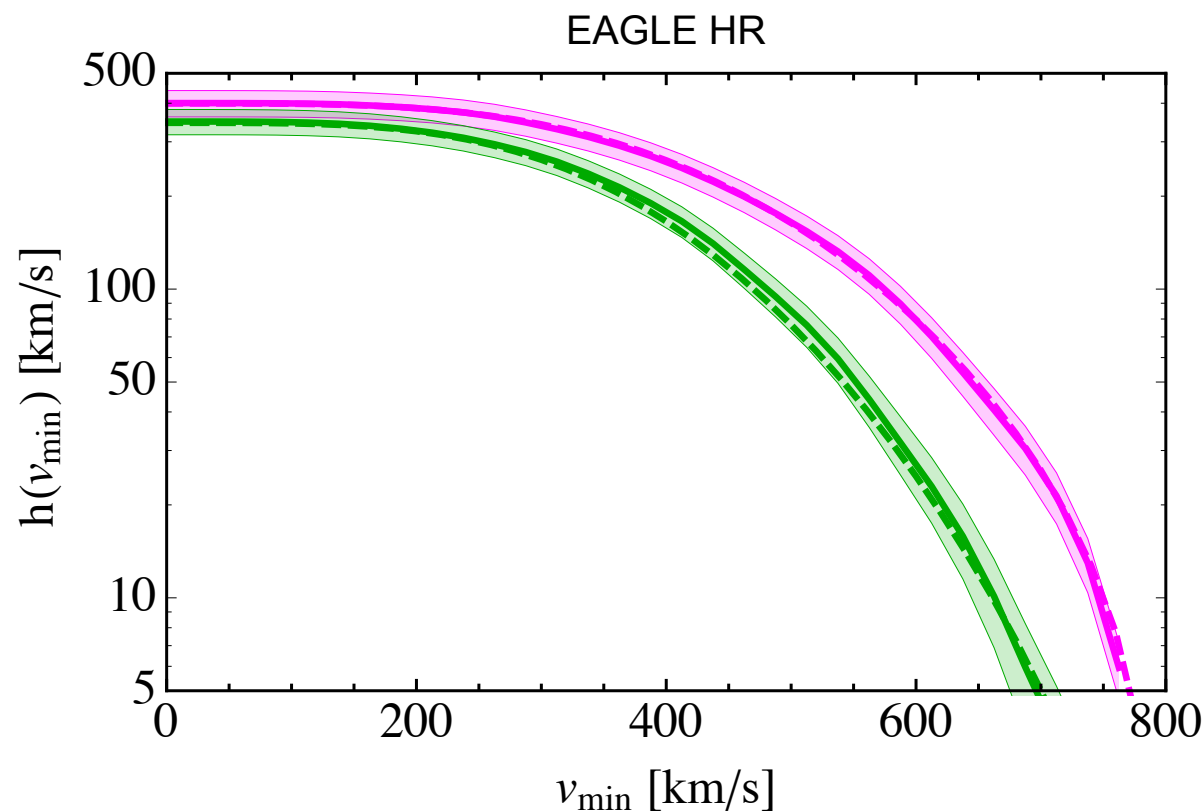
# Non-standard interactions

- For a very general set of non-relativistic effective operators:

Kahlhoefer & Wild, 1607.04418

$$\frac{d\sigma_{\chi N}}{dE_R} = \frac{d\sigma_1}{dE_R} \frac{1}{v^2} + \frac{d\sigma_2}{dE_R}$$

$\eta(v_{\min}, t)$        $h(v_{\min}, t) = \int_{v > v_{\min}} d^3v v f_{\text{det}}(\mathbf{v}, t)$



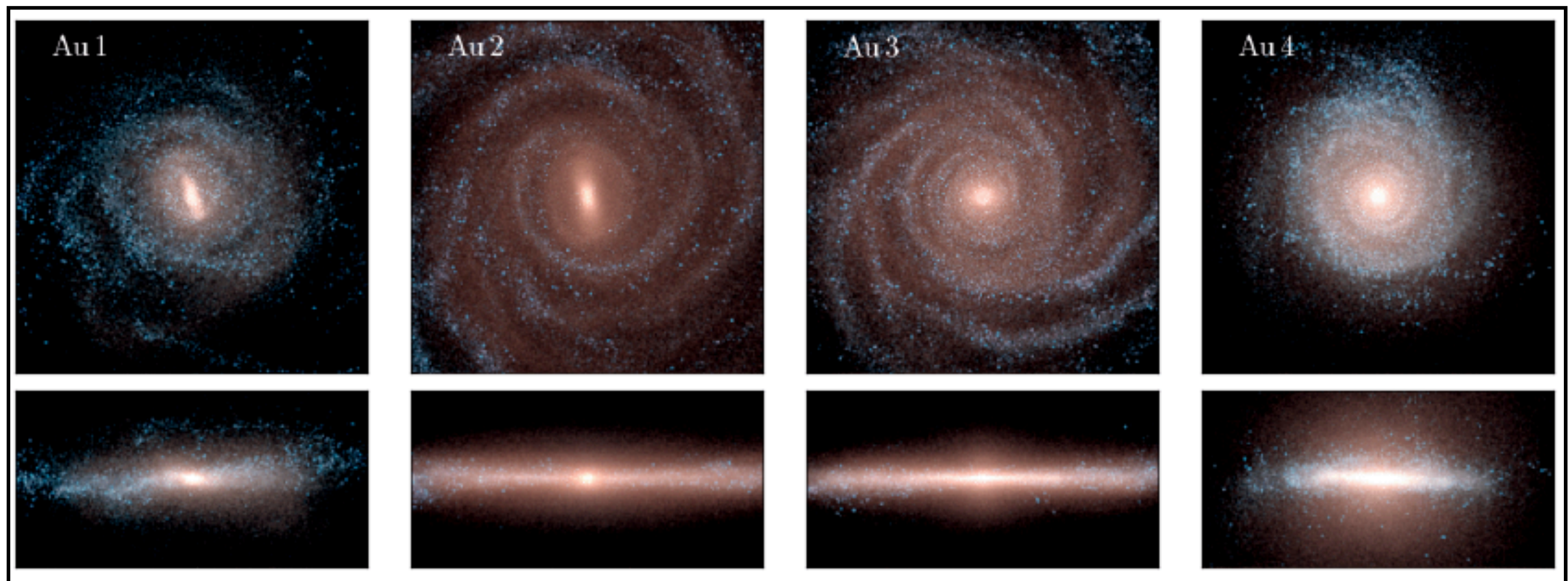
Bozorgnia & Bertone, 1705.05853

- Best fit Maxwellian  $h(v_{\min})$  falls within the  $1\sigma$  uncertainty band of the  $h(v_{\min})$  of the simulated haloes.

# Future perspective

New high resolution simulations available:

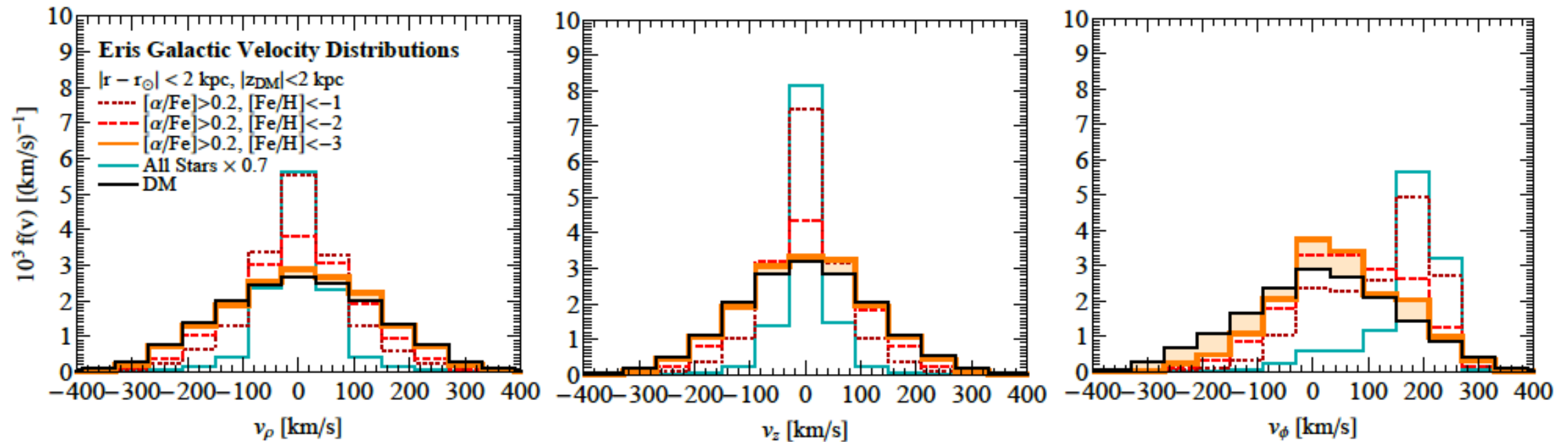
**Auriga simulations:** 30 hydrodynamic simulations of MW size haloes



- Search for correlations between the local DM and stellar velocity distributions.

# Future perspective

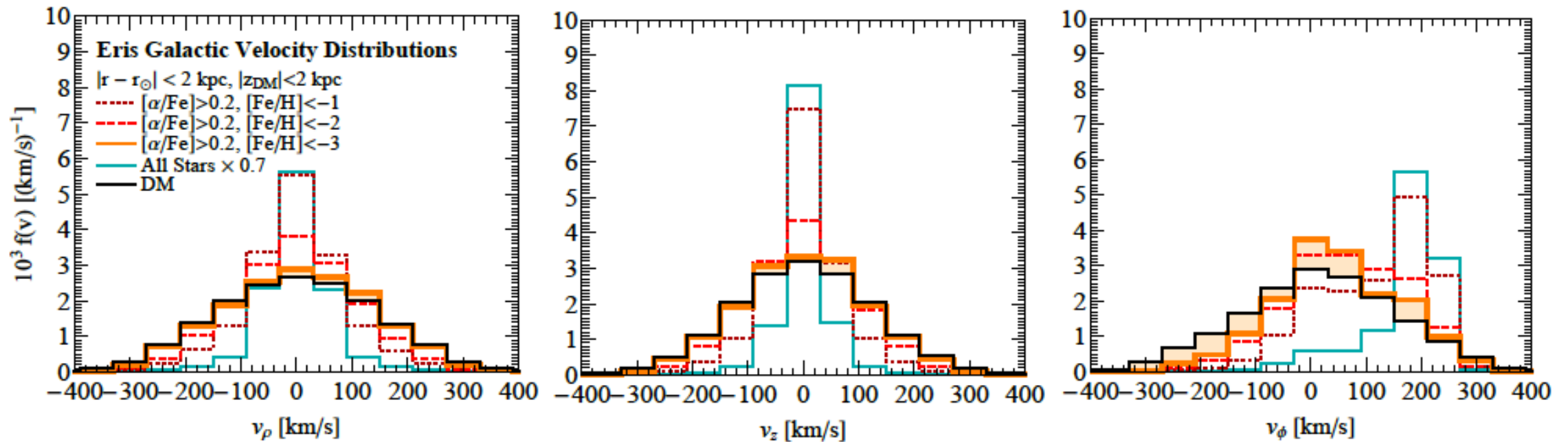
*Are the DM and stellar velocity distributions correlated?*



Herzog-Arbeitman, Lisanti, Madau, Necib, 1704.04499

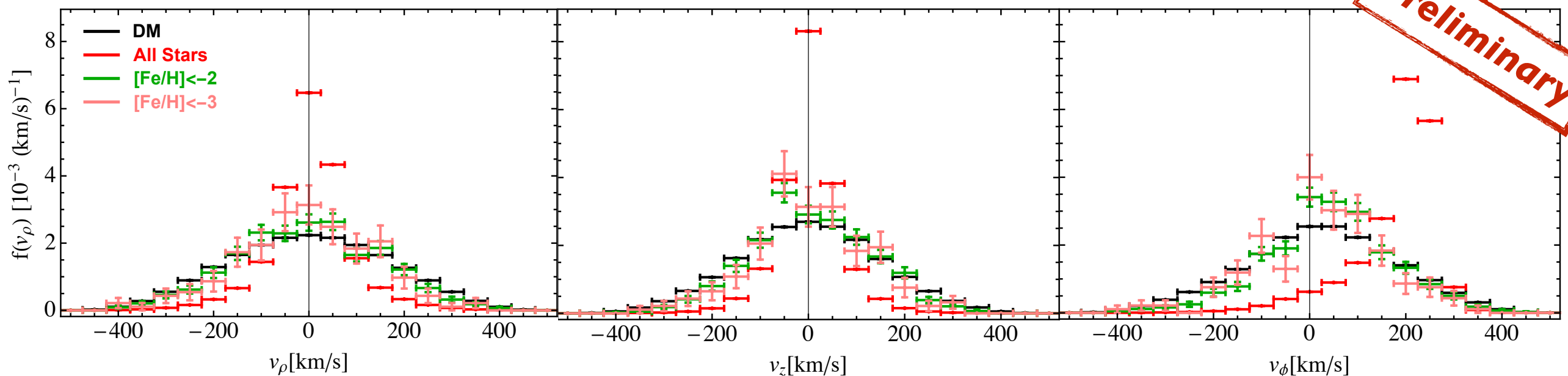
# Future perspective

Are the DM and stellar velocity distributions correlated?



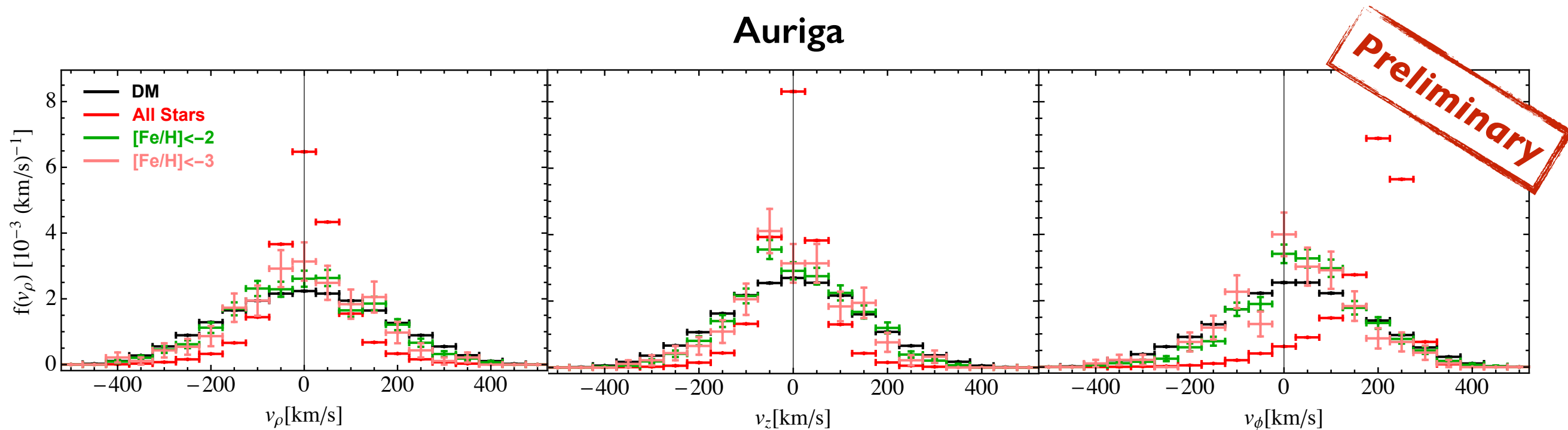
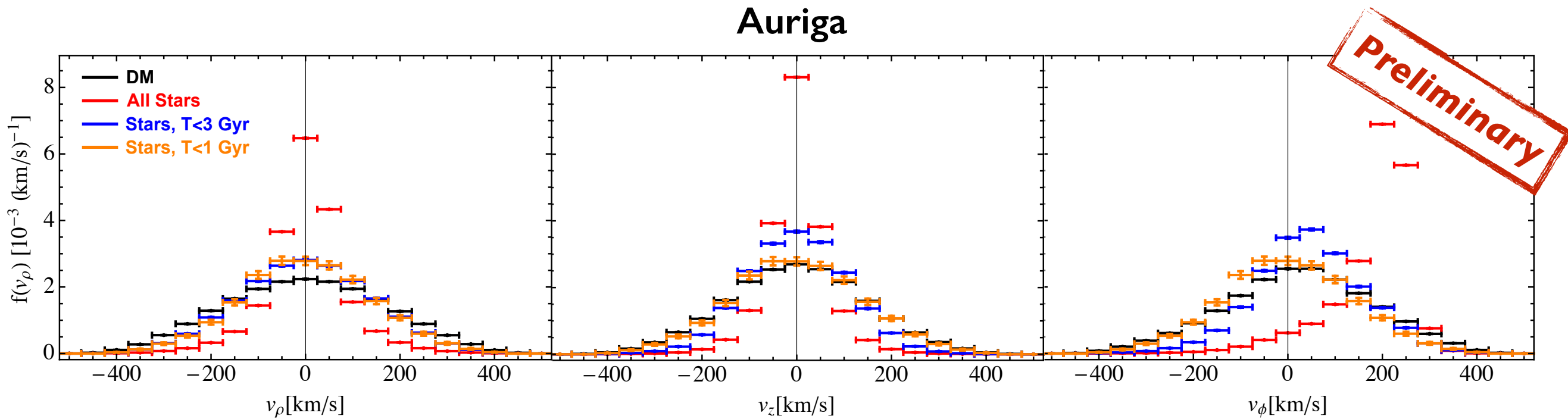
Herzog-Arbeitman, Lisanti, Madau, Necib, 1704.04499

## Auriga



# Future perspective

*Are the DM and stellar velocity distributions correlated?*



# Prospects for indirect DM searches

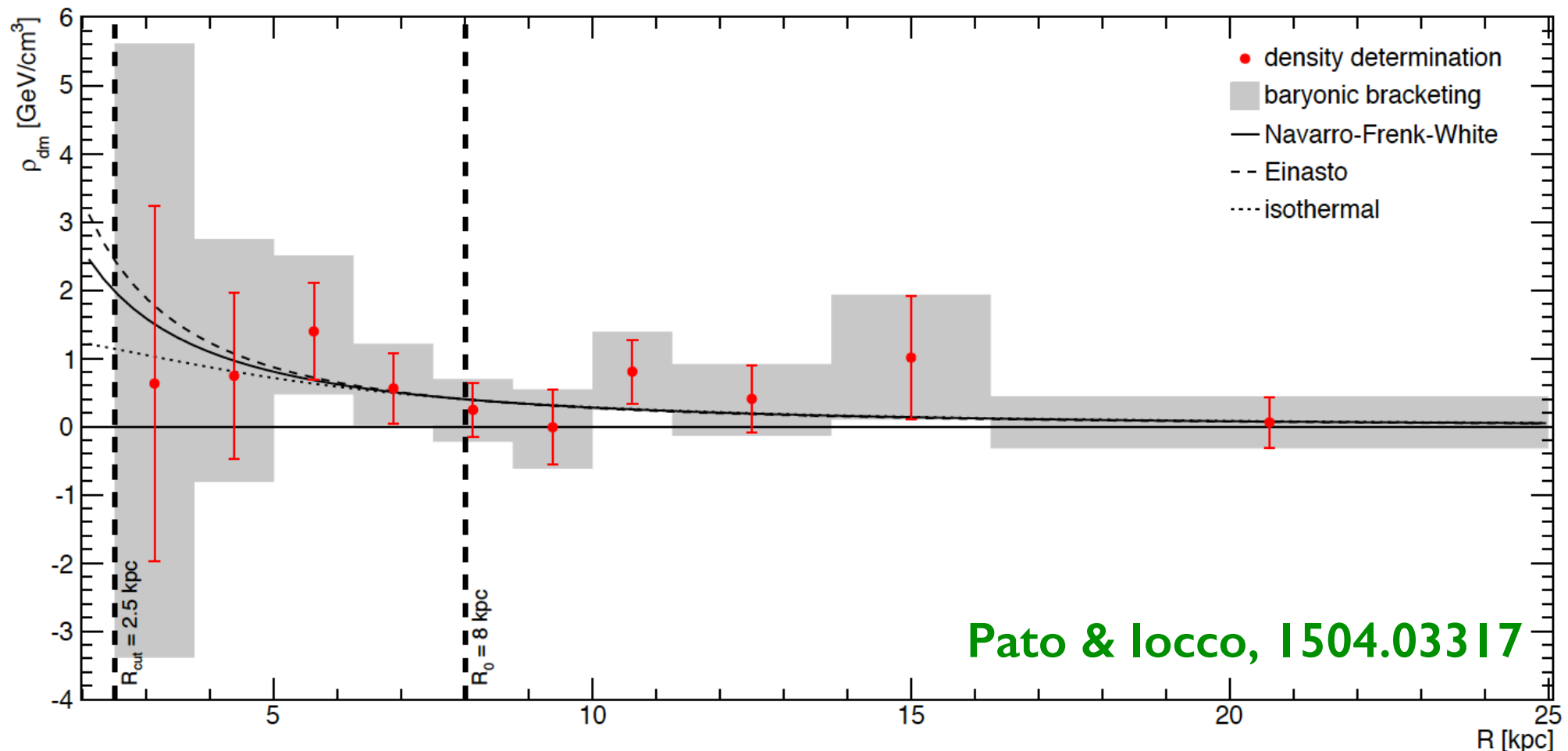
# Indirect DM searches

- Expected gamma-ray flux from DM annihilation:

$$\frac{d\Phi_\gamma}{dE} = \frac{\langle\sigma v\rangle}{8\pi m_\chi^2} \frac{dN_\gamma}{dE} \int_{\text{l.o.s.}} ds \rho^2(r(s, \psi))$$

astrophysics

- Large uncertainties in the DM density profile in the inner few kpc.



# Indirect DM searches

- Expected gamma-ray flux from DM annihilation:

$$\frac{d\Phi_\gamma}{dE} = \frac{\langle\sigma v\rangle}{8\pi m_\chi^2} \frac{dN_\gamma}{dE} \int_{\text{l.o.s.}} ds \overset{\text{astrophysics}}{\rho^2(r(s, \psi))}$$

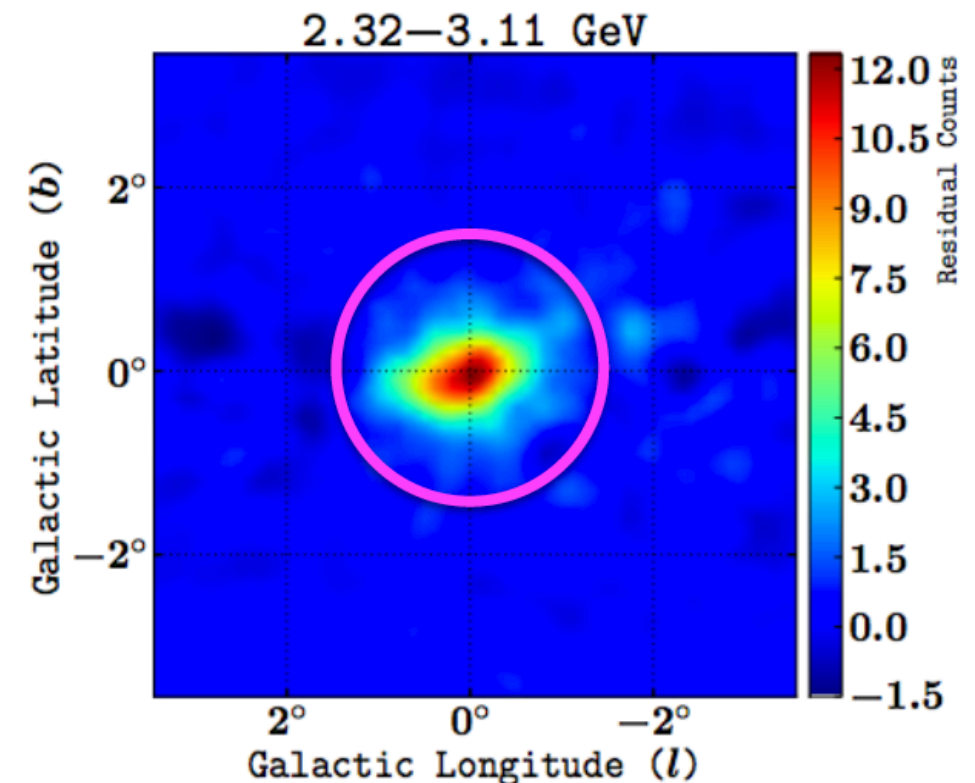
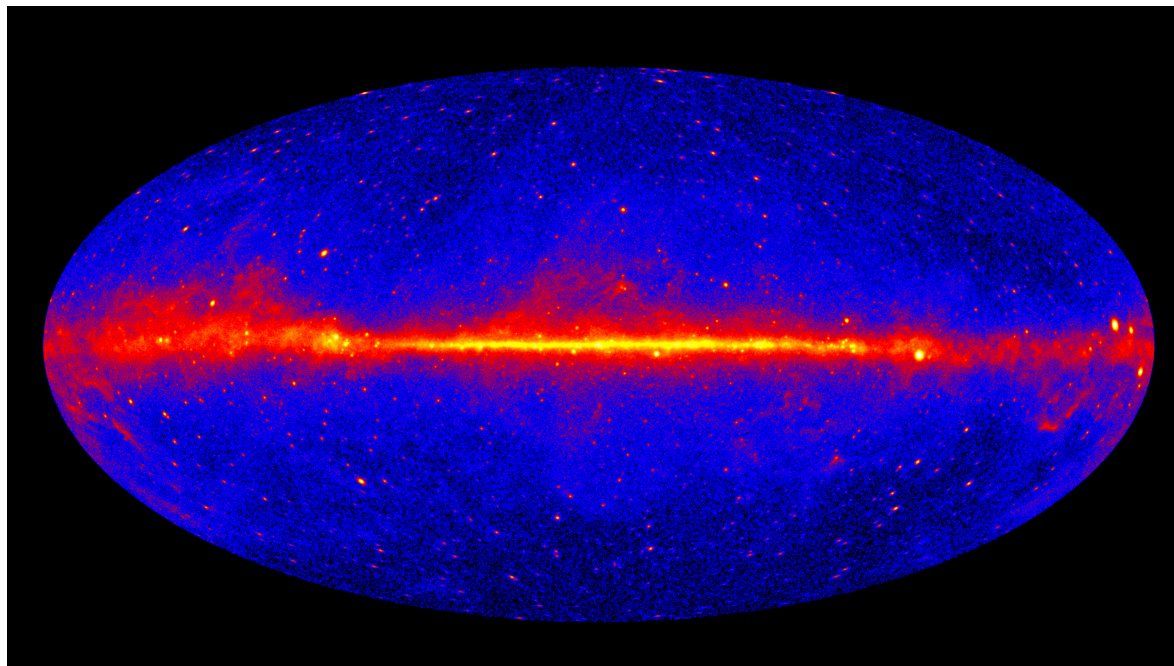
- Large uncertainties in the DM density profile in the inner few kpc.

## Use cosmological simulations:

- DMO simulations predict NFW profile:  $r^{-\gamma}$ , where  $\gamma \approx 1$  in the inner few kpc.
- What is the DM density profile for **MW-like galaxies** in hydrodynamical simulations?

# Galactic centre GeV excess

- Unexplained excess of gamma rays in Fermi-LAT data from the centre of our Galaxy, above the known astrophysical background. **Hooper & Goodenough '09, Vitale & Morselli '09, ...**



**Macias & Gordon, 1312.6671**

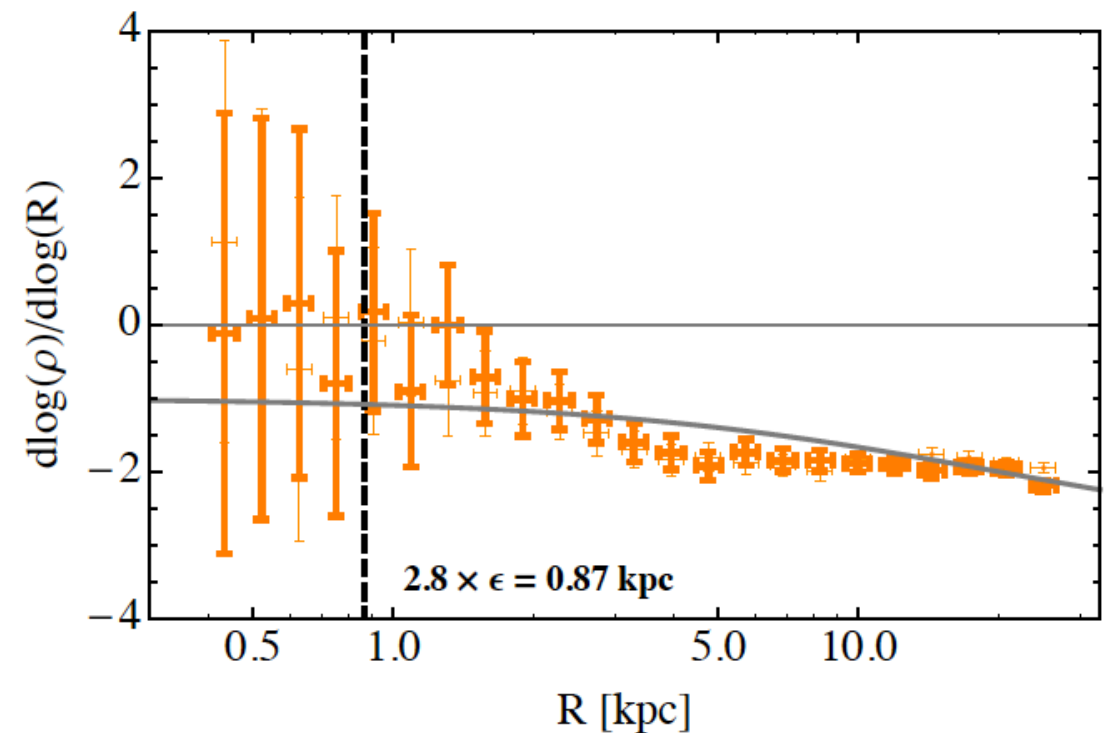
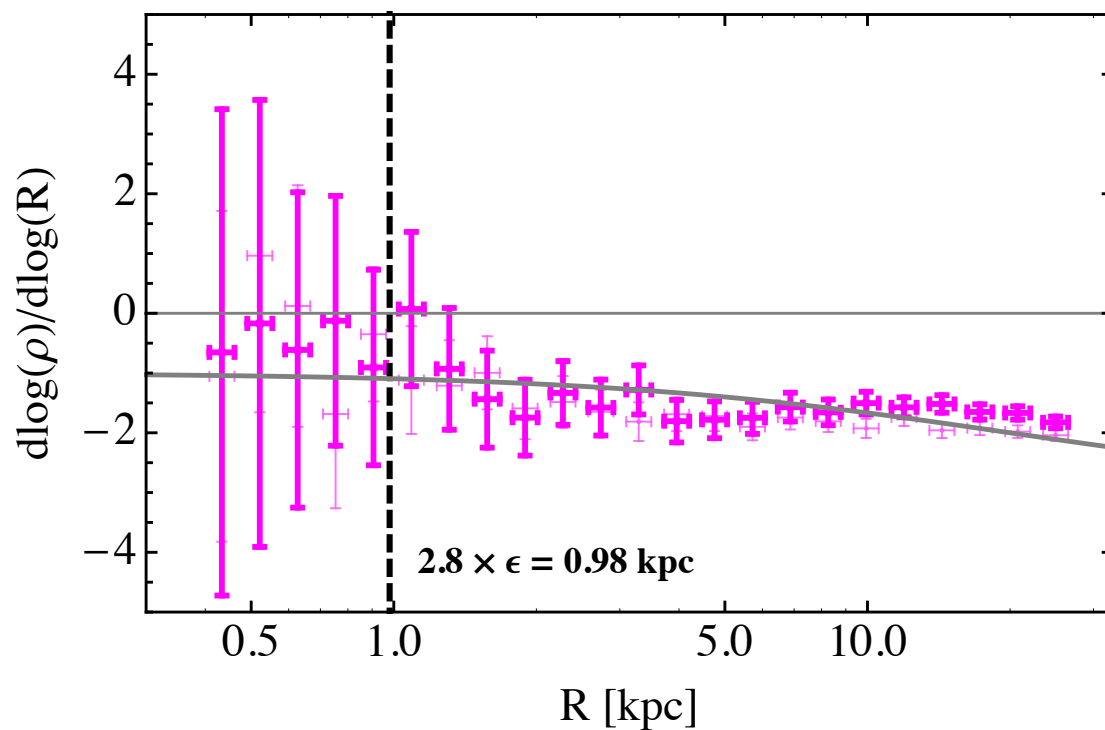
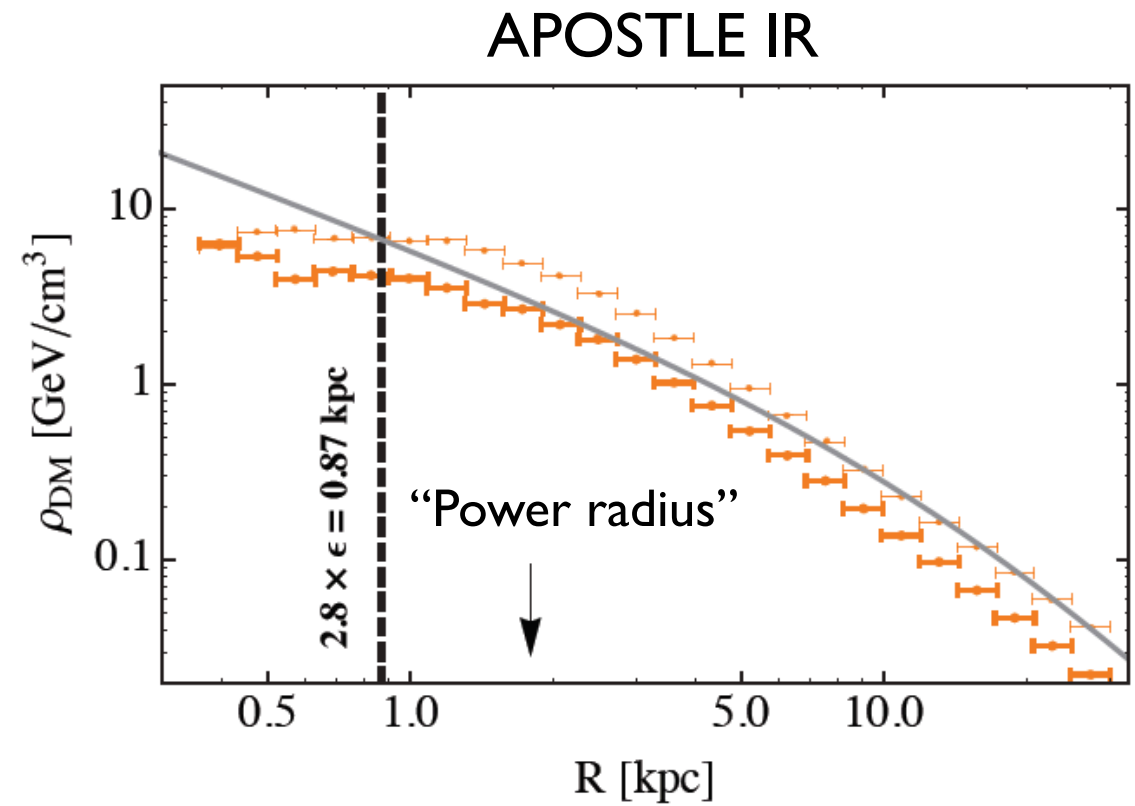
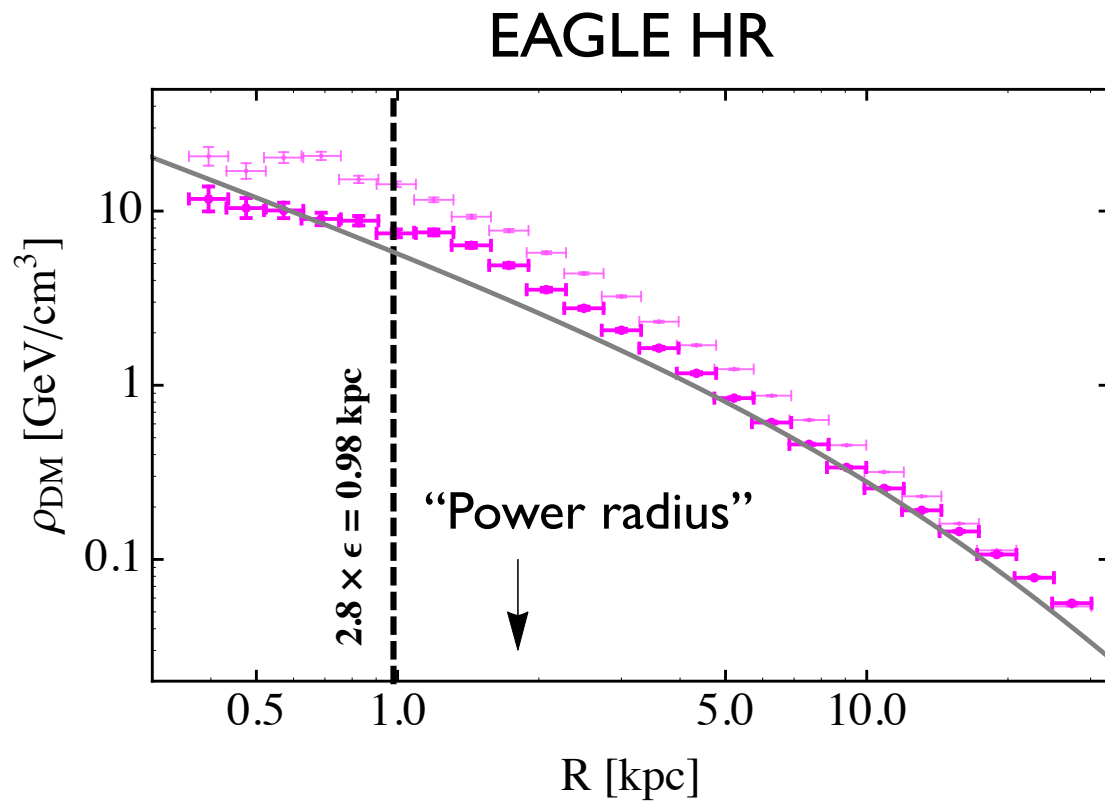
- DM interpretation:**  
Best fit value for the inner slope:  $\gamma = 1.26 \pm 0.15$
- Other interpretations:** *unresolved millisecond pulsars, diffuse photons from cosmic rays, stellar source population in the Galactic bulge, ...*

# Galactic centre GeV excess

- Test the DM density profile predicted by hydrodynamical simulations against the GeV excess data.
- **Additional selection criterion of MW-like galaxies:** substantial stellar disk component.

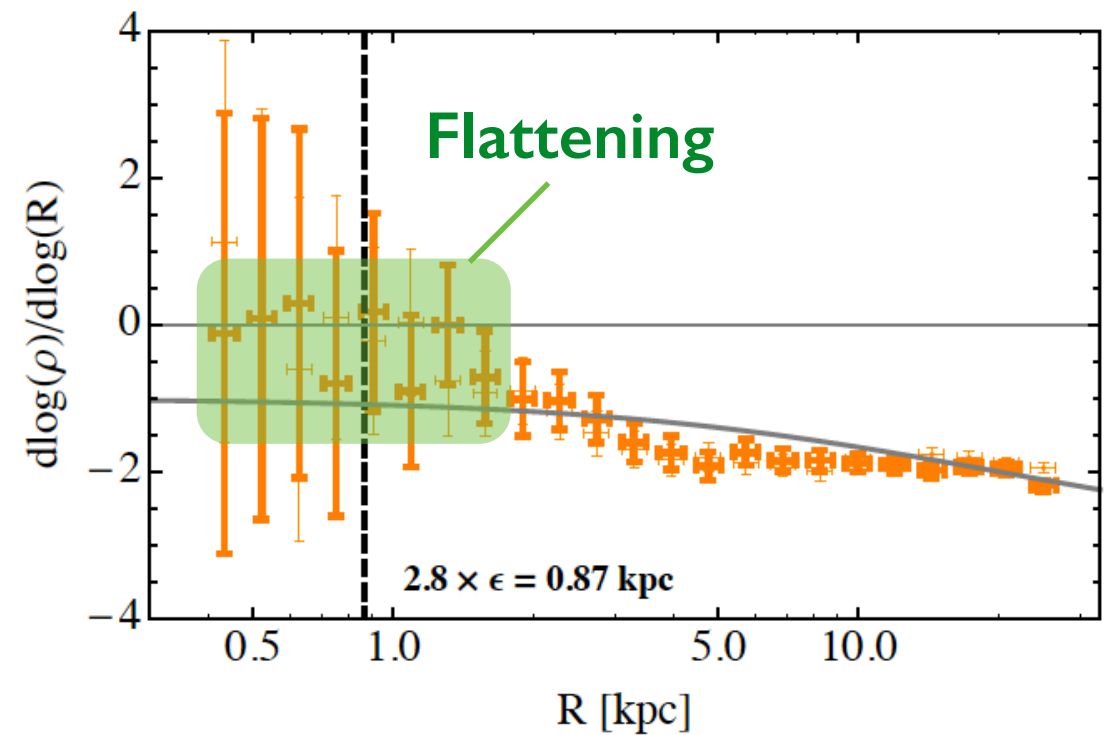
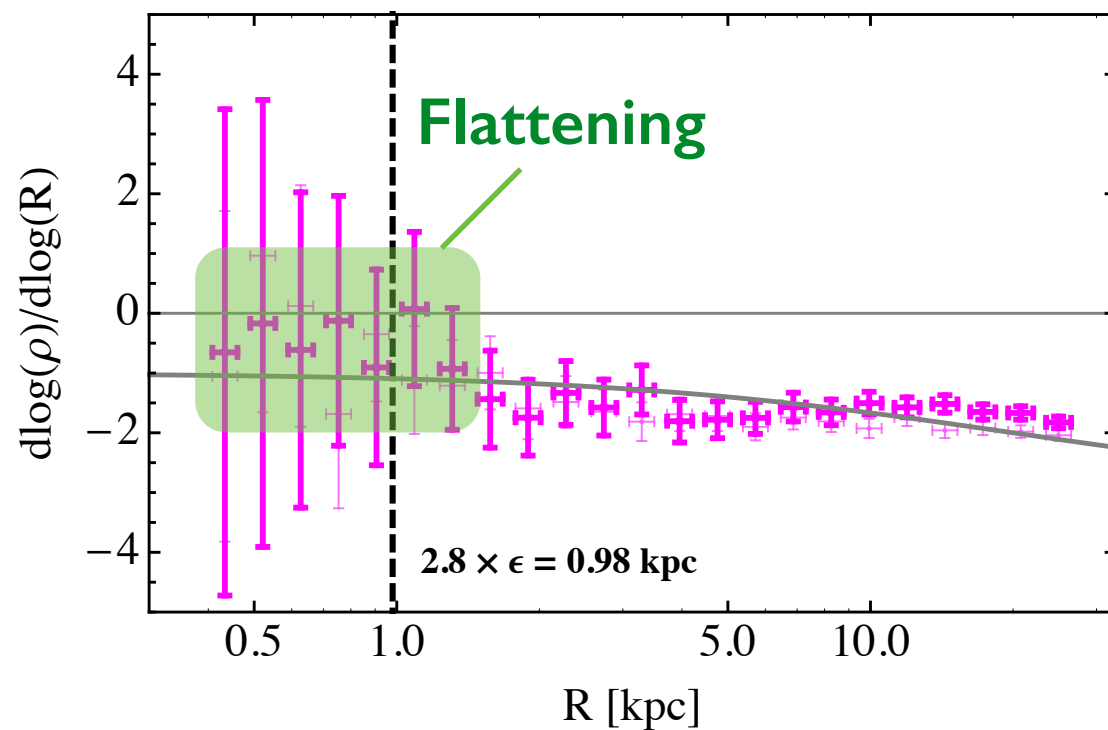
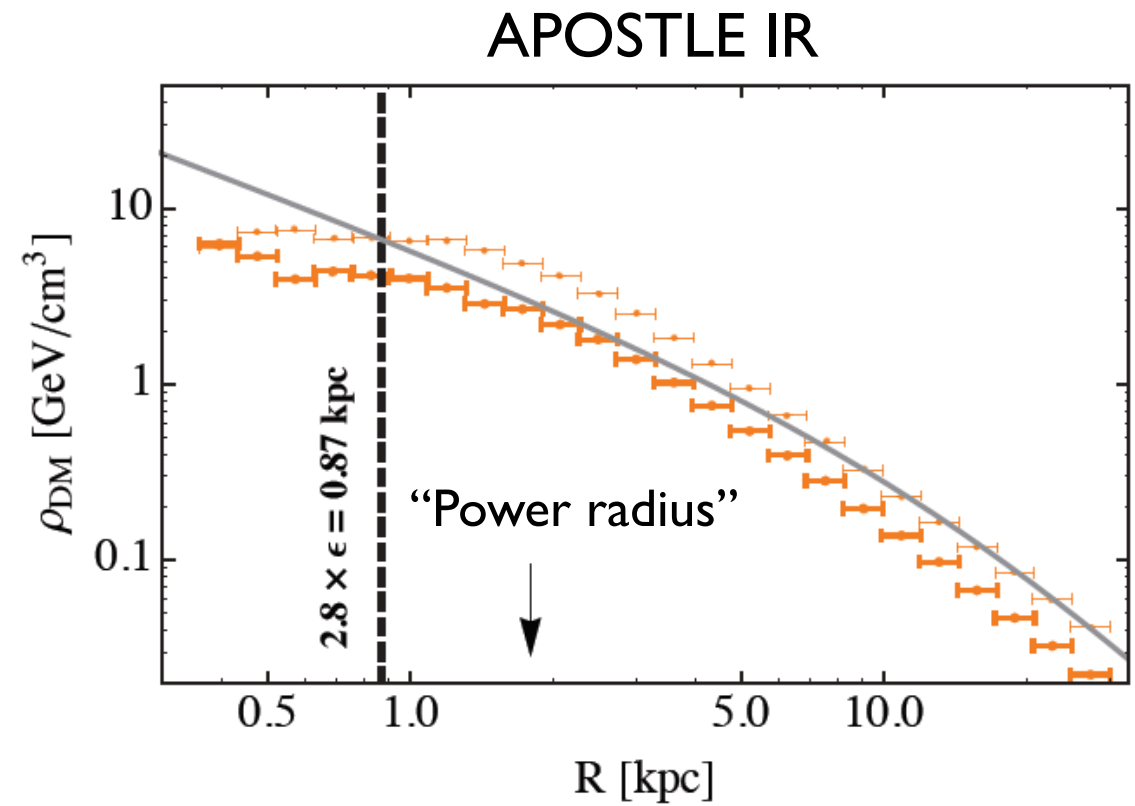
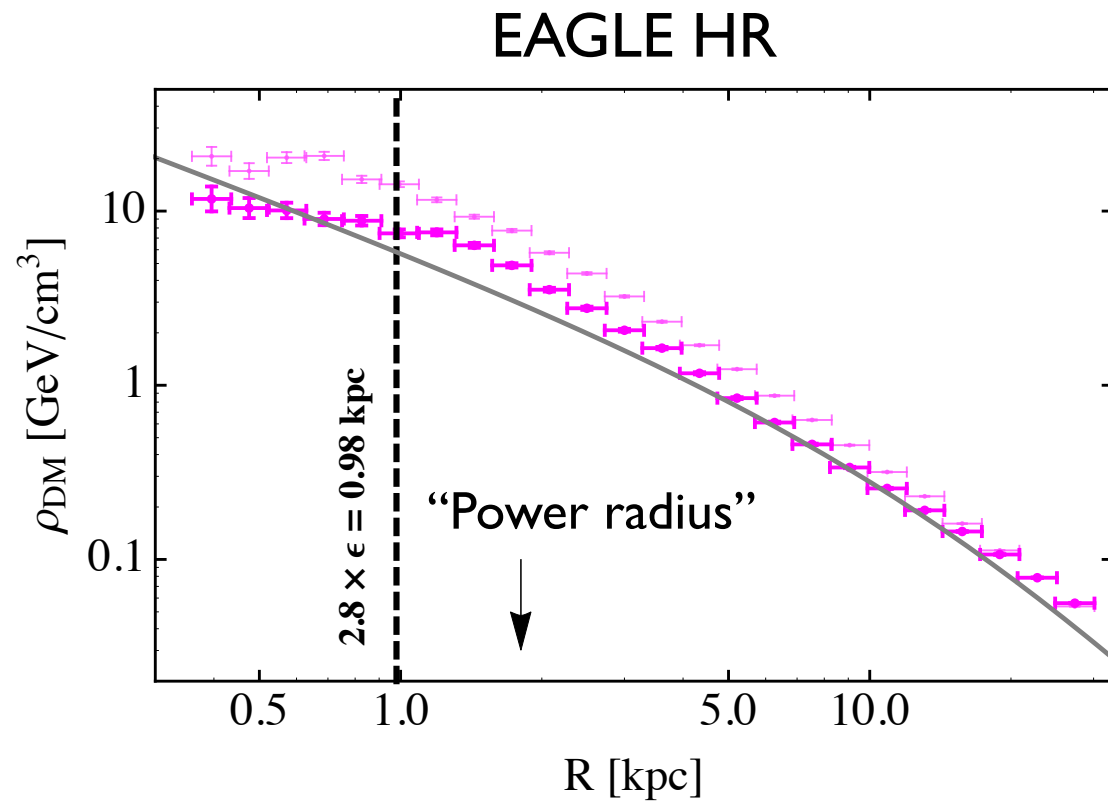
4 MW analogues:  
2 EAGLE + 2 APOSTLE

# DM density profiles



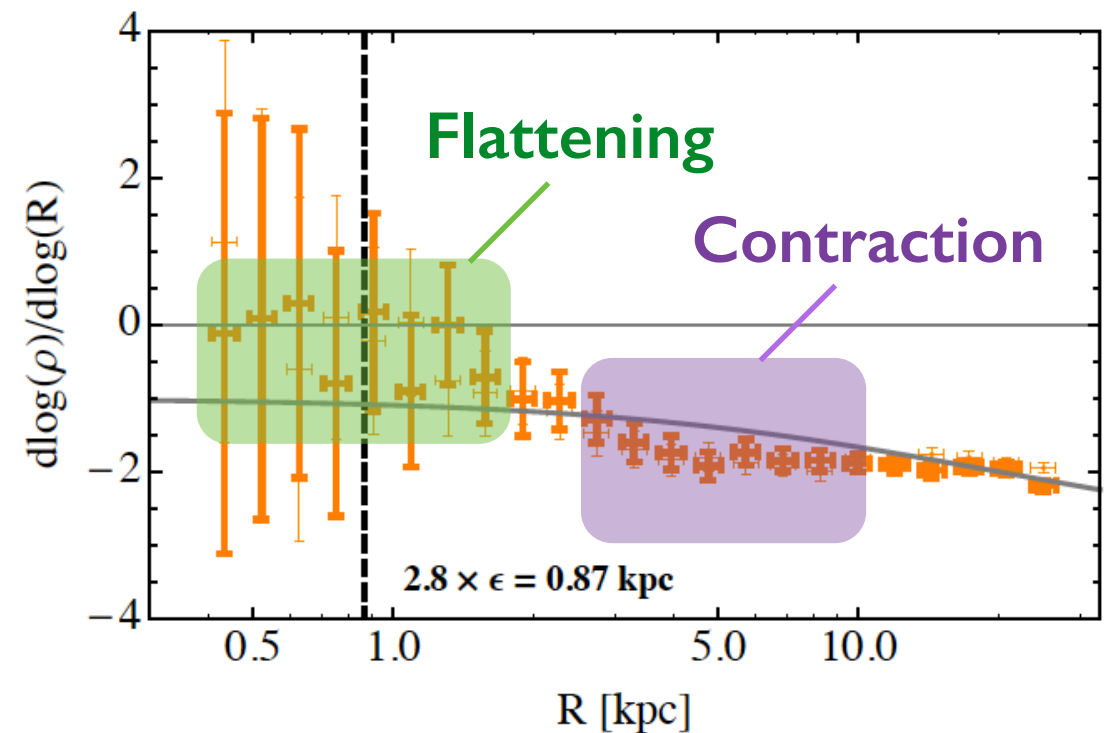
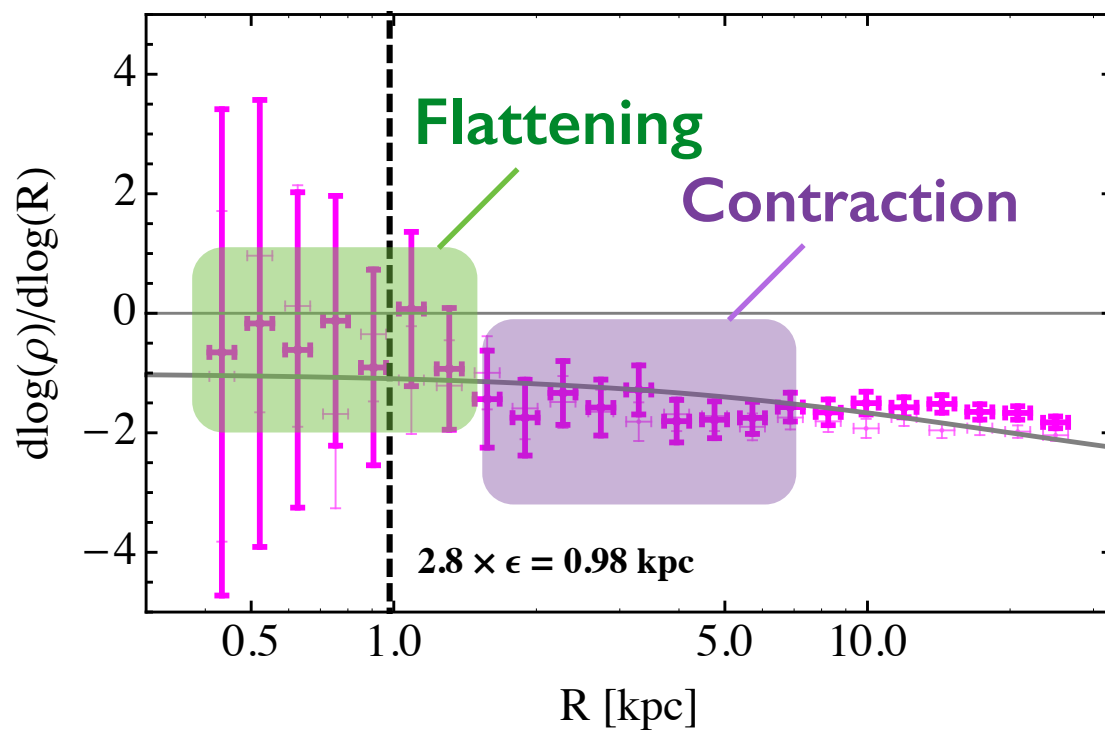
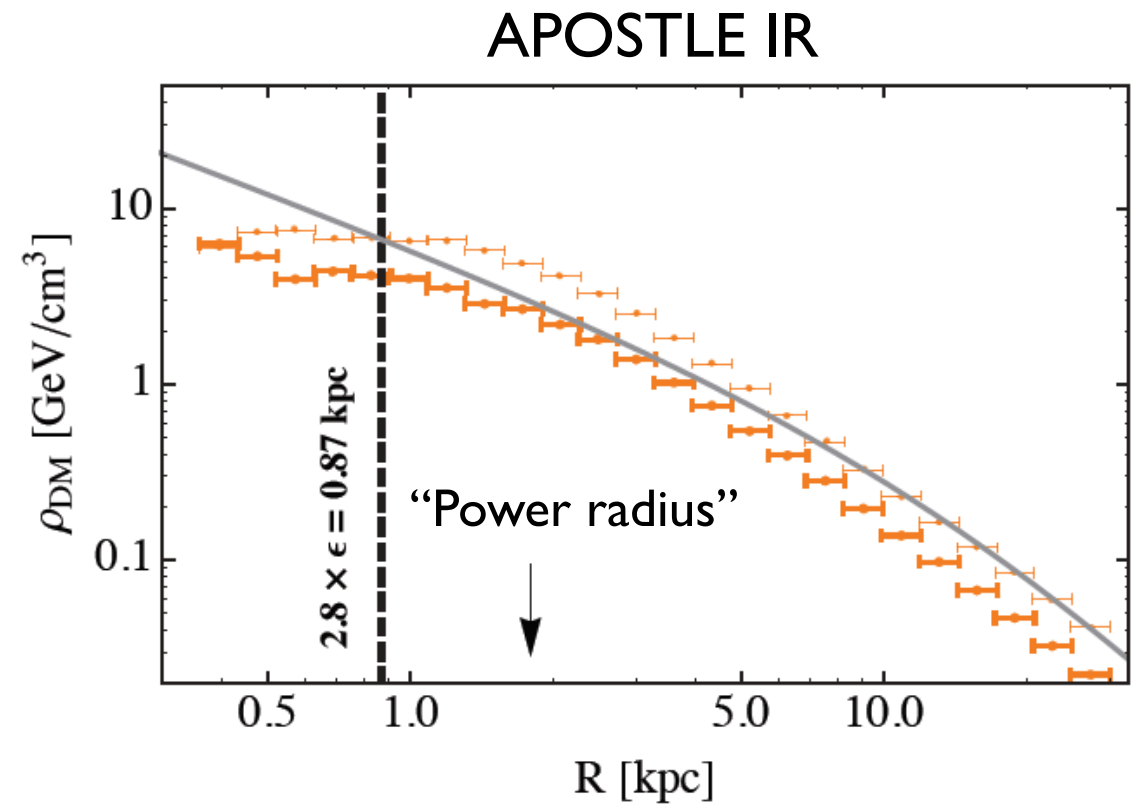
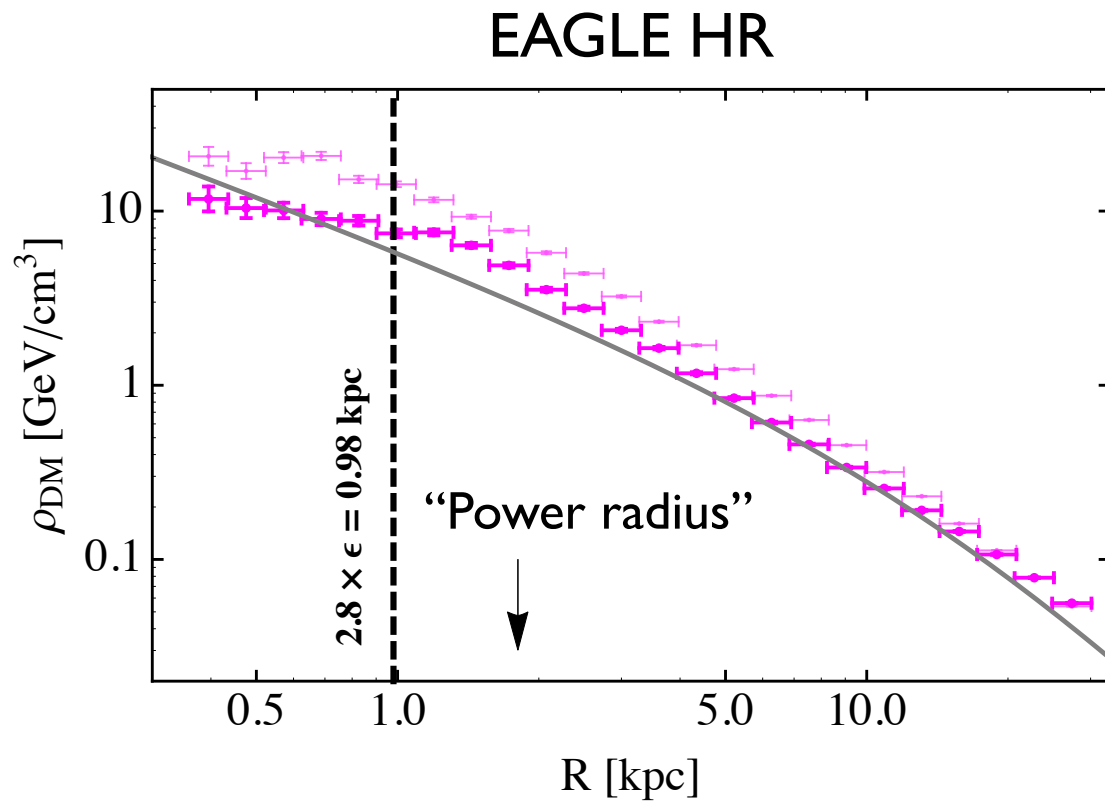
Calore, Bozorgnia et al., 1509.02164

# DM density profiles



Calore, Bozorgnia et al., 1509.02164

# DM density profiles



Calore, Bozorgnia et al., [1509.02164](#)

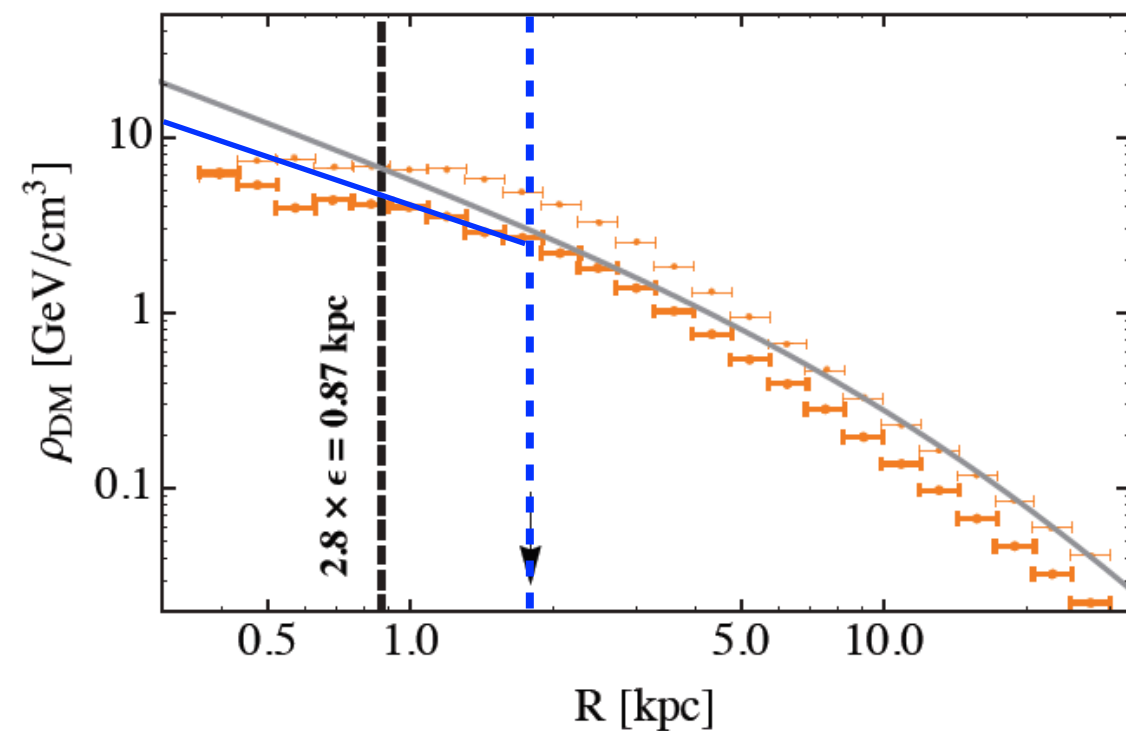
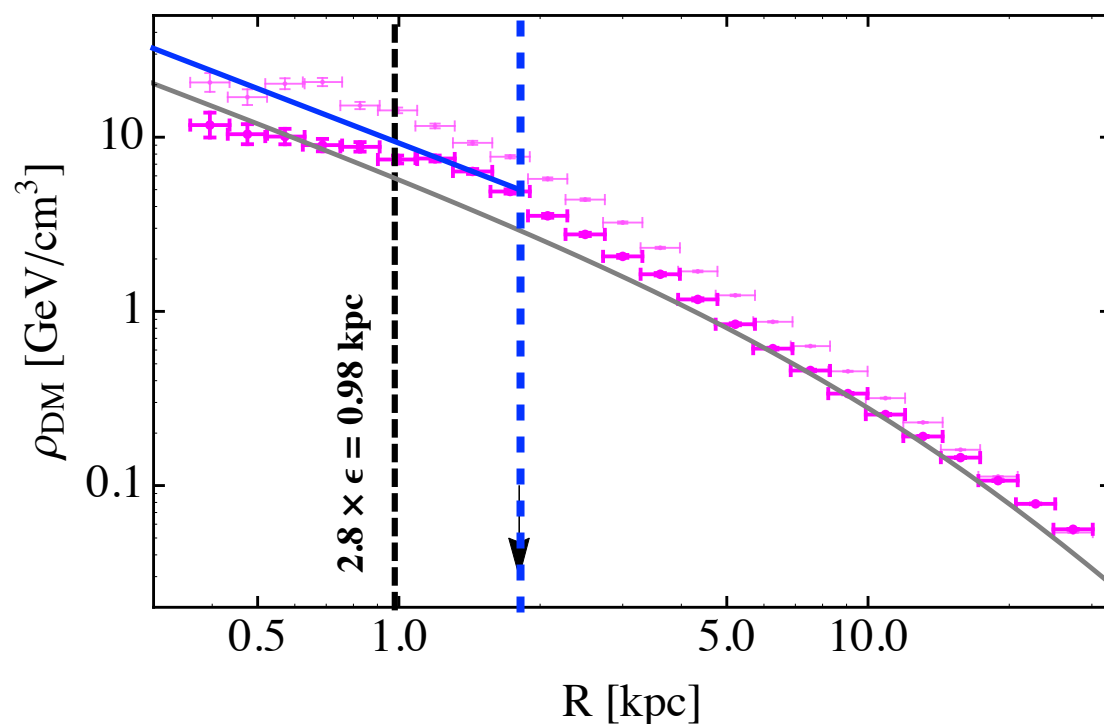
# DM density profiles

- GeV excess data analyzed in the region:

$$2^\circ \leq |b| \leq 20^\circ \ \& \ |l| \leq 20^\circ$$

radial scale: 0.3 - 3 kpc

- **A very conservative approach:** power-law extrapolation with maximal asymptotic slope at the Power radius.

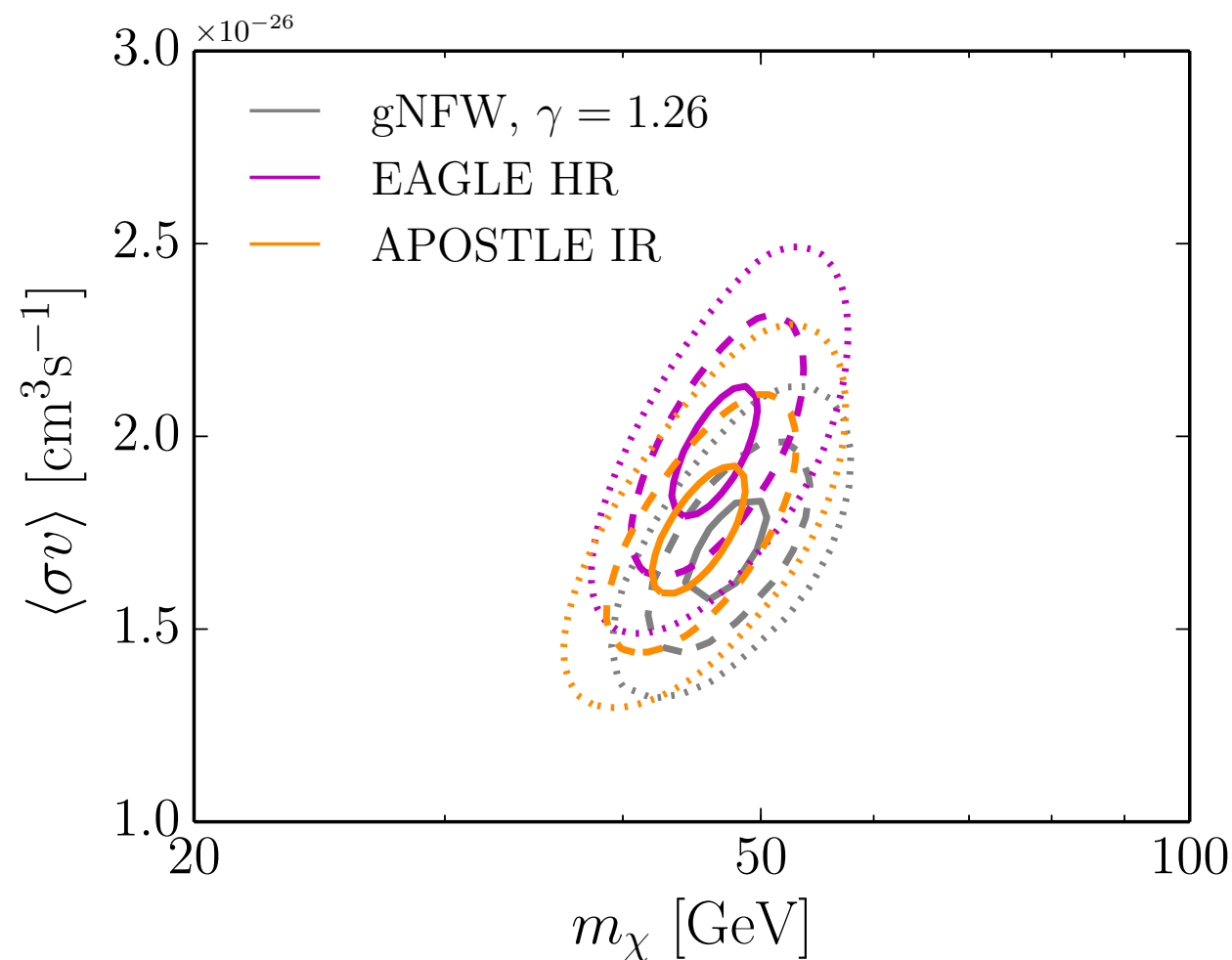


EAGLE HR (2 haloes):  $0.94 < \gamma_{\max} < 0.98$  at  $R_{P03} = 1.8$  kpc

APOSTLE IR (2 haloes):  $0.50 < \gamma_{\max} < 0.62$  at  $R_{P03} = 1.8$  kpc.

# Fitting the GeV excess

- Assuming 100% annihilation into b-quarks:



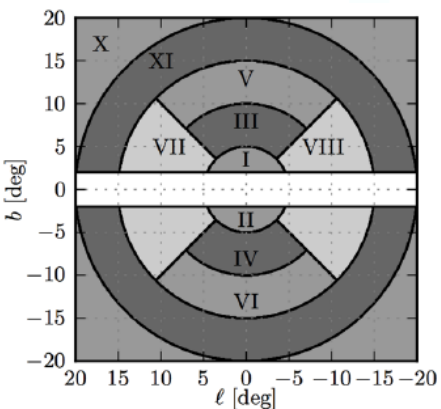
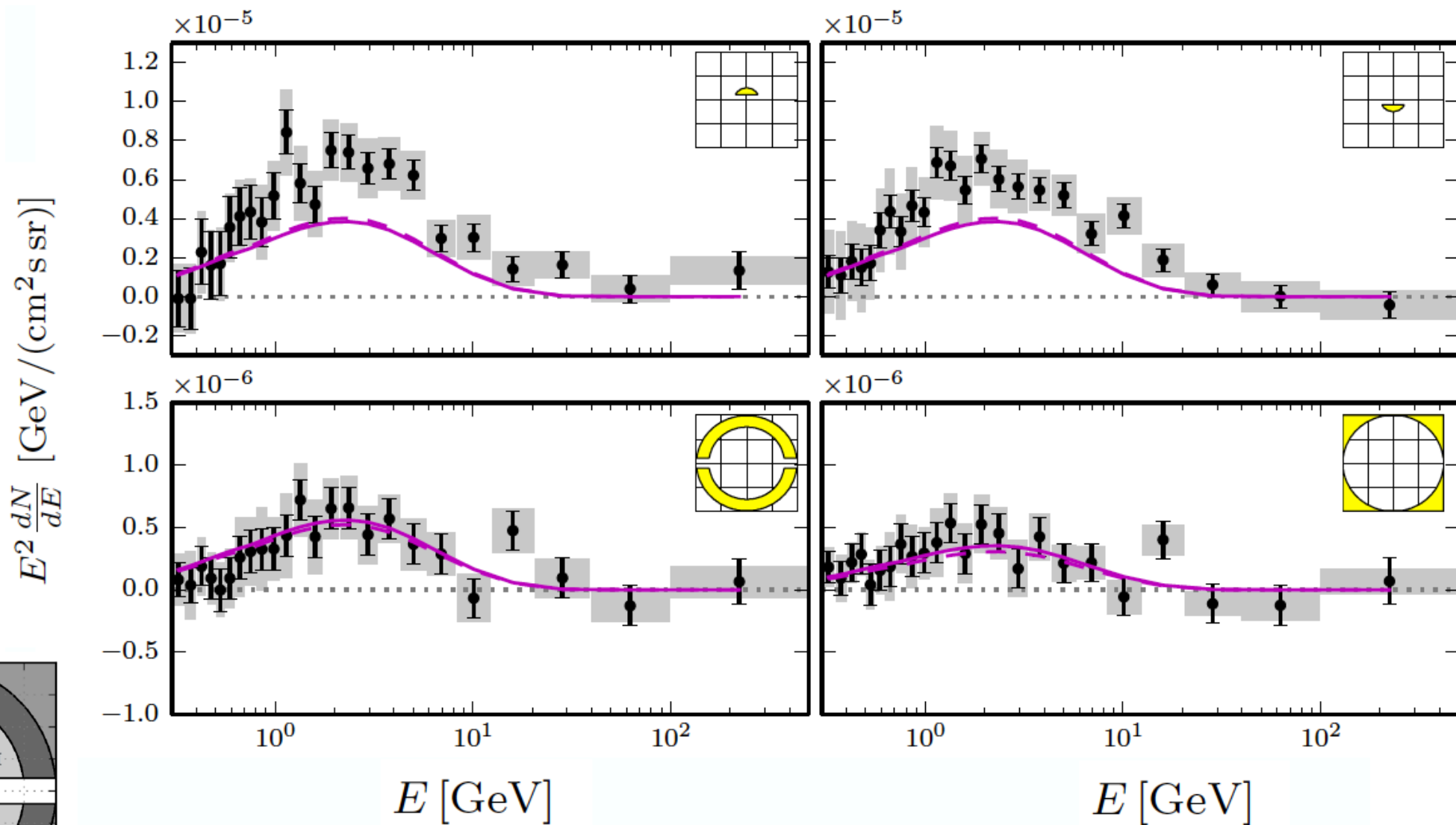
- Similar constraints on DM mass and annihilation cross section, but significantly worse fit.

(238 dof)

Profile	$\langle\sigma v\rangle [\times 10^{-26} \text{ cm}^3/\text{s}]$	$m_\chi [\text{GeV}]$	$\chi^2$	$p$ -value
gNFW ( $\gamma=1.26$ )	$1.71 \pm 0.11$	$47.32 \pm 1.07$	223.9	0.73
EAGLE HR	$1.96 \pm 0.14$	$46.37 \pm 1.37$	246.3	0.34
APOSTLE IR	$1.76 \pm 0.16$	$45.36 \pm 2.96$	283.9	0.02

# Fitting the GeV excess

- Even under our very conservative assumption, DM density profiles of our MW-like galaxies do not reproduce the correct morphology of the GeV excess in the inner most regions.



Calore, Bozorgnia et al., 1509.02164

# Summary

- To make *precise quantitative predictions* for the DM distribution from simulations → Identify MW analogues by taking into account *observational constraints on the MW*.

# Summary

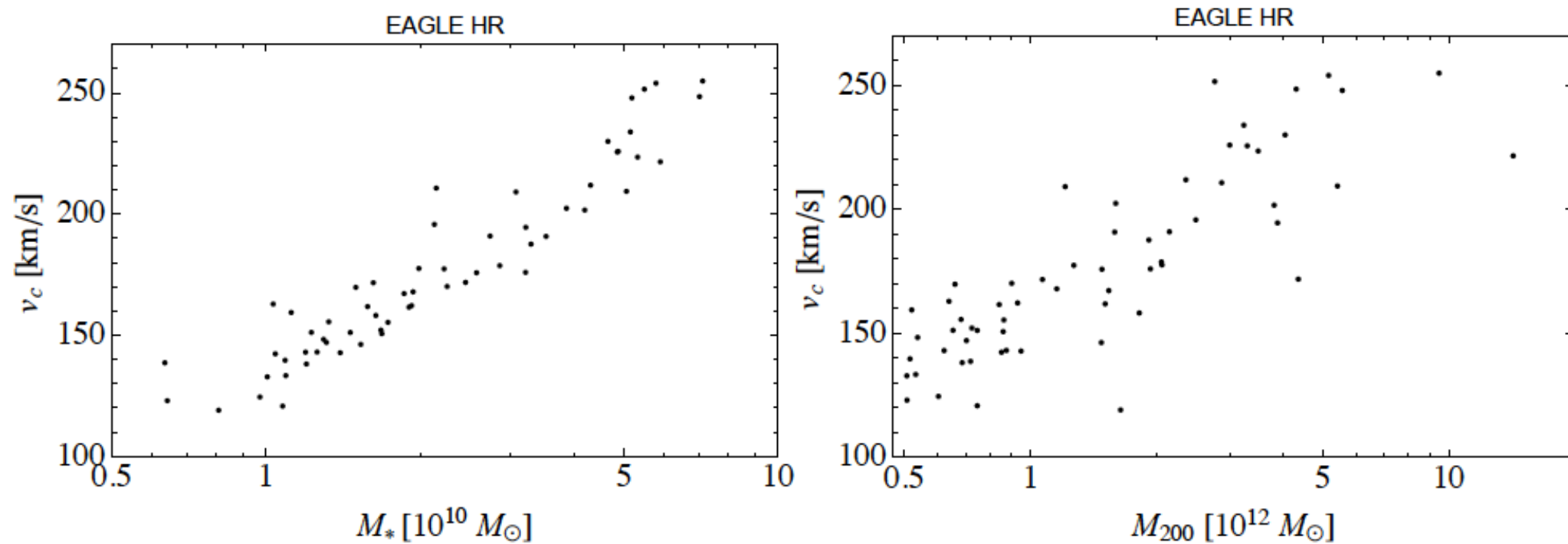
- To make *precise quantitative predictions* for the DM distribution from simulations → Identify MW analogues by taking into account *observational constraints on the MW*.
- **Local DM density** agrees with local and global estimates. *Constraints from Gaia could be used in future simulations.*
- **DM density profiles** show flattening in the inner few kpc and contraction up to 10 kpc.
- **Halo integrals** of MW analogues match well those obtained from *best fit Maxwellian velocity distributions*.  $v_{\text{peak}} \neq v_c$

# Summary

- To make *precise quantitative predictions* for the DM distribution from simulations  $\longrightarrow$  Identify MW analogues by taking into account *observational constraints on the MW*.
- **Local DM density** agrees with local and global estimates. *Constraints from Gaia could be used in future simulations.*
- **DM density profiles** show flattening in the inner few kpc and contraction up to 10 kpc.
- **Halo integrals** of MW analogues match well those obtained from *best fit Maxwellian velocity distributions*.  $v_{\text{peak}} \neq v_c$
- Maxwellian works for the analysis of direct detection data.  $\longrightarrow$  *Can substantially reduce astrophysical uncertainties by a better selection of MW-like galaxies in simulations.*
- DM density profiles of MW-like galaxies fail to reproduce the GeV excess.

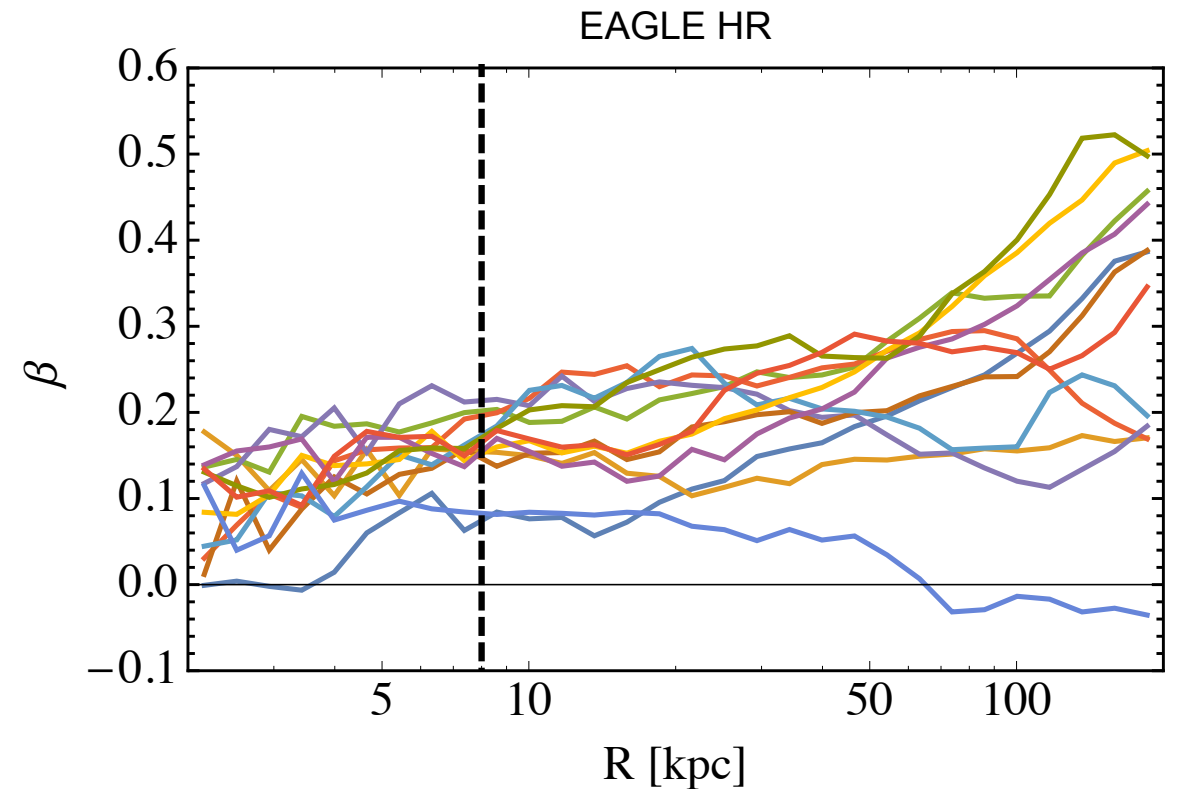
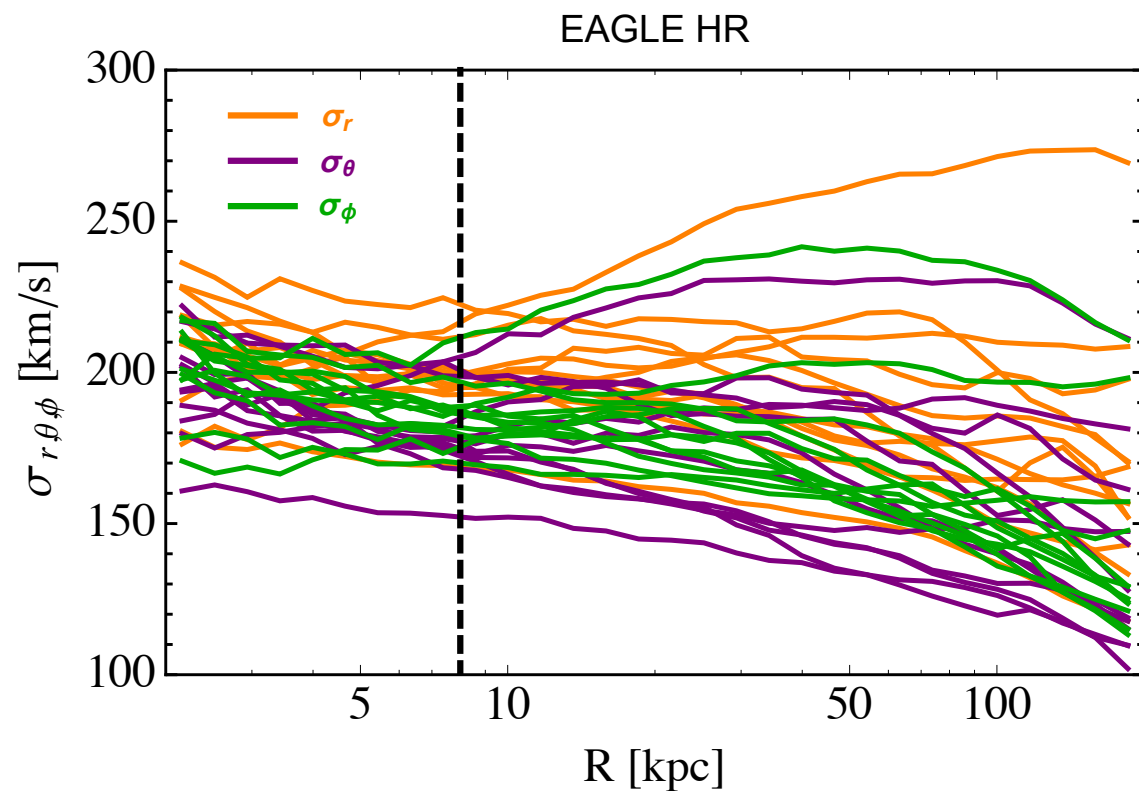
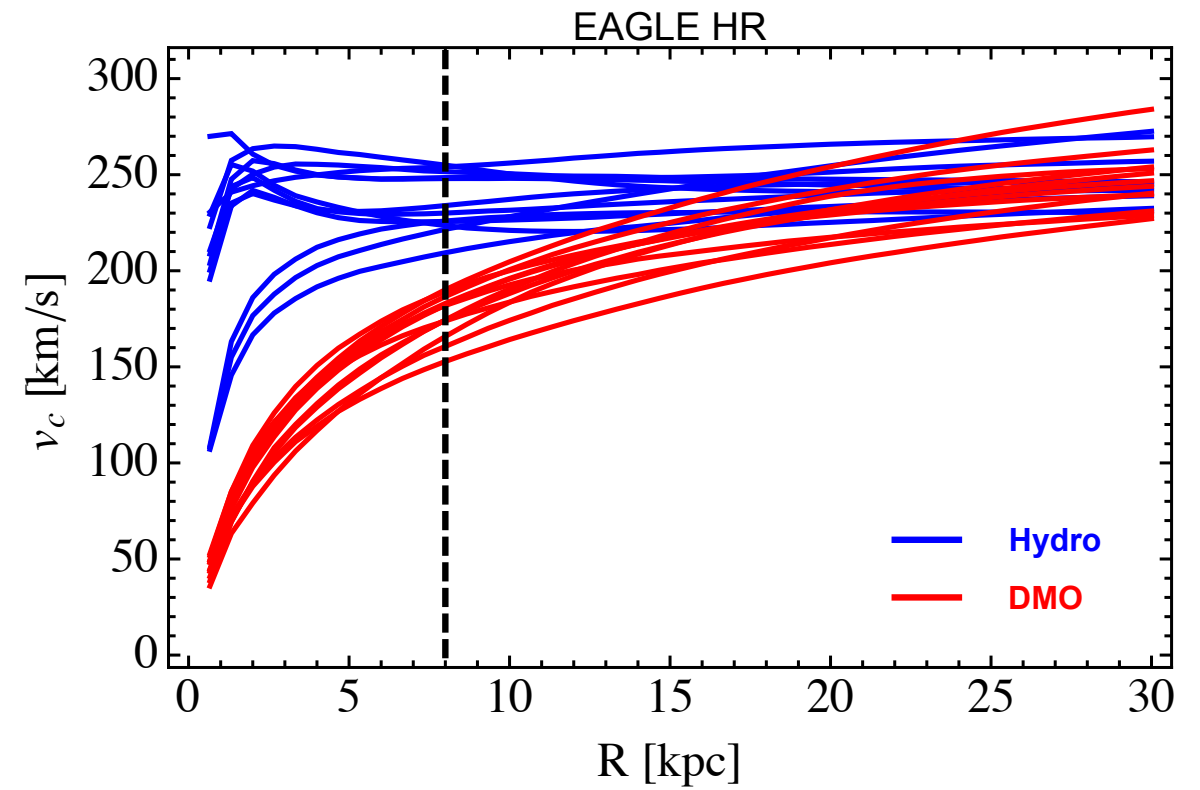
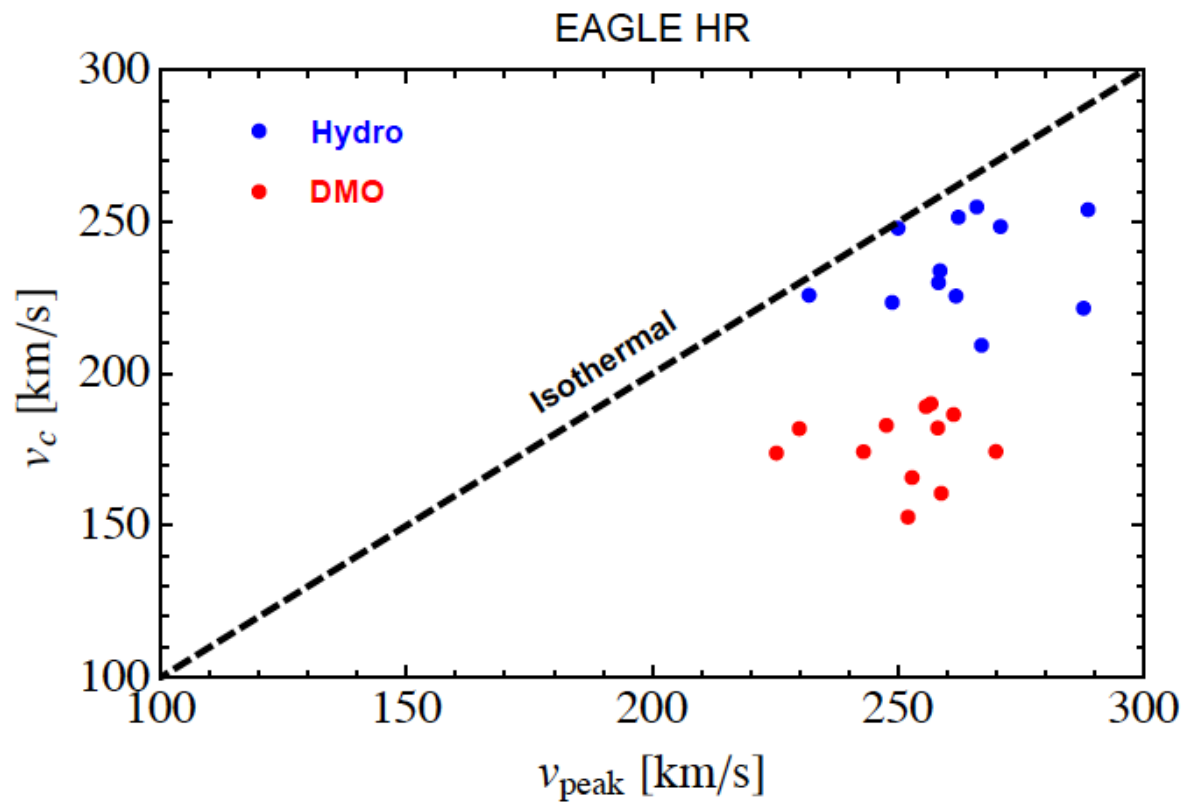
# Backup Slides

# Selection criteria for MW analogues



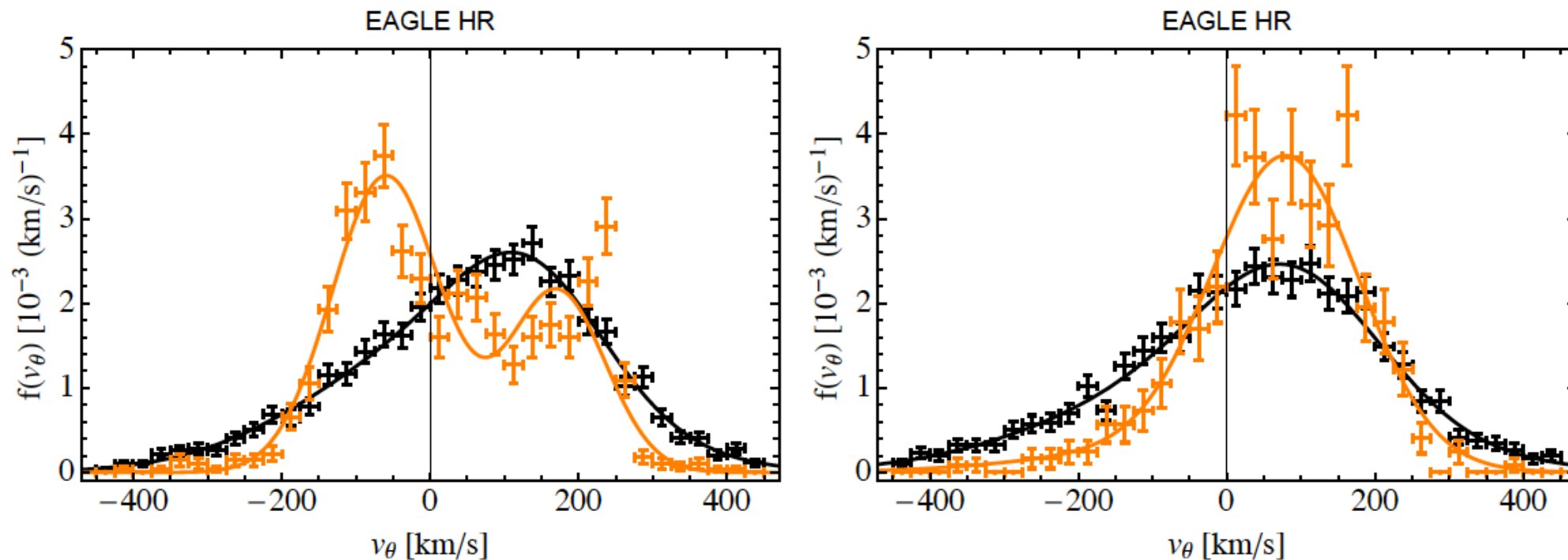
- ▶  $M_*$  strongly correlated with  $v_c$  at 8 kpc, while the correlation of  $M_{200}$  with  $v_c$  is weaker.
- ▶  $M_*(R < 8 \text{ kpc}) = (0.5 - 0.9)M_*$ .
- ▶  $M_{\text{tot}}(R < 8 \text{ kpc}) = (0.01 - 0.1)M_{200}$ .
- ▶ Over the small halo mass range probed, little correlation between  $M_{\text{DM}}(R < 8 \text{ kpc})$  and  $M_{200}$ .

# Departure from isothermal



# Searching for dark disks

DM and stellar velocity distributions:



- ▶ Fit with a double Gaussian. Difference in the mean speed of second Gaussian between DM and stars is 35 km/s in the left, and 7 km/s in the right panel.
- ▶ Fraction of second Gaussian is 32% in the left panel and 43% in the right panel.

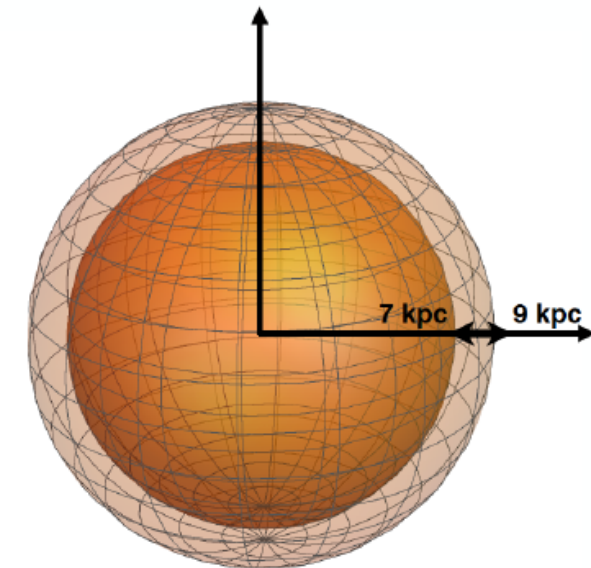
# Searching for dark disks

Is there an enhancement of the local DM density in the **Galactic disc** compared to the **halo**?

- ▶ Compare the the average  $\rho_{\text{DM}}$  in the torus with the value in a spherical shell at  $7 < R < 9$  kpc.

$\rho_{\text{DM}}^{\text{torus}}$  is larger than  $\rho_{\text{DM}}^{\text{shell}}$  by:

2 – 27% for 10 haloes,  
greater than 10% for 5 haloes, and  
greater than 20% for only two haloes.



- ▶ The increase in the DM density in the disc could be due to the DM halo contraction as a result of dissipational baryonic processes.

# Halo shapes

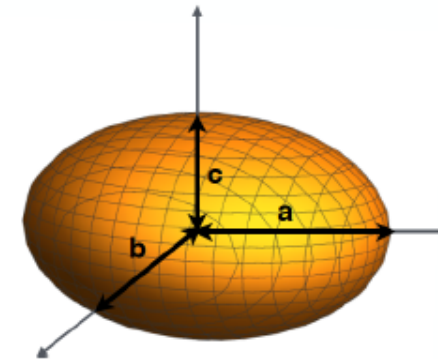
- ▶ To study the shape of the inner ( $R < 8$  kpc) DM haloes, we calculate the inertia tensor of DM particles within 5 and 8 kpc.  
⇒ ellipsoid with three axes of length  $a \geq b \geq c$ .
- ▶ Calculate the **sphericity**:  $s = c/a$ .
  - ▶  $s = 1$ : perfect sphere.  $s < 1$ : increasing deviation from sphericity.
  - ▶ At 5 kpc,  $s = [0.85, 0.95]$ . At 8 kpc,  $s$  lower by less than 10%.
  - ▶ Due to dissipational baryonic processes, DM sphericity systematically higher in the hydrodynamic simulations compared to DMO haloes in which  $s = [0.75, 0.85]$ .

# Halo shapes

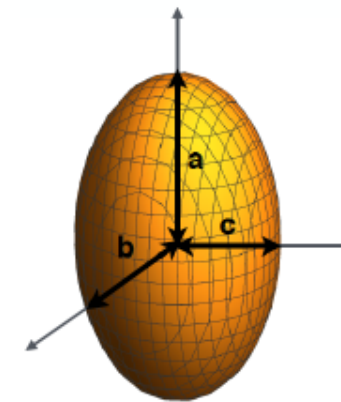
- ▶ Describe a deviation from sphericity by the triaxiality parameter:

$$T = \frac{a^2 - b^2}{a^2 - c^2}$$

- ▶ Oblate systems,  $a \approx b \gg c \Rightarrow T \approx 0$ .



- ▶ Prolate systems,  $a \gg b \approx c \Rightarrow T \approx 1$ .



- ▶ In the hydro case, since inner haloes are very close to spherical, deviation towards either oblate or prolate is small. **DMO counterparts** have a preference for *prolate* inner haloes.

# Parameters of the simulations

Simulation	code	$N_{\text{DM}}$	$m_g [M_{\odot}]$	$m_{\text{DM}} [M_{\odot}]$	$\epsilon$ [pc]
Ling <i>et al.</i>	RAMSES	2662	–	$7.46 \times 10^5$	200
Eris	GASOLINE	81213	$2 \times 10^4$	$9.80 \times 10^4$	124
NIHAO	EFS-GASOLINE2	–	$3.16 \times 10^5$	$1.74 \times 10^6$	931
EAGLE (HR)	P-GADGET (ANARCHY)	1821–3201	$2.26 \times 10^5$	$1.21 \times 10^6$	350
APOSTLE (IR)	P-GADGET (ANARCHY)	2160, 3024	$1.3 \times 10^5$	$5.9 \times 10^5$	308
MaGICC	GASOLINE	4849, 6541	$2.2 \times 10^5$	$1.11 \times 10^6$	310
Sloane <i>et al.</i>	GASLOINE	5847–7460	$2.7 \times 10^4$	$1.5 \times 10^5$	174

## Properties of the selected MW analogues

Simulation	Count	$M_{\text{star}} [\times 10^{10} M_{\odot}]$	$M_{\text{halo}} [\times 10^{12} M_{\odot}]$	$\rho_{\chi}$ [GeV/cm <sup>3</sup> ]	$v_{\text{peak}}$ [km/s]
Ling <i>et al.</i>	1	$\sim 8$	0.63	0.37–0.39	239
Eris	1	3.9	0.78	0.42	239
NIHAO	5	15.9	$\sim 1$	0.42	192–363
EAGLE (HR)	12	4.65–7.12	2.76–14.26	0.42–0.73	232–289
APOSTLE (IR)	2	4.48, 4.88	1.64–2.15	0.41–0.54	223–234
MaGICC	2	2.4–8.3	0.584, 1.5	0.346, 0.493	187, 273
Sloane <i>et al.</i>	4	2.24–4.56	0.68–0.91	0.3–0.4	185–204

# Parameters of the simulations

## Auriga simulations

Resolution level	$\frac{m_{\text{DM}}}{[M_{\odot}]}$	$\frac{m_{\text{b}}}{[M_{\odot}]}$	$\frac{\epsilon}{[\text{pc}]}$
4	$3 \times 10^5$	$5 \times 10^4$	369
5	$2 \times 10^6$	$4 \times 10^5$	738
3	$4 \times 10^4$	$6 \times 10^3$	184

# Morphology of simulated haloes

- ▶ Select simulated galaxies whose stellar kinematics show a disc component, rather than ellipticals or undergoing mergers.
- ▶ Characterize the morphology of each simulated galaxy by looking for evidence of coherent rotation.
- ▶ Use the distribution of angular momentum vectors of individual particles relative to the net angular momentum of the galaxy to discriminate between discs (coherent rotation) and spheroids (no coherent rotation).
- ▶ Derive the distribution of the stellar orbital circularity parameter,

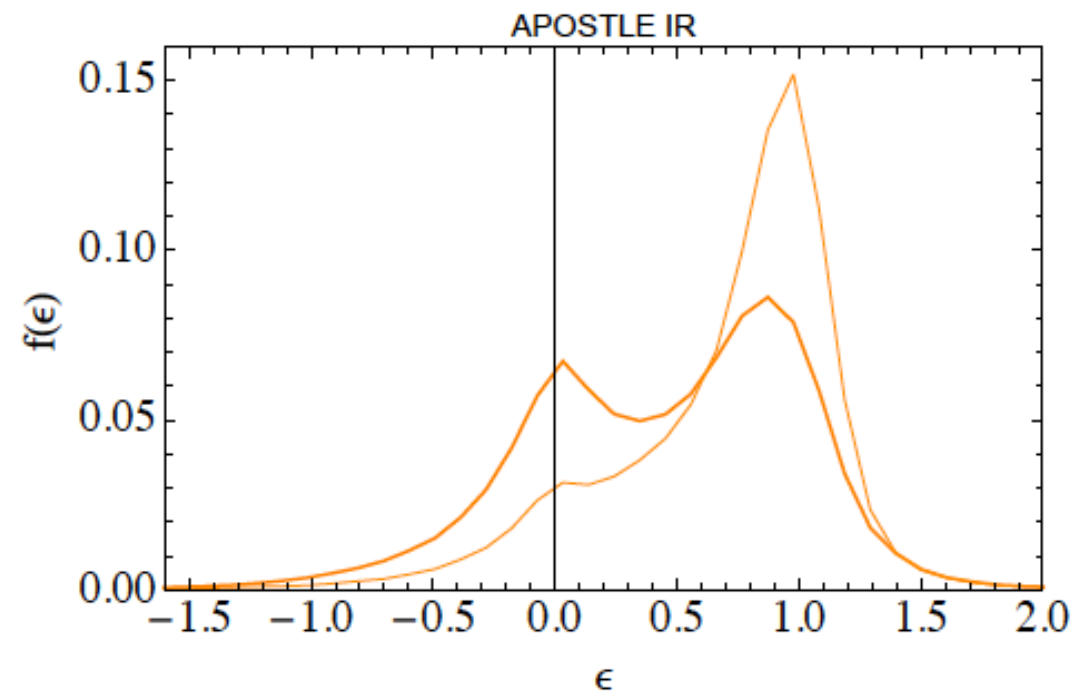
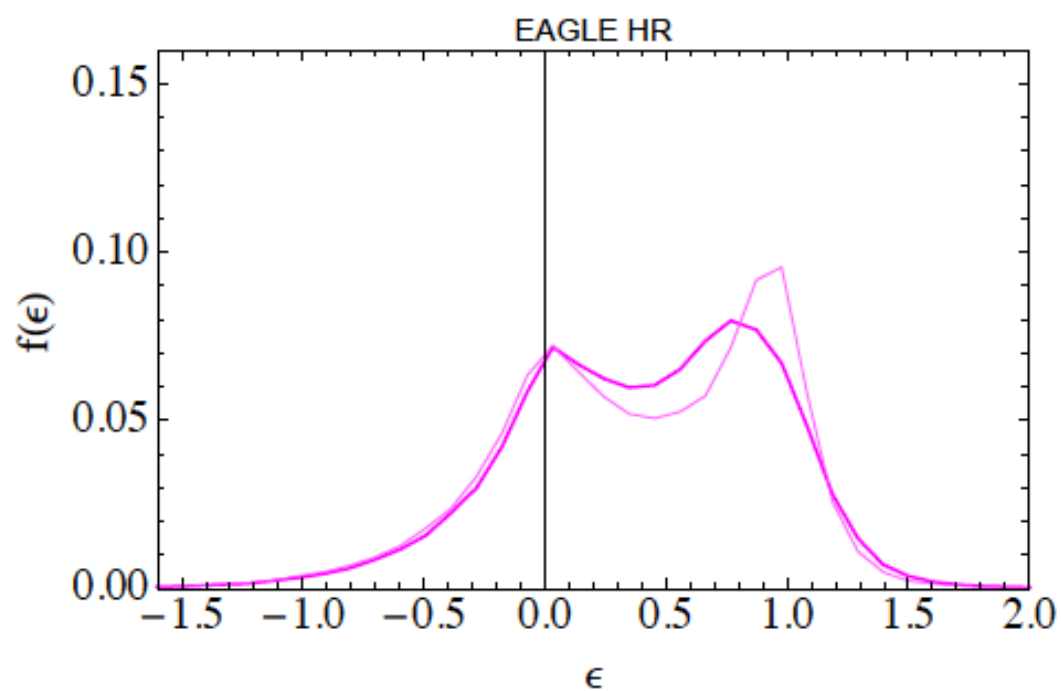
$$\epsilon(r) = \frac{j_z}{j_c(r)}$$

A distribution peaked at  $\epsilon = 1 \Rightarrow$  disc

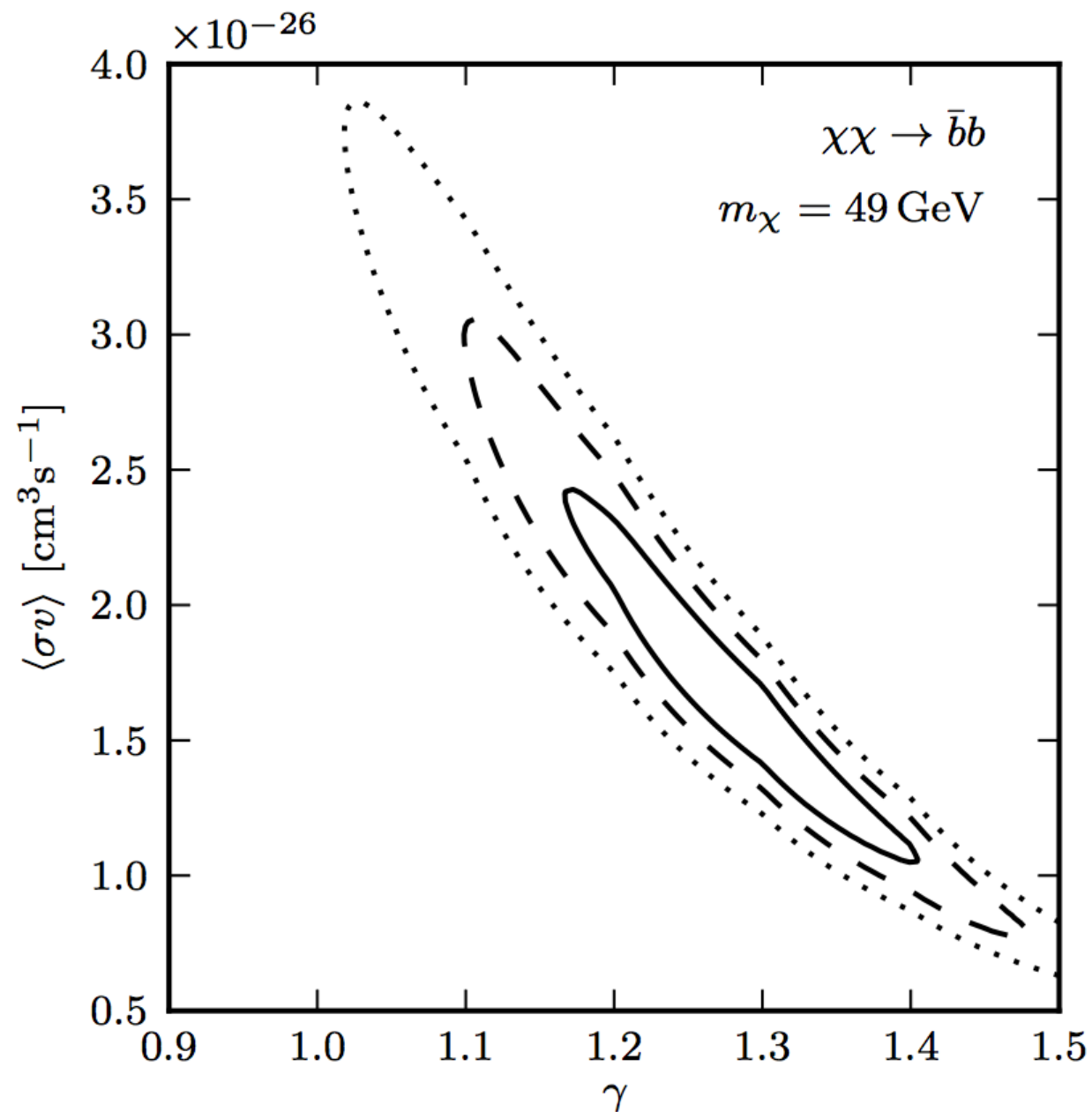
An almost symmetric distribution around  $\epsilon = 0 \Rightarrow$  spheroidal system

# Morphology of simulated haloes

- ▶ We retain a galaxy if the stellar fraction in the range  $\epsilon > 0.45$  is larger than 50%.
- ▶ With this criterion we can identify galaxies that have a dominant disc, and remove galaxies that show an almost symmetric distribution around  $\epsilon = 0$ .



# GeV excess spatial profile

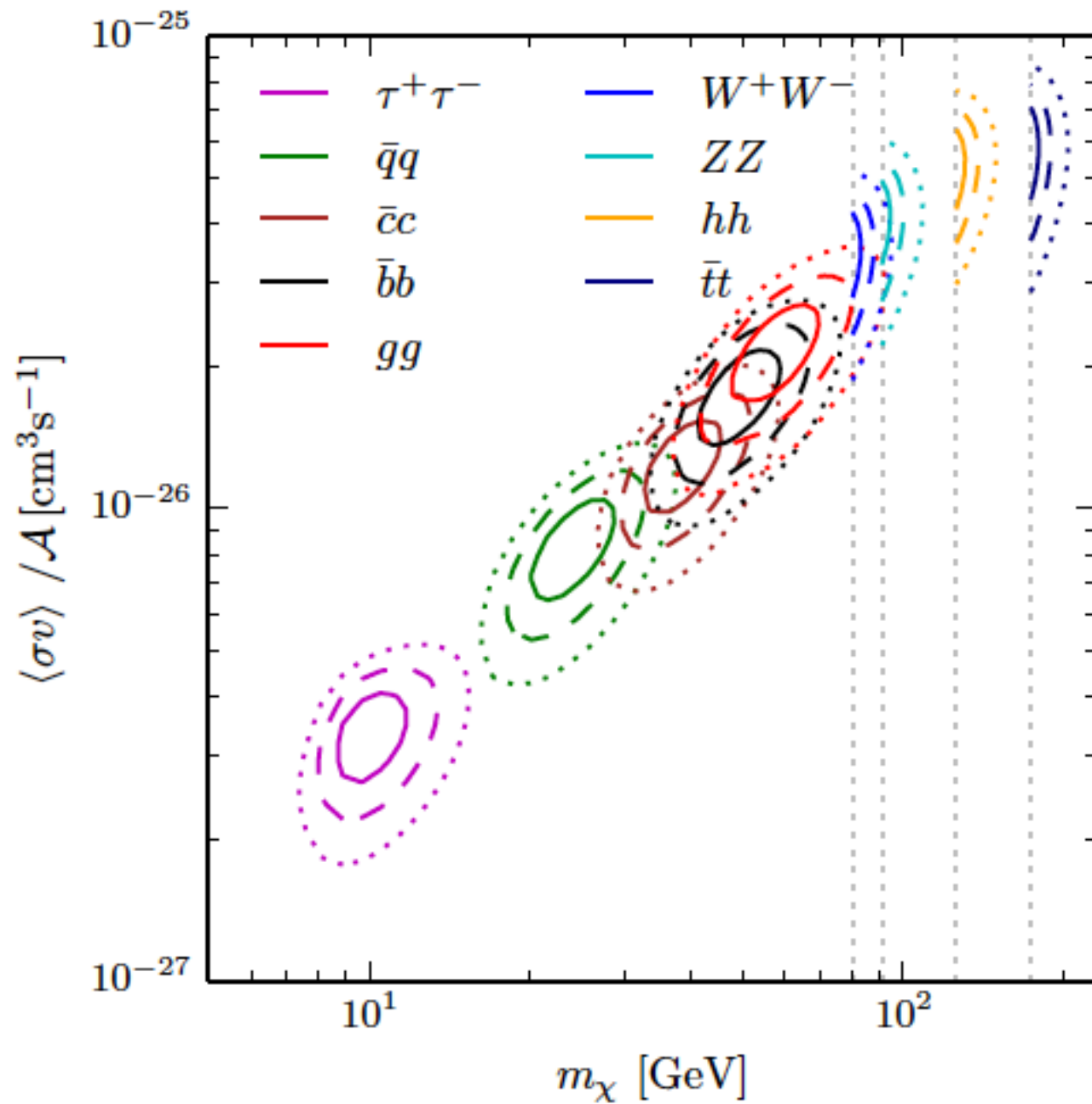


Generalized NFW:

$$\rho(r) = \rho_s \frac{r_s^3}{r^\gamma (r + r_s)^{3-\gamma}}$$

Calore et al., I409.0042

# GeV excess DM interpretation



Channel	$\langle\sigma v\rangle$ ( $10^{-26} \text{ cm}^3 \text{ s}^{-1}$ )	$m_\chi$ (GeV)	$\chi^2_{\min}$	$p$ -value
$\bar{q}q$	$0.83^{+0.15}_{-0.13}$	$23.8^{+3.2}_{-2.6}$	26.7	0.22
$\bar{c}c$	$1.24^{+0.15}_{-0.15}$	$38.2^{+4.7}_{-3.9}$	23.6	0.37
$\bar{b}b$	$1.75^{+0.28}_{-0.26}$	$48.7^{+6.4}_{-5.2}$	23.9	0.35
$\bar{t}t$	$5.8^{+0.8}_{-0.8}$	$173.3^{+2.8}_{-0}$	43.9	0.003
$gg$	$2.16^{+0.35}_{-0.32}$	$57.5^{+7.5}_{-6.3}$	24.5	0.32
$W^+W^-$	$3.52^{+0.48}_{-0.48}$	$80.4^{+1.3}_{-0}$	36.7	0.026
$ZZ$	$4.12^{+0.55}_{-0.55}$	$91.2^{+1.53}_{-0}$	35.3	0.036
$hh$	$5.33^{+0.68}_{-0.68}$	$125.7^{+3.1}_{-0}$	29.5	0.13
$\tau^+\tau^-$	$0.337^{+0.047}_{-0.048}$	$9.96^{+1.05}_{-0.91}$	33.5	0.055
$[\mu^+\mu^-]$	$1.57^{+0.23}_{-0.23}$	$5.23^{+0.22}_{-0.27}$	43.9	$0.0036]_{\text{JES}}$

Calore et al., 1411.4647